Integrated analysis of small RNA, transcriptome and degradome sequencing provides new insights into floral development and abscission in yellow lupine (Lupines luteus L.)

Paulina Glazinska (pglaz.pg@gmail.com)
Nicolaus Copernicus University https://orcid.org/0000-0002-8299-2976
Milena Kulasek
Nicolaus Copernicus University
Wojciech Glinkowski
Nicolaus Copernicus University
Waldemar Wojciechowski
Nicolaus Copernicus University
Jan Kosiński
Adam Mickiewicz University

Research article

Keywords: Yellow lupine, miRNA, phased siRNA, RNA-seq, degradome, sRNA, flower development, abscission, auxin

Posted Date: May 14th, 2019

DOI: https://doi.org/10.21203/rs.2.9588/v1

Version of Record: A version of this preprint was published at International Journal of Molecular Sciences on October 16th, 2019. See the published version at https://doi.org/10.3390/ijms20205122.

Abstract

Background Yellow lupine (Lupinus luteus L., Taper c.) is an important legume crop. However, its flower development and pod formation are often affected by excessive abscission. Organ detachment occurs within the abscission zone (AZ) and in L. luteus primarily affects flowers formed at the top of the inflorescence. The top flowers' fate appears determined before anthesis. The organ development and abscission mechanisms utilize a complex molecular network, not yet not fully understood, especially as to the role of miRNAs and siRNAs. We aimed at identifying differentially expressed (DE) small ncRNAs in lupine by comparing small RNA-seq libraries generated from developing upper and lower raceme flowers, and flower pedicels with active and inactive AZs. Their target genes were also identified using transcriptome and degradome sequencing. Results Within all the libraries, 394 known and 28 novel miRNAs and 316 phased siRNAs were identified. In flowers at different stages of development, 30 miRNAs displayed DE in the upper and 29 in the lower parts of the raceme. In comparisons between upper and lower raceme flowers, a total of 46 DE miRNAs were identified. miR393 and miR160 were related to the upper and miR396 to the lower flowers and pedicels of non-abscising flowers. In flower pedicels we identified 34 DE miRNAs, with miR167 being the most abundant of all. Most siRNAs seem to play a marginal role in the processes studied herein, with the exception of tasiR-ARFs, which were DE in the developing flowers. The target genes of these miRNAs were predominantly categorized into the following Kyoto Encyclopedia of Genes and Genomes (KEGG) pathways: 'Metabolism' (15,856), 'Genetic information processing' (5,267), and 'Environmental information processing' (1,517). Over 700 putative targets were categorized as belonging to the 'Plant Hormone Signal Transduction pathway'. 26,230 target genes exhibited Gene Ontology (GO) terms: 23,092 genes were categorized into the 'Cellular component', 23,501 into the 'Molecular function', and 22,939 into the 'Biological process'. Conclusion Our results indicate that miRNAs and siRNAs in yellow lupine may influence the development of flowers and, consequently, their fate by repressing their target genes, particularly those associated with the homeostasis of phytohormones, mainly auxins.

Background

Yellow lupine is a crop plant with remarkable economic potential. Thanks to its ability to fix nitrogen, it does not need fertilizers, and its protein-rich seeds may be an excellent source of protein in animal feed [1–3]. The crop yield is determined by the number of formed pods, and in yellow lupine this value is significantly limited by its high flower abscission level [1]. *Lupinus luteus* flowers are stacked in whorls along the common stem forming a raceme. Pods are formed at the lowest whorls, while the flowers above them fall off [4]. The estimated percentage of dropped flowers is 60% at the 1st (and lowest) whorl, 90% at the 2nd whorl, and ~100% at the whorls above them. Thus, the problem of flower abscission generates large economic losses in agriculture [1].

Plant organ abscission is an element of the developmental strategy related to reproduction, defense mechanisms or disposal of unused organs [5, 6]. In most species, the key players involved in activation of the abscission zone (AZ) are plant hormones, among which auxin (IAA) and ethylene (ET) play the key

roles [7, 8]. An increased concentration of auxin in the distal region of pedicel (between the flower and the AZ), as compared to its concentration in the proximal region (between the AZ and the peduncle), is a prerequisite for organ abscission [5, 6, 9]. Our previous transcriptome-wide study [10] proved that the abscission of yellow lupine flowers and pods is associated, *inter alia*, with intensive changing of auxin catabolism and signaling. Genes encoding auxin response factors *ARF4* and *ARF2* were more expressed in generative organs that were maintained on the plant, in contrast to the mRNA encoding auxin receptor *TIR1* (*Transport Inhibitor Response 1*), which is accumulated in larger quantities in shed organs [10].

Since (i) some micro RNAs (miRNAs) and small interfering RNAs (siRNAs) restrict the activity of certain *ARFs* [11, 12] and members of the *TAAR (TIR1/AFB AUXIN RECEPTOR)* family encoding auxin receptors [13], and since (ii) we proved that the precursor of miR169 is accumulated in increased quantities in yellow lupine's generative organs undergoing abscission [10], we predict that sRNAs play significant roles in orchestrating organ abscission in *L. luteus*.

miRNA is a cluster of 21-22-nt-long regulatory RNAs formed as a result of the activity of *MIR* genes in certain tissues and at certain developmental stages [14–16], and also in response to environmental stimuli [17–19]. *MIR* genes encode two consecutively formed precursor RNAs, first pri-miRNAs and then pre-miRNAs, which are subsequently processed by DCL1 (Dicer-like enzyme) into mature miRNAs [20, 21]. *MIR* genes are often divided into small families encoding nearly or completely identical mature miRNAs [22]. miRNA sequences of 19-21 nucleotides are long enough to enable binding particular mRNAs by complementary base pairing, and allow either for cutting within a recognized sequence or for translational repression (reviewed in [23]). Plant miRNAs are involved in, for instance, regulating leaf morphogenesis, establishment of flower identity, and stress response [17–19, 24–26]. Some of them also form a negative feedback loop by influencing their own biogenesis, as well as the biogenesis of some 21-nt-long siRNAs called trans-acting siRNAs (ta-siRNAs). ta-siRNAs are processed from non-coding *TAS* mRNAs, which contain a sequence complementary to specific miRNAs [27, 28]. There is also a large group of plant sRNAs that are referred to as phased siRNA, which are formed from long, perfectly double-stranded transcripts of various origins, mainly processed by DCL4 [29, 30].

Numerous studies on sRNA in legumes (e.g. *Glycine max*, *G. soja* [31], *Medicago truncatula* [32]*, M. sativa* [33], *Arachis hypogaea* [34]*, Lotus japonicus* [35] and *Phaseolus vulgaris* [36]) have primarily focused on stress response and nodulation (also reviewed in [37]), or have been entirely carried out *in silico* [38]. In lupines, the knowledge on the roles of regulatory RNAs function, is still negligible [39]. Importantly, the involvement of regulatory sRNAs in mechanisms behind the maintenance/abscission of generative organs has never been explored before. This study aims to investigate the role of low molecular regulatory RNAs (miRNAs and phased siRNAs) and their target genes in *Lupinus luteus* flower development and abscission.

To achieve this goal, ten variants of sRNA libraries were prepared and NGS sequencing was performed. We identified both known and presumably new miRNAs and siRNAs from flowers at different developmental stages, specifically the lower flowers (usually maintained and developed to pods) and the upper flowers (usually shed before fruit setting). Moreover, in our comparisons of libraries from the upper and lower flowers, differentially expressed miRNAs were found. In order to identify the miRNAs involved exclusively in

flower abscission, we compared sRNA libraries from the pedicels of flowers that were maintained on the plant and those that were shed. A transcriptome-wide analysis was carried out to identify the target genes for the recognized sRNAs, and a degradome-wide analysis to confirm the processing of the target sequences for a number of conserved or new *Lupinus luteus* sRNAs. Our results of an NGS analysis of small RNA, transcriptome and degradome libraries indicate that miRNAs play a vital role in regulating yellow lupine flower development, both generally and depending on the flower's location on the inflorescence. Furthermore, these molecules also display differential accumulation during flower abscission.

Methods

Plant Material and Total RNA Extraction

Commercially available seeds of yellow lupine cv. Taper were obtained from the Breeding Station Wiatrowo (Poznań Plant Breeders LTD. Tulce, Poland). Seeds were treated with 3,5ml/kg Vitavax 200FS solution (Chemtura AgroSolutions, Middlebury, United States) to prevent fungal infections and inoculated with live cultures of Bradyrhizobium lupine contained in Nitragina (BIOFOOD s.c., Walcz, Poland) according to seed producer's recommendations [187].

All the research material (flowers and flower pedicels) used for RNA isolation was collected from field-grown plants cultivated in the Nicolaus Copernicus University's experimental field (in the area of the Centre for Astronomy, Piwnice near Torun, Poland; 53°05'42.0"N 18°33'24.6"E) according to producer's agricultural recommendations [187] until the time of fowering. Flowers were collected 50 to 54 days after germination from the top and bottom parts of the inflorescence and were separated into four categories based on the progression of their development, and thus: Stage 1 – closed green buds, parts of which were still elongating. Stage 2 – closed yellow buds, around the time of anther opening. Stage 3 – flowers in full anthesis. Stage 4 – flowers with enlarged gynoecia from the lower parts of the inflorescence, or aging flowers from the upper parts of the inflorescence. Based on their position on the inflorescence, flowers in each of the stages were additionally tagged as either upper (UF) or lower flowers (LF), resulting in eight different variants: UF1, UF2, UF3, UF4, LF1, LF2, LF3 and LF4. Flower pedicels from flowers undergoing abscission (FPAB) or maintained on the plant (FPNAB) were also collected, as in our previous study [10]. The full list of sample names with descriptions is available in the Additional File 1: Table S1.

Total RNA extraction was performed using the miRNeasy Mini Kit (Qiagen, Venlo, the Netherlands) with a modified protocol including an increased volume of the QIAzol lysis reagent in the initial phase of extraction (due to the exceptionally high level of nucleic acids in some of the samples), and on-column DNA digestion was carried out with the RNase-Free DNase Set (Qiagen, Venlo, the Netherlands) to avoid any DNA contamination in the samples. Total RNA quality and quantity was evaluated by performing standard agarose gel electrophoresis (1,2% agarose gel in 0,5 TBE buffer) and a Nanodrop ND-1000 spectrophotometer (Thermo Scientific Waltham, Massachusetts, U.S.A) measurement. The RNA Integrity Number (RIN), as well as the concentration of RNA diluted following the standards required for NGS, were measured with the 2100 Bioanalyzer (Agilent Santa Clara, California, U.S.A) using the Small RNA Kit

(Agilent Santa Clara, California, U.S.A). All samples sent for NGS sequencing had adequate concentrations of RNA and RIN ranging from 8.9 to 10.0, indicating an excellent quality of the isolated RNA.

RNA Library Construction and NGS Sequencing

Small RNA libraries were prepared from the total RNA using the NEBNext Multiplex Small RNA Library Prep kit for Illumina (New England Biolabs Ipswich, Massachusetts, U.S.A) and subsequently sequenced on the HiSeq4000 platform (Illumina, San Diego, CA, U.S.A) in the 50SE (single-end) mode. All libraries were constructed in two biological replicates.

Transcript libraries were prepared from the total RNA using the NEBNext Ultra Directional RNA Library Prep Kit for Illumina (New England Biolabs Ipswich, Massachusetts, U.S.A) and sequenced on the HiSeq4000 platform in the 100PE (paired-end) mode.

Degradome Library Construction and Target Identification

For degradome sequencing, total RNA from UF3-LF3 samples was pooled. The protocol for degradome library preparation comprised the following steps: (i) mRNA isolation, where poly (A)-containing mRNA molecules are purified from total RNA using poly (T) oligo-attached magnetic beads, (ii) synthesis and subjugation of cDNA to ligate 5' adaptors, and purification of the resulting products with TAE-agarose gel electrophoresis, (iii) PCR amplification to enrich the final products, (iv) library quality validation on the Agilent Technologies 2100 Bio-analyzer and using the ABI StepOnePlus Real-Time PCR System (Applied Biosystems, Foster City, California U.S.A.), and (v) sequencing of the prepared library on the HiSeq4000 platform in the SE50 mode.

After sequencing, the reads were filtered using fastq_quality_filter from the Fastx-Toolkit package (http://hannonlab.cshl.edu/fastx_toolkit/) with at least 95% of nucleotides in each read demonstratinga quality >= 20 (Phred Quality Score) with -p 95 and q 20. The filtered Degradome-seq data, sequences of mature miRNA/siRNA and the assembled transcriptomes were processed with the CleaveLand4 package [56] to determine the cleavage sites for sRNA using default program settings. The final results were filtered based on the P-value <0.05.

The construction and sequencing of all the above-mentioned libraries were performed by Genomed S.A (Warszawa, Poland) and BGI (Shenzhen, China).

Identification of Known and Potential novel miRNAs and phased siRNA

Small RNA-Seq Data Pre-processing

Adapter-free sRNA reads were subjected to quality filtering with fastq_quality_filter from the FASTX-Toolkit package (http://hannonlab.cshl.edu/fastx_toolkit/) using –p 95 and –q 20 parameters (http://hannonlab.cshl.edu/fastx_toolkit/commandline.html#fastq_quality_filter_usage). Then, redundant and counting read occurrences (i.e. raw expression values) were identified with the fastx_collapser from the same package.

Short reads were compared against noncoding RNAs from Rfam [43, 44] and both mature miRNA and their precursors from miRBase [45–50]. The comparison was performed with Bowtie [188] allowing for no mismatches. In the columns 'miRBase annotation' of presented Tables, names of identical miRNAs from miRBase are provided. Additionally, identified miRNAs were classified into MIR families deposited in the miRBase.

The nucleotide length distribution of small RNAs from all the ten libraries (Fig. 1) was plotted using the ggplot2 R package [189]. The miRNA accumulation in all the ten libraries expressed in reads per milion (RPM) (Fig. 4) was plotted using the R packages: ggplot2 [189] and gridExtra [190].

Identification of Known and Novel miRNAs

A search for miRNAs was done in the two following ways. Mature miRNAs with sequences and lengths identical to known plant miRNAs from miRBase were identified using a similarity search at the mature miRNA level. In an alternative approach, we applied ShortStack [52] with default settings. This tool identifies miRNAs based on their mapping against a reference genome. Since no genome was available for the studied species, we used a *de novo* approach for transcriptome assembly instead. The latter method allowed for identification of miRNAs that were not similar to anything within miRBase, and these miRNAs were assigned as new.

Identification of ta-siRNAs (phased siRNAs)

ShortStack [52] was used to identify small RNAs that were being cut in phase from longer precursors. Similarly to miRNAs, the transcriptomes were used as references, since no genome sequence was available. In order to obtain the highest quality set of these sRNAs,
only top 200 candidates were selected from each sample, based on the phased score value provided by ShortStack. Finally, lists of such sRNAs from all samples were merged into a single dataset of non-redundant phased siRNAs (Additional File 1: Table S8). The expression values were calculated in the similar manner as in the case of miRNAs.

Analysis of Differentially Expressed si- and miRNAs

A differential expression analysis was performed with the DESeq2 R package [191].
The files containing raw read counts for miRNAs/siRNAs from treatment and control replicates were used as input, and only candidates with an adjusted p-value (q-value) below 0.05 were kept. The heatmaps displaying the expression profiles and hierarchical clustering of miRNAs, the fold change of differentially expressed miRNAs and p-values (Fig. 4) were plotted using the following R packages: ComplexHeatmap [192], circlize [193] and dendextend [194]. For flowers (Fig. 4a), the expression matrix was z-scaled prior to clustering using a scale() R function.

Due to the ineffectiveness of the Venn diagram approach in the visualization for more than 5 sets, common miRNAs in each intersection of 8 datasets were visualized using the UpSetR R package [55]. The frequency cutoff was set at zero (Additional File 3: Figure S2).

Evolutionary Conservation of miRNAs

As a result of adopting the similarity search approach in our miRNA search strategy, all the identified miRNAs were evolutionarily conserved, i.e. they could be found in at least one other plant species. In order to get more insight into the evolutionary relationship of miRNAs between species (at the miRNA family level), an additional analysis was performed. In detail, *L. luteus* miRNAs were assigned to miRNA families based on miRBase classification, and the same was done for the sequences of all *Eudicotyledons* species present in miRBase, with the exclusion of *Gossypium arboretum* (which has only one sequence deposited in the database that cannot be classified as belonging to any known miRNA family). miRNAs from 52 species were compared against *L. luteus* miRNAs in order to count the numbers of miRNA family members shared amongst the species. Same analysis was performed again for 9 *Fabaceae* species.

Validation of sRNA-seq Expressed miRNAs

Validation of differentially expressed (DE) miRNAs and siRNAs was performed using the Stem Loop RT-qPCR technique, according to [195]. To increase the accuracy and efficiency of the reaction, the pulse RT approach was applied to reverse the transcription step based on [196] using total RNA and the SuperScript III Reverse Transcriptase (Thermo Fisher Scientific Waltham, Massachusetts U.S.A) in a 20 μl reaction volume. The reverse transcription consisted of two steps: 30 min of pre-incubation at 16°C, followed by 60 cycles at 30°C for 30s, 42°C for 30s and 50°C for 1s. The subsequently performed qPCR was performed using specific primers designed according to [196], modified so that the UPL9 hydrolysis probe (Roche, Basel, Switzerland) could be used for maximum accuracy and background reduction. This reaction was performed using the SensiFAST Probe No-ROX kit (Bioline meridian bioscience Cincinnati, Ohio, U.S.A) and the LightCycler 480 (Roche, Basel, Switzerland). Each 20 μl reaction contained 1 μl cDNA template (transcribed from ~100 ng of total RNA for less expressed miRNAs and 25 ng of total RNA for more expressed miRNAs), 1 μl of 10 μM qPCR specific forward primer, 1 μl of 10 μM Universal-qPCR primer, 10 μl of 2x SensiFAST Probe No-ROX Mix, 0.2 μl of 10 μM UPL9 probe and 6.8 μl ddH_2O. qPCR was executed by pre-incubation at 95°C for 10 min, followed by 45 cycles of 95°C for 10 s, 59°C for 30 s, and 72°C for 1 s. The signal from the probe was detected during the amplification step. The threshold was set automatically and the threshold cycle (CT) was recorded. Each experiment consisted of three biological and technical replicates. The relative expression levels of the miRNAs were calculated using the method, and the data were normalized to the CT values for the *β actin* gene (expression level of this reference gene was measured according to [10]). All primer sequences are given in the Additional File 2: Table S13.

RNA-Seq: de novo Transcriptome Assembly and Target Gene Expression Analysis

The transcriptome was assembled *de novo* from RNA-Seq data using Trinity v 2.4.0 with default settings as in our previous study [10]. The expression level was estimated at both the unigene and isoform levels and described by FPKM: the number of reads per unigene normalized to the library size and transcript length (Fragments Per Kilobase Of Exon Per Million Fragments Mapped) using RSEM [197] as previously described [10].

Finding Targets for sRNAs

To find targets for known and novel miRNAs, we used the psRNATarget tool [57] with the default Schema V2 (2017 release) and an expectation score of up to 4. Here, the miRNA targets were searched for among the assembled transcriptomes. The same analysis was performed for phased siRNAs.

Gene Ontology (GO) and KEGG Analysis of Target Genes

In order to estimate the potential roles of the identified sRNAs and transcripts in biological processes, GO annotations of genes targeted by the identified miRNAs were downloaded from the Gene Ontology10, NCBI11, and UniProt12. The Bioconductor GOseq package [198] was used for a GO enrichment analysis. A KEGG annotation and enrichment analysis was performed to determine the metabolic pathways. The GO terms and KEGG pathways were considered to be significantly enriched with the corrected P-value of 0.05, which was calculated using a hypergeometric test [199].

Data submission to Sequence Read Archive (NCBI)

The RNA-Seq and small RNA-Seq data have been uploaded to the SRA database and are available under BioProject ID PRJNA419564 and Submission ID SUB3230840.

Results

Sequencing and Annotation of Yellow Lupine sRNAs

Ten variants of small RNA libraries from developing flowers and flower pedicels were constructed and sequenced as described in the material and methods section and Additional File 1: Table S1. Single-end deep sequencing was performed on the Illumina HiSeq4000 platform. After removing low-quality reads, a total of 303,267,263 reads (from 14,186,278 to 15,504,860 reads per library) and 128,060,403 unique reads (from 5,677,701 to 6,990,061 per library) were obtained (Additional File 1: Table S2). The length distribution of the small RNAs (15-30 nt) revealed that a length of 24 nt was the most frequent and that of 21 nt was the second class amount of the clean and redundant reads (Additional File 1: Table S2, Fig. 1), which was compliant with many other RNA-Seq experiments (e.g. [40–42]) and correlated with the abundance of siRNAs and miRNAs, respectively. The unique reads were annotated against Rfam [43, 44] and miRBase [45–50] databases, and from the latter both mature (named in tables as ‘miRBase’) and precursor sequences (named as ‘Hairpin’) were taken into account. However, many of them remained unassigned (Table 1, Additional File 1: Table S2). The unique sequences were annotated into different RNA classes against the Rfam database using BLAST [51].

The small RNA sequences have been clustered into several RNA classes, such as known miRNAs, rRNA, tRNA, sn/snoRNA and others (Table 2, Additional File 1: Table S3). A total of 690,436 sRNAs were annotated into 20 libraries, with the highest number observed in the upper flowers and abscising pedicles. Between these libraries, the most abundant classes were rRNAs and tRNAs, with average values of 26,390

and 3,726 sequences, respectively, followed by snoRNAs and different subtypes of snRNAs with average values ranging from 863 to 876 sequences (Table 2, Additional File 1: Table S3).

Identification of Known, Conserved miRNAs

After analyzing the results of the alignment against miRBase [45–50], 394 unique miRNAs containing 366 conserved miRNAs were identified in the ten samples (Additional File 1: Table S4). The number of the identified miRNAs in each library is shown in Table S. The largest number of known miRNAs (181) was observed in the Lower Flowers stage 3 (LF3) and the smallest (148) in the Upper Flowers stage 1 (UF1) (Additional File 1: Table S1). The identified miRNAs belonged to more than 67 families (Additional File 1: Table S4), while most of them belonged to the MIR156, MIR159 and MIR166 families, with more than 35 members in each (Fig. 2a).

Evolutionary Conservation of microRNAs Identified in *Lupinus luteus*

To explore the evolutionary roles of the known miRNAs identified in yellow lupine, these RNAs were compared with the sequences of almost all (i.e. 52) *Eudicotyledons* species present in miRBase [45–50]. *Gossypium arboretum* was excluded from this comparison as there is only one (and, additionally, unclassified) sequence deposited in the database for it. The same analysis was performed exclusively against nine *Fabaceae* species. As shown in Figure 2b, the 67 known miRNA families exhibited different numbers of homologous sequences in both the comparisons. Twenty of them were the most conserved ones, i.e. had homologues in over 20 species (Fig. 2b, shaded in blue). Six miRNA families were conserved at a moderate level: MIR393, MIR403, MIR2111 across 10-19 species, and MIR535, MIR319, MIR1507 across 5-9 species (Fig. 2b, shaded in yellow and magenta, respectively). Sixteen miRNA families showed a low level of conservation (had homologues in 2-4 species) (Fig. 2b, shaded in green). Finally, the last group consisted of ten members and displayed homology to miRNAs in only one species across the analyzed dataset Fig. 2b, shaded in orange). As many as 15 miRNA families identified in yellow lupine flowers were not present in eudicots. There were also two species for which no member of the considered miRNA families was present in the dataset: *Gossypium herbaceum* (*ghb*) and *Populus euphratica* (*pau*). For these species only one and eight miRNAs, respectively, were identified and uploaded to miRBase.

Our comparison across legumes revealed that 8 miRNA families were highly conserved in this taxon, i.e. had homologues in 5-9 species out of 9 (Fig. 2b, lower panel, shaded in magenta), 18 had homologues in 2-4 legumes (Fig. 2b, shaded in green), and 2 had homologues only in one plant, *Glycine max* (Fig. 2b, shaded in orange). A surprisingly high number (39) of miRNA families identified in yellow lupine flowers were not conserved across *Fabaceae*, probably due to still incomplete list of miRNAs in these taxa.

Identification of Novel miRNAs

With the use of the ShortStack software [52], 28 candidates for novel miRNAs were identified (Table 3). This tool identifies miRNAs based on their mapping against a reference genome. As no genome was available for the studied species, we used a transcriptome instead (statistical data on *de novo* assembly is in Additional File 1: Table S5). The results obtained were filtered against mature miRNAs from miRBase,

and unique sequences received names in the following format: “Ll-miRn(number)” (for example: Ll-miRn1). All of these 28 sequences were 21-24 nt in length, with 68% of them being 21nt long (Table 3). Interestingly, many of these unique miRNAs showed similarity to precursor miRNAs from miRBase, which led to the conclusion that they might be new members of the already known families: MIR167 (Ll-miRn12 and -n27) and MIR169 (Ll-miRn3, -n11 and -n15) (Table 3) and hinted that they might be exclusive to yellow lupine. The length of their precursor sequences ranged from 71 to 246 nt and their free energy (MFE) ranged from -32,3 to -144,9 kcal/mol for the secondary hairpin structure. The expression of these novel miRNAs was also highly diversified across all the libraries. Ll-miRn26 was present only in the LF1 sample, while Ll-miRn21 was present in all the sRNA libraries and had an expression ranging from 3,982.82 to 11,421.55 RPM (Additional File 1: Table S6).

Analysis of the Expression Abundance of Known miRNA Families in *Lupinus luteus*

Since miRNA expression across all libraries displayed high variation, we put the data into five categories based on the maximum value (Fig. 3). Two miRNAs, namelyLl-miR341 and Ll-miRn21, showed expression maxima of over 10,000 RPM. Maximal expression of another two, Ll-miR260 and Ll-miR384, ranged from 2,000 to 10,000 RPM. Thirteen miRNAs showed expression maxima ranging from 100 to 2,000 RPM. The most numerous category with 33 elements was the one for miRNAs with expression maxima ranging from 10 to 100 RPM. Another 24 miRNAs were expressed with the maximal RPM values between 1 and 10. The expression value of the five least abundant miRNAs did not exceed 1 RPM (Fig. 3, Additional File 1: Table S7).

Identification of Phased siRNA in Yellow Lupine

Numerous reports and studies point to the important role of phased siRNA not only in stress response mechanisms, but also in growth regulation (reviewed in e.g. [53]). Therefore, we decided to investigate the role of siRNAs during yellow lupine inflorescence development. To achieve this, ShortStack [52] was used to identify small RNAs that were being cut in phase from longer precursors. We identified 316 siRNA ranging from 21 to 25 nt in length, of which 71% were 24nt long (Additional File 1: Table S8, Additional File 1: Figure S1). The identified siRNAs displayed a highly differential expression pattern. The highest level of expression was observed in Ll-siR308, -274, -249, -206, -191, -161 and -108 (Additional File 1: Table S9), and ranged from 39 to 579 RPM in all the samples. Some of the sequences showed organ-specific expression; for example, Ll-siR4, -13, -173 were present only in the pedicels of abscising flowers (FPAB), while Ll-siR308 showed an elevated expression in the pedicels (FPAB and FPNAB) (Additional File 1: Table S9). On the other hand, Ll-siR246, -291 and -56 were present almost exclusively in the youngest flowers in the lower part of inflorescence (LF1). The least abundant siRNAs were Ll-siR50, -175, -250 and-263, which were present only in one library (Additional File 1: Table S9).

Analysis of the Expression Profile of the Identified sRNAs During Yellow Lupine Flower Development

In order to investigate the dynamics of the identified sRNAs’ expression during floral development in yellow lupine, we established a wide scope comparison of the following growth stages of flowers from the upper (UF2 vs UF1, UF3 vs UF2 and UF4 vs UF3) and lower (LF2 vs LF1, LF3 vs LF2 and LF4 vs LF3) parts of the

inflorescence (Table 4, Additional File 1: Table S10, Fig. 4). The analyses resulted in the identification of 30 differentially expressed (DE) miRNAs in the lower and 29 in the upper flowers (Table 4), as well as 14 and 7 siRNAs, respectively (Additional File 1: Table S11).

Between UF2 vs UF1, there was a change in the expression of 8 miRNAs, of which 4 were up-regulated. Among these DE sequences, there were 2 sequences belonging to MIR359 and MIR166 families each, as well as one representative of each of the MIR159, MIR167, MIR396 and novel Ll-miRn10 families. Ten DE miRNAs were identified in a comparison of UF3 vs UF2, of which only one Ll-miR258 (miR166 homologue) was up-regulated. The remaining miRNAs were down-regulated and consisted of 3 sequences belonging to the MIR390 and MIR396 families each, and single miRNAs from the MIR168, MIR408 and MIR396 families. A comparison of the UF4 vs UF3 libraries revealed 12 DE miRNAs, of which 7 were up-regulated. The most numerous group was that of members of the MIR390 family, followed by 2 members of MIR167 and MIR319, and singular representatives of MIR398, MIR164 and MIR858, with one novel Ll-miRn11 (Table 4).

During the development of flowers from the lower part of the inflorescence, the miRNAs accumulation dynamics was different. The highest number of the identified DE miRNAs were found comparing the youngest flowers (LF2 vs LF1), while, interestingly, a complete lack of DE miRNAs was found when comparing the oldest flowers: LF4 vs LF3 (Table 4). In our comparison of LF2 vs LF1, among the 18 DE miRNAs (6 of which were up-regulated) the most numerous group were novel miRNAs, with 5 sequences, namely Ll-miRn22, -27, -10, -3 and -31, followed by members of the MIR396 family (4 sequences, all down-regulated). Subsequently, among the DE miRNas shown in this comparison we found members of the MIR156 and MIR168 families (2 each), followed by single sequences from the MIR166, MIR159, MIR390, MIR858 and MIR393 families. Between the LF2 and LF3 stages we confirmed that there was a change in the accumulation of 11 miRNAs (6 of which were up-regulated), and this pertained to two members of the MIR166 and MIR399 families each, Ll-miRn1 and Ll-miRn22, which were followed by single representatives of the MIR390, MIR395, MIR858, MIR398, MIR408 families (Table 4).

As regards siRNAs during flower development in yellow lupine, almost every differentially expressed siRNAs were up-regulated. In the lower part of the inflorescence, similarly to miRNAs, there were no differences between the LF4 and LF3 stages. During upper flower development, the most DE siRNAs were identified in a comparison of UF2 vs UF1, and the least (only one) when comparing UF3 vs UF2. One noteworthy observation was the presence of the same siRNAs in the comparisons of UF2 vs UF1 and LF2 vs LF1, namely Ll-siR281, -308 and -249, which suggests that an increase in their accumulation is important during phase 1 to phase 2 transition in the development of yellow lupine's flowers, regardless of their position on the inflorescence. The complete dataset can be found in (Additional File 1: Table S11).

In order to identify miRNAs the presence of which is either common and unique depending on the developmental stage of the upper and lower flowers in lupine, Venn diagrams were constructed (Fig. 5 a and a, Additional File 1: Table S12) using Venny 2.1 [54]. The results of these analyses revealed that approximately 70% of the identified miRNAs were common in all developmental stages of both the upper (Fig. 5a) and lower flowers. (Fig. 5b). However, miRNAs unique to certain developmental stages were also found (Fig. 5 and Additional File 1: Table S12). The findings concerning the abundance of miRNAs in

various combinations of 8 datasets are displayed in Additional File 3: Figure S2 as an UpSet R plot [55]. The total numbers of miRNAs detected in each experimental variant are shown as horizontal bars in the bottom left corner. The histogram demonstrates the number of miRNAs corresponding to a given combination, indicated by the dots connected by lines below each bar. The most numerous set with 155 elements was the one with an intersection of all 8 variants. As many as 17 miRNAs were assigned exclusively to stage 3 flowers collected from the lowest whorl (LF3), while for the other 7 variants this number ranged between 6 and 2.

Comparison of Differentially Expressed sRNAs Between Developing Flowers From the Lower and Upper Whorls of the Raceme

In order to determine the differences in sRNA expression in developing yellow lupine flowers, comparative analyses of both the upper and lower flowers was performed for each developmental stage of the inflorescence (LF1 vs UF1, LF2 vs UF2, LF3 vs UF3 and LF4 vs UF4) (Table 5, Fig. 4, Additional File 1: Table S10). In general, 46 DE miRNAs were identified, of which twelve DE miRNAs were from stage 1, eleven from stage 2, eleven from stage 3 and 2 from stage 4 of the flower development process. Interestingly, all UF1 miRNAs were down-regulated, contrary to stage 2 miRNAs all of which were up-regulated. As forUF3 miRNAs, 5 of them were up-regulated, with 6 down-regulated. In UF4, one miRNA (Ll-miR445, homologous to miR319) was up-regulated, while Ll-miR100 homologous to miR390 was down-regulated (Table 5). In the first stage of development, the most numerous group of DE miRNAs was that of the novel sequences (Ll-miRn3, -25, -29 and -30), followed by sequences annotated as miR396 (3 miRNAs). The remaining miRNAs were single sequences annotated as miR167, miR395, miR390 and miR171. In the second stage of flower development,miRNAs belonging to MIR319 family were identified as the largest group (5 sequences), followed by two DE miRNAs annotated as miR160 and miR396, respectively, and singular ones annotated as miR394 and miR393. The third stage turned out to be the most diverse, with 2 representatives of the miR160 family, followed by single sequences annotated as miR394, -393, -858, -159, -396, -5490, -1861 and miR5168. As regards phased siRNAs, only 4 of them displayed differential expression, namely Ll-siR119 in stage 1 and Ll-siR224, -100 and -146 in stage 4. These results might suggest that, firstly, miRNAs display differential expression in each and every stage of flower development, regardless of flower position on the inflorescence, and secondly, that miRNAs seem to be much more important than phased siRNAs are with regard to yellow lupineflower differentiation.

Analyses of the Venn diagrams we created (Fig. 5c), displaying the presence profiles for the library miRNAs, revealed that in each comparison between the upper and lower flowers (UF1 vs LF1 etc.) around 80% of the identified sequences were common for both the upper and lower flowers (Fig. 5c). However, in each comparison we were able to identify miRNAs unique to each stage of the development and each flower position. For example, 20 miRNAs were exclusively present in LF1, while 12 miRNAs were unique to UF1. The detailed information on these comparisons can be found in Additional File 1: Table S12. It is worth noting, however, that Ll-miR224/miR393 were only present in the upper flowers in every stage of development, while in the lower flowers no common miRNAs were found. Despite this, in the lower flowers the presence of members of the MIR396 family (two in LF1, four in LF3 and two in LF2), 3 members of MIR171 in LF1, 3 members of MIR395 in LF2, and two members of the MIR159 family in LF3 and LF4 each,

was observed. Interestingly, the presence of miR319 (two members for UF1, UF2 and UF4 each) could be found in the upper flowers apart from Ll-miR224. Additional analyses of miRNAs common for specific developmental stages regardless of the flower's position on the inflorescence (UF1LF2, UF2LF2, UF3LF3, UF4LF4) (Additional File 1: Table S12, Additional File 4: Figure S3a) revealed that for stage 1 there were no unique and common miRNAs (that would not be present in the other stages). For stages 2 and 3, 6 miRNAs each were identified, with 3 unique miRNAs for stage 4.

Comparison of Differentially Expressed sRNAs between Flower Pedicels with Active and Inactive Abscission Zones

In order to identify sRNAs possibly involved in yellow lupineflower abscission, mi- and siRNA expression patterns for flower pedicels with an active abscission zone (AZ) (FPAB) and inactive AZ (FPNAB) were compared. As a result, 34 DE miRNAs (including 5 novel ones) (Table 6) and 20 phased siRNAs (Additional File 1: Table S11) were identified. 14 miRNAs and 9 siRNAs were up-regulated, while the rest remained down-regulated in FPNAB. Among the up-regulated miRNAs, the most numerous family was MIR167 (5 members), followed by MIR398 (3 members). Among the down-regulated miRNAs, the most abundant were MIR390, MIR396 and MIR395 with 3 members each (Table 6, Fig. 4b). With regard to siRNAs, the most up-regulated in FPANB were Ll-siR173, -4 and -13, and the most down-regulated was Ll-siR208 (Additional File 1: Table S11).

An analysis of the Venn diagrams based on the presence of the identified miRNAs revealed that approx. 80% of the miRNAs were present in both abscising and non-abscising flower pedicles (Fig. 5d). However, 23 miRNAs remained unique to FPAB and 17 to FPNAB (Fig. 5d, Additional File 1: Table S12). Additional comparative analyses of the miRNAs common to the flowers and pedicels revealed miRNAs unique to pedicels only (23 miRNAs), as well as those unique to the pedicels of abscising flowers (20) and non-abscising flowers (14), which were completely absent in the flowers. (Additional File 1: Table S12, Additional File 4: Figure S3b). The sequences unique to FPAB only consisted of, i.a., Ll-miR76/miR169 (sRNA-seq ID/miRBase annotation), Ll-miR420 and -430 belonging to the MIR319 family, as well as auxin related Ll-miR333/miR160 and Ll-miR282/miR167. In FPNAB, 4 members of the MIR156 family (Ll-miR404, -404, -306, -304) and 3 members of the MIR396 family (Ll-miR383, -197 and -196) could be found (Additional File 1: Table S12).

Validation of the Identified sRNAs in RNA-seq

In order to validate the data generated using deep sequencing technology and to confirm the expression patterns of the identified sRNA, we employed stem-loop (SL) qRT-PCR of the 8 identified sRNAs (six conserved miRNAs, one novel miRNA and two siRNAs) (Additional File 2: Table S13). The qPCR results were similar to sRNA-seq data (Fig. 6). For example, in the qRT-PCR analysis the Ll-siR254 expression increased as the flower developed, showing a positive correlation with the deep sequencing results. Ll-siR249 was preferentially accumulated in yellow lupine pedicels, both in qPCR and RNA-seq. The distinct and strong expressions of miR155 in LF1 and miR281 in FPAB were also similar in both the experiments (Fig. 6). The results of the expression analysis of these sRNAs supported the validity of our sRNA-Seq.

Identification of sRNA Target Genes using Degradome and psRNATarget Analysis

In order to estimate accurately the biological function and impact of certain miRNAs, their target genes needed to be identified first. To this effect, we constructed degradome libraries from pooled samples of stage 3 upper and lower parts of the inflorescence (Additional File 2: Table S14). Through total degradome library sequencing, 19,353,278 raw reads were obtained (Additional File 2: Table S14a). After quality filtering, the degradome data were aligned to the reference transcriptome with CleaveLand 4 [56] to find sliced miRNA and siRNA targets. After processing and an analysis, a total of 14,077 targets were identified, and after filtering with a p-value < 0.05, 538 targets emerged (501 targets for 178 known miRNAs and 37 targets for 13 novel miRNAs) (Additional File 2: Table S15). For the phased siRNAs, 3,340 targets were initially identified, and after filtering their number dropped to 89 targets for 46 siRNAs (Additional File 2: Table S16). The results obtained through CleaveLand4 were divided into categories from 0 to 4 in the following manner: 4 –only one read at this position, 3 - >1 read, but below or equal to the average* depth of coverage on the transcript, 2 - >1 read, above the average* depth, but not the maximum on the transcript, 1 - >1 read, equal to the maximum on the transcript when there was >1 position at the maximum value, 0 - >1 read, equal to the maximum on the transcript when there was just 1 position at the maximum value [56]. Through our analyses, for the categories ordered from 0 to 4, we obtained (after p-value filtering) 353, 54, 65, 17, 47 miRNA targets and 33, 18, 11, 19, 8 siRNA targets, respectively (Additional File 2: Table S14b). Exemplary target t-plots and sequences of the miRNAs and target mRNAs are shown in Figure 7.

As expected, many of the targets for evolutionarily conserved miRNAs were compliant with literature data. For example, Ll-miR329/miR160-5p (sRNA-seq ID/miRBase annotation) targeted *ARF16* and *ARF18*, the Ll-miR415/miR171b targeted *SCL6*, Ll-miR341/miR319q targeted *TCP2*, Ll-miR224/miR393a-5p targeted *TIR1*, Ll-miR401/miR156k targeted *SPL2* and *SPL12*, and Ll-miR229/miR396a-5p targeted *GRF3*, *GRF4*, and *GRF5* (Additional File 2: Table S15). A comparison of the expression of 4 exemplary miRNAs and their target genes (Fig. 7) confirmed the reverse-correlation in the accumulation of miRNAs and an abundance of mRNA target genes, especially in flower pedicels. In the flowers, this correlation was not so obvious, presumably because of the organ's more complex nature (with its various elements, such as the stamen and the pistil), where regulation could be tissue-specific. In the case of some of the identified mi- and siRNAs, we were unable to determine the targets with a degradome analysis, which might have been caused by the lack of a sufficient amount of cleavage products ensuing from using only stage 3 flowers to construct the library. In order to find the plausible missing target genes, the psRNATarget tool (2017 update) [57] was employed, which rendered putative target genes through a comparison of the sRNAs with the reference transcriptome containing data from all of the samples. Using this method, we managed to establish putative target genes for most of the mi- and siRNAs, obtaining (with expectation from 0 to 4) 66.102 miRNA and 32.725 siRNA targeted transcripts. A full list of the targets identified using the psRNATarget or degradome analysis for DE miRNAs, siRNAs and novel miRNAs is contained in Tables 3, 4, 5, 6 and Additional File 2: Table S16. Targets for all of them are shown in Additional File 2: Tables S15, 16, 17 and 18.

Function of the Potential miRNAs Targets

Our transcriptome analysis against the Kyoto Encyclopedia of Genes and Genomes (KEGG) revealed the putative function of many targets of the miRNAs identified in yellow lupine. Most of the sequences in the main KEGG categories belonged to Metabolism (15,856), followed by Genetic information processing (5,267), Environmental information processing (1,517), Cellular processes (1,326) and Organismal Systems (800) (Additional File 5: Figure S4). A full list of KEGG pathways and numbers of the assigned sequences is shown in (Additional File 6: Figure S5 and Additional File 7: Figure 6). One of the most represented sub-categories was Signal transduction (1,484), with over 700 putative targets in the Plant Hormone Signal Transduction pathway, where almost every sequence was frequently targeted with multiple miRNAs (Fig. 8). The second most notable pathway was mitogen-activated protein kinase (MAPK) signaling, which was associated with different abiotic and biotic stress factors, with 350 putative targets distributed across every described stress response (Additional File 8: Figure S7). A complete dataset on the KEGG analysis can be seen in (Additional File 2: Table S19).

In order to investigate the functions played by the miRNAs identified in yellow lupine flowers, we submitted miRNA targets to a Gene Ontology (GO) category analysis. Among the 27,547 targets of known and novel miRNAs identified with psRNATarget, 26,230 targets exhibited GO terms (Additional File 2: Table S20). 23,092 genes were categorized to 'Cellular component', 23,501 to 'Molecular function', and 22,939 to 'Biological process'. Figure 9a shows target gene percentages for each GO category. The largest proportion of targets classified to 'Cellular component' was attributable to 'cell', 'cell part' and 'organelle'. The majority of targets involved in the 'Molecular function' category were classified as 'binding' and 'catalytic activity'. Within 'Biological process', most of the targets were categorized as 'cellular' and 'metabolic process' (Fig. 9a, Additional File 2: Table S20). Within the 'Flower development' category, the targets of 37 miRNAs fit within GO terms related to phytohormones (Fig. 9b), and the targets of 69 miRNAs were categorized to GO terms related to the development of flower parts (Fig. 9c).

Discussion

Yellow lupine has a great potential as a substitute for soybean in animal feed production in Europe. An ability to limit the economic drawbacks resulting from excessive flower abscission would be the most convincing argument for lupine cultivation. This, however, can only be achieved if we understand the plant's biology, especially the molecular basis for the development and maintenance of lupine flowers, of which little is known. Therefore, we believe that the pathways controlling these processes deserve intensive research focus. The commonly used NGS technique allows for comprehensive analyses of sRNAoms, transcriptoms, and degradomes, as well as identification of sRNAs and their target genes in both model and non-model plants, for example: tomato [58], soybean [59], *Arabidopsis* [60, 61], oilseed rape [62], *Brassica juncea* [63], lily [64, 65], peanut [66], orchardgrass [67] or wheat [68, 69].

Our previous analyses of yellow lupine transcriptomes resulted in the identification of transcripts of many genes involved in flower and pod abscission, and suggested sRNA involvement in this process [10]. What is puzzling, our observations of *L. lupinus* floral development indicate that their fate (abscission or pod formation) is determined prior to AZ activation. Therefore, we performed comparative analyses between

sRNAs from flowers developing on upper and lower parts of the raceme. Identifying the miRNAs and their target genes involved in the above-mentioned processes will further our knowledge of the biology of not only lupines, but plants in general, since the role played by sRNA in organ abscission is still obscure.

Functions of miRNA/Target Modules During Yellow Lupine Flower Development

Involvement of sRNAs in flower development has undergone intense investigation and already been explored in many plant species, such as wild rice (*Oryza rufipogon*) [70], hickory (*Carya cathayensis Sarg)* [71], yellow-horn (*Xanthoceras sorbifolia*) [72], spring orchid (*Cymbidium ensifolium*) [73], and roses (*Rosa* sp.) [74]. Our sRNA-seq analyses have not only shed light on the molecular mechanisms that control flower development in one more plant species and confirmed the involvement of known miRNAs, such as miR159, miR167 or miR172, in this process [75], but we have also explored the roles of sRNAs in flower abscission and identified species-specific miRNAs.

In order to identify miRNAs and their target genes involved in flower development and abscission in *L. luteus* we conducted comprehensive analyses of ten sRNA and ten transcriptome libraries, and performed one degradome sequencing. The libraries were created for flowers in different developmental stages located in the top and bottom whorls of the raceme, and for flower pedicels with active and inactive AZs. This approach resulted in the identification of 394 conserved miRNAs belonging to 67 families, 28 novel miRNAs and 316 phased siRNAs. Additionally, we found their target genes and, consequently, were able to identify their functions. We also described miRNAs characteristic of the subsequent stages of flower development independently from the flower's position on the raceme, and identified miRNAs present only in either upper or lower flowers, in the particular stages of development.

Known sRNAs and Their Target Genes are Involved in Regulating Flower Development in Yellow Lupine

We explored the large set of data concerning flower development that we obtained through sRNA-Seq analysis, focusing on three aspects: (i) conserved miRNAs involved in flower morphogenesis and development, (ii) expression dynamics during flower development, (iii) miRNAs specific for particular developmental stages.

Conserved miRNA families associated with flower morphogenesis and development

Among the known and conserved miRNAs we spotted a number of miRNAs commonly associated with flower morphogenesis and development, belonging to, *inter alia*, the MIR156/157, MIR159, MIR165/166, MIR167 and MIR172 families (reviewed in [26]).

Within the degradome data sets, we found target genes of two out of four differentially expressed *L. lupinus* miRNAs belonging to the MIR156/157 family (Ll-miR124 and Ll-miR401), encoding squamosa promoter-binding-like proteins 13B (*SPL13B*) and *SPL2*, respectively. Studies have shown that miR156 is necessary for maintaining anther fertility in *Arabidopsis*, by orchestrating the development of primary tapetum cells and primary sporogenous cells [76]. In this plant, *SPL13B* expression is strictly limited by miR156 to anther tapetum in young buds, while *SPL2* is weakly expressed in parietal and sporogenous

cells and the surrounding cell layers in young flowers [76], where it is targeted by miR156 to regulate pollen maturation [77].

The net of factors that regulate pistil development include miR156-targeted members of the SPL gene family, such as *SPL3* and the miR156-resistant *SPL8* gene, with both of them redundantly controlling gynoecium patterning through interfering with auxin homeostasis and signaling. What is striking, none of miRNAs identified in yellow lupine targets *SPL3, which* positively regulates the MADS box genes *APETALA1* (*AP1*), *FUL* and *LFY*, central regulators of flowering [78]. In *Arabidopsis*, down-regulation of miR156-targeted *SPLs* resulted in a shortened style and deformed gynoecium [79]. Other studies on mutants have shown, that the aforementioned *SPL* genes cooperate with *ARF3*, a master regulator of gynoecium development and morphogenesis [80], which directly regulates transcription of several genes involved, among others processes, in auxin synthesis, transport, signaling and response [81].

miR159 was shown to target the conserved *GAMYB-like* genes that are a part of the GA signaling pathway [82, 83]. In *A. thaliana*, by affecting the expression of *MYB33* (*MYB DOMAIN PROTEIN 33*) and *MYB65*, miR159 influences the *LFY* transcription level and gibberellin-dependent flowering induction. Moreover, the same miRNA also regulates proper flower development [84–86]. miRNA159 also regulates morphogenesis of the stamen, and male fertility [85], probably by restricting *MYB33* expression by miR159 to stamen tissues during flower development [84].

Two transcription factors involved in pistil and stamen development, *ARF6* and *ARF8*, contain the target site for miR167 [87, 88]. The roles of miR167 and *ARFs* are conserved across different species [89]. For *Arabidopsis*, it has been proven that both these genes are involved in stamen filament elongation, anther dehiscence, stamen maturation and anthesis [90], and that *arf6 arf8* double mutants suffer from poor pollination [91]. By inducing jasmonic acid biosynthesis, *ARF6* and *ARF8* initiate anther dehiscence and flower bud opening and regulate perianth growth [91–93] However, these genes may also act in a jasmonic acid-independent way, by influencing the transcriptional activity of *GH3*, which results in a shift in the free auxin level [94, 95]. In tomato, a reduction in the accumulation of the miR167-targeted *ARF6* and *ARF8* leads to the lack of trichomes on the style surface, failed pollen germination and, consequently, sterility [96].

Recent research into multiple plant species has shown that miR172 targets genes belonging to the *APETALA2* (*AP2*, *TOE1*, *TOE2*, *TOE3*) family. miR172 is part of the photoperiodic flower induction pathway and is associated with the functioning of the ABCE model of floral development [97]. Overexpression of *MIR172* causes formation of a phenotype characterized by the absence of perianth, transformation of sepals into pistils and early flowering [97].

Our study showed the presence of at least one member of all these families in flowers (Fig. 2, Additional File 1: Table S7), which indicated that in lupine the families were crucial in generative development, as well. MIR156 and MIR159 are the most numerous families in *Lupinus luteus*, which suggests they play fundamental roles in its flower development processes.

Clusters of miRNAs depending on expression dynamics

The differentially expressed miRNAs identified in yellow lupine flowers were clustered by the dynamics of their expression (Z-scaled expression, to be precise) (Fig. 4). The first of the four clusters comprised miRNAs the accumulation of which increased as the flowers developed. The second cluster grouped all miRNAs the expression of which differed only in connection with the flower's position on the inflorescence. The third cluster comprised miRNAs the expression of which dropped as the flowers developed. The fourth cluster included miRNAs characterized by a heterogeneous trend in expression (Fig. 4).

The first cluster contained miRNAs belonging to the MIR166, MIR167, MIR319, MIR390 and MIR395 families. The first of these families includes Ll-miR177, which guides the cleavage of *RADIALIS*, a transcription factor from the MYB family that controls the asymmetric flower shape [98, 99], as well as Ll-miR258 and Ll-miR265, which probably target the Homeobox-leucine zipper protein ATHB-15. In *Arabidopsis*, both miR165 and miR166 target the same *HD-ZIP III* genes: *ATHB15*, *ATHB8*, *REVOLUTA (REV)*, *PHABULOSA* (*PHB*) and *PHAVOLUTA* (*PHV*) to regulate gynoecium and microspore development [21, 100–103]. An excessive expression of miR165 in the *MERISTEM ENLARGEMENT 1* (*MEN1*) *Arabidopsis* line causes a decrease in the expression of all of the aforementioned *HD-ZIP III* target genes and results in SAM disruption, which may take the form of an enlarged apical meristem, a shortened carpel and female sterility [104]. miR166 has also been shown to control embryonic SAM development in rice and maize [105, 106]. The MIR167 family members that accumulate in larger quantities during flower development are Ll-miR280, Ll-miR281 and Ll-miR285, targeting *ARF6* and *ARF8*. In the thermo-sensitive wheat line, an increased tae-miR167 expression in spikelet tissue generated the phenotype of cold-induced male sterility [107]. Similarly in citrus, nineteen members of the MIR167 family, including the diverse isomiRs, have been identified, whereas most of them displayed a significant up-regulation in the anthers of male sterile mutants [42]. Ll-miR445 and Ll-miR130 are members of the MIR319 family, while their putative target genes are *TCP4* and *MYB33*, respectively. In *Arabidopsis*, the miR319a/TCP4 regulatory module is necessary for petal growth and development. Moreover, the overexpression of *MIR319* reduces male fertility, and this defect is hypothesized to be caused by the cross-regulation of *MYB33* and *MYB65* by miR319 and miR159. As the miR319 target site within the *MYB33* and *MYB65* transcripts exhibits a lower match with miRNA than the miR159 target site, the latter is more efficient at regulating these genes and miR319 is their secondary regulator [108]. This regulatory network is even more complex. In *A. thaliana*, cooperation of three miRNAs and their target genes, namely miR159/*MYB*, miR167/*ARF6/ARF8* and miR319/*TCP4*, is a prerequisite for proper sepal, petal and anther development and maturation. miR159 and miR319 influence the expression of *MIR167* genes, which in turn affect each other. These miRNAs orchestrate plant development by regulating the activity of the phytohormones GA, JA and auxin [109]. An increased accumulation of miR167 and miR319 in the late stages of yellow lupine flower development could also be associated with regulating the growth and development of petals and anthers, as anthers in stage 3 of their development are already mature and split. Another miRNA showing a similar expression profile is Ll-miR9/miR390-5p. It targets the *TAS3* transcript, which in turn is a source of tasiR-ARF, a negative regulator of *ARF2*, *ARF3* and *ARF4* activity. This regulatory cascade plays a vivid role in plant development [110, 111]. The expression level of miR390 derived from *MIR390b* reflects auxin concentration in organs, while the repression of *ARF2*, *ARF3* and *ARF4* by tasiR-ARF is important for lateral organ development, including roots and leaves [11, 112–114], and flower formation [115]. Down-regulation of

ARF2 using RNA interference (dsRNAi) in *Arabidopsis* leads to delayed flowering, rosette leaf senescence, flower abscission and the opening of siliques [116].

Ll-miR118 and Ll-miR119, which target ATP sulfurylase 1, belong to the MIR395 family. In *Arabidopsis*, miR395 targets two gene families, ATP sulfurylases (*ATPS*) and sulfate transporter 2;1 (*SULTR2;1*), which are elements of the sulfate metabolism pathway [117]. ATPS regulates glutathione (GSH) synthesis and is an essential enzyme in the sulfur-assimilatory pathway [118, 119]. In cotton, the miR395-APS1 module is engaged in drought and salt stress response [120]. In *B. juncea* [63], miR395 presumably down-regulates *APS1* to cause an increase in *GSH* expression and suppress the oxidative stress. Sulfate is the main source of sulfur and is taken up by roots, transported throughout the plant and used for assimilation. Sulfate limitation forces a significant up-regulation of miR395 expression [121]. Consequently, during yellow lupine flower development the demand for sulfur probably increases, and the plant activates mechanisms for its efficient uptake.

Within the third cluster of miRNAs, the expression of which decreased as the flowers developed, there were homologues of miR390-3p, miR858, miR396-3p, miR168, miR408-3p and miR398 (Fig. 4). Ll-miR99, Ll-miR100 and Ll-miR102 are identical to miR390-3p (the so-called passenger strand, former star strand) and, probably similarly to miR390-5p, are able to guide *TAS3* cleavage. However, their expression showed an opposite trend to that of miR390-5p. A target gene of Ll-miR115/miR858 is *MYB5*, engaged in regulating seed coat development and trichome branching [122], although in *Arabidopsis* miR858 modulates another set of *MYB* genes, which are flavonoid-specific and control pathogen defense [123]. Another miRNA from the third cluster is Ll-miR155/miR396-3p (passenger strand), which guides cleavage of JMJ25 demetyhylase mRNA (confirmed in degradomes), involved in preserving the active chromatin state [124]. *ECERIFERUM1* (*CER1*), the target gene for another two homologues of miR396-3p, Ll-miR199 and Ll-miR200, is a homologue encoding an enzyme involved in alkane biosynthesis, and in cucumber is engaged both in wax synthesis and ensuring pollen viability [125]. This cluster also included a miRNA that negatively regulates elements involved in miRNA and ta-siRNA functioning, namely Ll-miR247/miR168 targeting *AGO1* mRNA [126]. Another miRNA clustered here was the highly conserved Ll-miR60/miR408-3p, which guides the processing of the mRNA of the copper-binding Basic Blue protein homologue (plantacyanin, PC). In *Arabidopsis*, PC plays a role in fertility, exhibiting the highest expression in the inflorescence, especially in the transmitting tract. Transgenic *A. thaliana* plants overexpressing the gene encoding this protein suffered from severely reduced fertility due to the lack of anther dehiscence and an improper twisted path of wild-type pollen germination [127]. What is puzzling is that in yellow lupine the expression of miR408 was high in stage 1 lower flowers and stage 2 lower and upper flowers, where both the anthers and the transmitting tract were immature, only to decrease in the subsequent stages. It is possible that in lupine PC is suppressed in an alternative way, or miR408 expression actually rises in the anthers and the pistil, although in a very local manner, and this trend is unnoticeable due to the high background from other tissues where the expression profile of this miRNA may be opposite. Especially so, since it has been shown that miR408 plays a role in other *Arabidopsis* organs, as well. Transgenic *Arabidopsis* plants overexpressing *MIR408* displayed altered morphology, including significantly enlarged organs, resulting in enhanced biomass and seed yield. Plant enlargement was shown to be primarily

caused by cell expansion rather than cell proliferation, and in transgenic plants it was correlated with stronger accumulation of the myosin-encoding transcript and gibberellic acid (GA). In addition, this plant line exhibited a higher concentration of copper in chloroplasts and an increased level of plastocyanin (PC) expression, resulting in a significantly higher photosynthetic rate [128].

miRNAs specific for particular developmental stage

Among the miRNAs identified in yellow lupine we spotted several that seemed to be crucial in particular stages of the plant's development (Table 4, Additional File 1: Table S9). For example, the largest quantities of miR159 (Ll-miR452 and Ll-miR454) were accumulated in stages 2 and 3 of the plant's development. They targeted Gamma-glutamyl peptidase 5 of an undefined function in plants, and an evolutionarily conserved target for *GAMYB*, respectively. As already mentioned, this could be associated with miRNA family cooperating with miR167 and miR319 in regulating *L. luteus* anther maturation early on in flower development. The accumulation of homologues of miR5168, miR1861, miR369-5p and miR5794 increased in stage 2 upper and lower flowers, while – interestingly – in the later stages these miRNAs were only present in lower flowers. According to degradome analysis, Ll-miR251/miR5168 guides cleavage of the mRNAs of the genes encoding the Homeobox-leucine zipper protein ATHB-14 and the chaperone protein dnaJ 13. The miR5168 sequence displays a great similarity to that of miR166, thanks to which they may perhaps share the same target gene *ATHB-14*, the putative transcription factor engaged in the adaxial-abaxial polarity determination in the ovule primordium [129]. As confirmed by yellow lupine degradome sequencing, Ll-miR229/miR396-5p targets *Growth-regulating factor 5* (*GRF5*) and *GRF4* transcripts. In *Arabidopsis*, miR396 plays an essential role in leaf growth by down-regulating *GRF*, which in turn interacts with *GRF-interacting factor 1* (*GIF1*) to take part in cell proliferation [130]. In this plant, *GRF5* is expressed in anthers at early stages of flower development and in gynoecia throughout the whole flower development, and transcripts of *GRF4* accumulate later in sepals, tapetum, and endocarpic tissues of ovary valves [131]. Additionally, miR396 impacts the carpel number by targeting *GRF6* [132]. Transgenic rice with OsmiR396 overexpression and *GRF6* knock-down suffers from open husks and sterile seeds [133]. *GRF6* cooperates with *GRF10* to transactivate the *JMJC* gene *706* (*OsJMJ706*) and *CRINKLY4 RECEPTOR-LIKE KINASE* (*OsCR4*) responding to GA, which is a prerequisite for the flower to successfully develop into a normal seed [133]. The presence of these miRNAs in yellow lupine flowers suggests that they regulate cell proliferation mainly in the pistil and the developing ovules. An increased share of miRNAs involved in cell division, namely miR396, miR319 and miR164, in NGS analyses was also observed in early grain development in wheat [69].

Involvement of New miRNAs in *L. luteus* Flower Development

Using ShortStack [52] software we predicted 28 candidates for new miRNAs (Table 3). Fifteen of them were new members of known families, for example MIR167 (Ll-miRn12 and Ll-miRn27), MIR172 (Ll-miR4), MIR393 (Ll-miR19) or MIR169 (Ll-miRn3, Ll-miRn11 and Ll-miRn15) (Additional File 1: Table S8). The other 13 had no homologues among known miRNAs and were recognized as lupine-specific miRNAs.

Some of the new miRNAs displayed differential expression during *L. luteus* flower development. Ll-miRn3, which shows similarity to pre-miR169, displayed differential expression in UF1 vs LF1 and LF2 vs LF1 library comparisons, wherein it is the most accumulated in LF1, and in flower pedicels (up-regulated in FPNAB). According to degradome data, this miRNA targets *SCARECROW2* (*SCR2*) homologue, a putative activator of the calcium-dependent activation of *RBOHF* that enhances reactive oxygen species (ROS) production and may be involved in cold stress response [134]. In rice roots, the SCARECROW genes play a role in cellular asymmetric division [135]. In this plant, *SCR2* expression is relatively high in flower buds and flowers, and after flowering rises in the leaves and roots [136]. In yellow lupine, this gene may be involved in intense cell divisions during early flower development and is down-regulated in the pedicels with an active AZ to stop its growth. Another frequently encountered DEM, Ll-miRn10, shows differential expression in LF2 vs LF1 and UF2 vs UF1 comparisons, being up-regulated in stage 1 flowers. Its target gene is *CIPK6* that is engaged in calcium-dependent CBL kinase activation, which in turn regulates potassium channel activity [137]. Ll-miRn22, which shows sequence similarity to pre-miR1507, is up-regulated in LF3 vs LF2 and LF2 vs LF1 library comparisons, and its expression escalates with flower development in the bottom whorl. The MiR1507 family is annotated as legume-specific [138]. Through analyses of our degradomic data we did not find its target gene, and the psRNATarget hit was the putative disease resistance RPP13-like protein 1. Unfortunately, this protein has been poorly described, therefore it is difficult to determine its function in yellow lupine flowers.

Noteworthily, the target genes of Ll-miRn1 and Ll-miRn30 identified through degradome sequencing are *SGS3* and *DCL2*, respectively, and the miRNAs are up-regulated in LF3 vs LF2 comparisons and down-regulated in UF1 vs LF1 comparisons, respectively. *SGS3*- and *DCL2*-encoded proteins are involved in sRNA biogenesis [139, 140]. Importantly, novel miRNA identified in soybean Soy_25 displays a high sequence similarity to Ll-miRn1 and also targets SGS3, which indicates that this regulatory feedback loop for sRNA biogenesis is common for *Fabaceae* [141]. These results indicate that *L. luteus* miRNAs play a regulatory role in siRNA biogenesis in early flower development.

miRNA Accumulation Varies in Lower and Upper Flowers in Different Stages of Development

One of our goals was to identify the sRNAs engaged in yellow lupine flower development, with a particular emphasis on the differences between flowers from lower and upper parts of the inflorescence, in order to gain an insight into how early the flower fate is determined.

In our study we spotted differences in miRNA accumulation patterns as early as the first stage of flower development. Lower flowers in this developmental stage exhibited higher expression of miR396-3p, miR393-3p, miR858, miR390-3p, miR167-5p, and miR319. From the second stage until the end of their development, upper flowers accumulated more miR319, miR394, miR160, and miR393 (Fig. 4, Table 5). The elevated expression levels of these miRNAs suggests a reduction in the abundance of the transcripts of their target genes encoding auxin receptors and auxin response factors. This in turn may have led to a reduction in auxin sensitivity, and through decreasing the number of transcription factors belonging to the TCP family, probably caused different cell proliferation profiles in comparisons of flowers collected from the upper and lower whorls.

miR393 participates in regulating several developmental processes in the leaves [142], and contributes to root architecture development [143], pathogen defense [144–146] and plant response to nitrogen limitation or changes in salinity [13, 143, 147, 148]. miR393 regulates the accumulation of transcripts encoding auxin receptors belonging to the TAAR family, which, in the presence of auxin, guide proteasomal degradation of AUX/IAA repressors, thus enabling transcriptional regulation by ARF. Changes in receptor abundance affect the sensitivity of the given tissue to auxin and this is how this molecule influences plant development [149].

In *A. thaliana*, miR160 directly controls three *ARF* genes, namely: *ARF10, ARF16* and *ARF17* [150]. It is involved in many processes in plants, e.g. flower identity specification, leaf development or fruit formation [150, 151]. In tomato, sly-miR160 is abundant in ovaries, and changes in its expression affect plant fertility [152]. Down-regulation of sly-miR160 by introducing a target mimic caused improper ovary patterning and thinning of the placenta already prior to anthesis. Changes in gynoecium shape were followed by changes in fruit morphology [152]. Moreover, the ectopic expression of *SlARF10A* caused by a mutation in the target site for miR160 (mSlARF10A) resulted in a similar phenotype, with an additional strictly limited number of seeds that failed to germinate [153]. In view of these facts, the higher expression of miR160 in lupine lower flowers early on in their development means that a slightly different organization of the gynoecia may be one of the crucial determinants of flower fate.

Flowers collected from the lower whorls displayed higher accumulations of miR5490, miR5794, miR1861, miR396-5p, miR395, miR166, and miR159-3p (Table 5). miR1861 and miR396 were recognized as positive cell proliferation and development regulators [154–156]. In rice, for example, miR1861 exhibited differential expression during grain filling [157], and its expression was higher in superior grains in comparison to inferior ones [154]. This is consistent with our results, and a higher occurrence of miR1861 and miR396 in lower flowers may be an indication of the plant investing more supplies in this part of the inflorescence.

sRNAs are Involved in Flower Abscission in *L. luteus*

Little is known about sRNA engagement in flower abscission. Research into the involvement of miRNAs in this process has been already carried out in cotton [158], tomato [152, 159], and sugarcane [160]. Our investigation provided a more comprehensive view of this process and allowed us to explore cues for abscission present long before AZ formation.

For a genome-wide investigation of miRNAs involved in the formation of the abscission layer in cotton, two sRNA libraries were constructed using the abscission zones (AZ) of cotton pedicels treated with ethephon or water. Among the 460 identified miRNAs, only gra-MIR530b and seven novel showed differential expression in abscission tissues [158], and these miRNAs have no homologues in our dataset.

In tomato, sly–miR160 regulates three auxin-mediated developmental processes, namely ovary patterning, floral organ abscission and lateral organ lamina outgrowth [152]. Down-regulation of sly-miR160 and the resulting higher expression of its target genes, transcriptional repressors of auxin response *ARF10* and *ARF17*, also resulted in the narrowing of leaves, sepals and petals and an impeded shedding of the perianth after successful pollination [152]. This was consistent with the higher accumulation of miR160 in

upper flowers designated to fall off. As this miRNA showed no differential expression in flower pedicels, it probably does not play a role in the executory module of abscission itself, but is rather part of a mechanism that determines flower fate.

Another research on tomato using sRNA and degradome sequencing libraries explored the roles of sRNAs in AZ formation in early and late stages of the process, additionally accelerated or not by ethylene or control treatment [161]. The study showed that in tomato pedicels, when compared to the early stages of abscission, in comparison to the early stage the accumulation levels of, *inter alia*, miR156, miR166, miR167, miR169, miR171 and miR172 rose in late stages of abscission, while the abundance of miR160, miR396 and miR477 dropped [161]. Although it is difficult to compare ethylene-treated tomato pedicel results to our data, it is worth noting that in the corresponding FPAB vs. FPNAB comparison in our study, the accumulation of miR396 was lower, and the levels of miR167 and miR166 were higher, as well (Table 6).

It has been proven for sugarcane that miR156, miR319-3p, miR396 and miR408 take part in leaf abscission [160]. In their study, both mature (5p) and passenger (3p) miRNAs from MIR167 family were up-regulated in leaf abscission sugarcane plants (LASP), comparing to leaf packaging sugarcane plants (LPSP) (which corresponds to the FPAB vs. FPNAB comparison in our study). A total of four pairs of mature and passenger miRNAs were differentially expressed in this comparison, and they were members of the MIR156, MIR167 and MIR393 families [160]. Apart from the above-mentioned sugarcane miRNAs, miR396, miR395 and miR171 were up-regulated in this library comparison, as well. Four miRNAs, namely miR164, 166, 159, 319-3, showed an opposite trend [160]. In our study, both mature and passenger members of the MIR167 family were leaders among DEMs, too, (Table 6) pointing to their crucial role in both vegetative and generative organ abscission. Significantly, this applies to evolutionarily distant taxa: both monocots and dicots.

The situation is different for miR396. In contrast to sugarcane, passenger miR396-3p in yellow lupine is mainly accumulated in the pedicels with an inactive AZ (Table 6). It is also abundant in flowers from the lower whorls (Table 5), which suggests that in yellow lupine miR396-3p and miR396-5p (present in LF3) are engaged in maintaining flowers on the plant. This is probably related to the fact that this miRNA* may have different target genes in different organisms due to the higher rates of change characteristic of passenger miRNAs [162]. Thus, it is possible that in *L. luteus* miR396-3p targets other genes than it does in sugarcane.

Possible miRNA-dependent Regulatory Pathways that Participate in Both Development and Abscission in Yellow Lupine Flowers

Auxin-related sRNAs Involved in Regulating Flower Development and Abscission

Recent studies have shown that sRNA activity is associated with hormonal regulation of plant development through influencing the spatio-temporal localization of the hormone response pathway [163].

The auxin signal transduction pathway mainly consists of the three elements discussed below. Auxin is perceived by members of the TAAR family, namely TIR1 and its homologues AUXIN SIGNALING F-BOX PROTEIN (AFB), F-box proteins comprised in the SCF complex (SKP1-Cullin -F-box-RBX1). Downstream these receptors there are AUX/IAA repressor proteins and ARF transcription factors [151, 164, 165]. The expression of TAAR receptors is regulated by miR393 and secondary ta-siRNA derived from their own transcripts [13]. miR167 and miR160, by affecting the *ARF6*, *ARF8* [88] and *ARF10*, *ARF16, ARF17* [166] transcript accumulation, respectively, are able to modulate the expression of *GH3-like* [167] and, by this, influence auxin-regulated plant development. It has been proven that the expression of *ARF2*, together with *ARF3* and *ARF4*, is regulated by the ta-siRNA/miR390 module [168]. In the two-hit model, ta-siRNA-containing the *TAS* transcript is recognized by two miR390 molecules, one of which guides its cleavage, and the other, in a complex with AGO7, serves as a primer for complementary strand synthesis, with its subsequent processing ultimately resulting in ARF-targeting siRNA biogenesis [169].

In our study, among the differentially expressed sRNAa in flowers and flower pedicels, there were members of the MIR167, MIR160, MIR393 and MIR390 families, as well as phased siRNAs targeting *ARF2*, *ARF3*, and *ARF4*. This fact suggests a vivid role of auxin-related sRNAs in flower development and abscission in *L. luteus* and confirms our previously published results of transcriptome-wide analyses [10], where we observed differences in expression levels of genes encoding several elements of the auxin signal transduction pathway.

When comparing organs to be abscised with those to be maintained, Ll-miR281 belonging to the MIR167 family was down-regulated in the UF1 vs LF1 comparison, but in the FPAB vs FPNAB comparison this miRNA, together with Ll-miR276, Ll-miR280, and Ll-miR39, was up-regulated. During flower development, the accumulation of Ll-miR285 changed as the flower at the top of the inflorescence entered stage 2 (UF2 vs. UF1) and, subsequently, the expression of Ll-miR280 and Ll-miR281 shifted as it entered stage 4 (UF4 vs. UF3). The relatively high number of members of the MIR167 family showing differential expression in the studied variants indicates that miR167 is one of the key regulators of flower development and abscission in yellow lupine.

Ll-miR224, a member of the MIR393 family, which guides cleavage of *TIR1* mRNA , was identified as differential and unique for the upper part of lupine inflorescence, which makes it a molecular marker of flowers fated to fall off.

Three members of the MIR160 family displayed differential expression, namely Ll-miR332 and Ll-miR329 in UF2 vs LF2, and Ll-miR332 and Ll-miR333 in UF3 vs LF3, all being up-regulated. As already mentioned, these miRNAs may promote flower abscission.

Strikingly, our sRNA-seq analyses showed differential expression of three miRNAs identical with miR390-3p deposited in miRbase for other plant species. These miRNAs (Ll-miR99, Ll-miR100 and Ll-miR102) were down-regulated in all of the following comparisons: between upper vs lower flowers (UF1 vs LF1, UF4 vs LF4), between pedicels (FPAB vs FPNAB), and between flowers in different stages of development (LF2 vs LF1, UF3 vs UF2). There was one exception, namely that of Ll-miR9, which was identical to, *inter alia*, aly-

miR390a-5p or ath-miR390a-5p (miRBase), which was up-regulated in the LF3 vs LF2 and UF4 vs UF3 comparisons. The differential expression and functioning of passenger miRNAs has already been described. The research carried out by Xie and Zhang 2015 on cotton showed that the formation of some miRNA*s, such as miR172* and miR390*, was associated with the phases of the plant's growth. These miRNA*s were up-regulated in seedlings, but down-regulated in other growth stages [170]. Therefore, miRNA*s can be specifically expressed in various tissues to maintain the steady state of the organism. Our degradome analysis showed for yellow lupine that Ll-miR9/miR390-5p was able to guide the cleavage of the *TAS3* transcript. There is no certainty as to the status of its passenger strand, and further research is required in order to identify its accumulation and function in the organs concerned.

ARF2, *ARF3* and *ARF4* are possibly down-regulated in the processing that is guided by Ll-siR249 and Ll-siR308, which were shown to be differential in the LF2 vs LF1 and UF2 vs UF1 comparisons (Table 4), and which are identical to tasiR-ARFs in many plant species according to the tasiRNAdb database [171] (data not shown). These tasi-ARFs probably originate from *TAS3* transcript (TRINITY_DN55534_c4_g1) containing two binding sites for miR390 (data not shown). Ll-miR9/miR390, differentially expressed in LF3 vs LF2 and UF4 vs UF3, and, surprisingly, also Ll-siR240, guide cleavage of another *TAS3* mRNA (TRINITY_DN54998_c6_g5_i2) (Figure S8) which contains only one target site for miR390 (data not shown). This is the first report on *TAS3* processing regulated by siRNA. The target site for Ll-siR240 is shifted by 10 nucleotides relative to the target site for Ll-miR9/miR390 (Additional File 2: Figure S8). The expression of Ll-siR249, Ll-siR308 and Ll-miR9 showed a similar profile, as it rose during flower development and was the highest in the pedicels (Fig. 7). Ll-siR240 accumulated proportionally to *TAS3*, which means that it was least expressed in the pedicels, while in flowers its expression increased with time (Additional File 2: Table S21). The identified target transcripts belonging to the *ARF2*, *ARF3* and *ARF4* families showed organ-specific differential expression, which indicated their strongly local regulation by siRNA (Additional File 2: Table S21). The presence of all the elements of the miR390/TAS3/tasiR-ARF module among the DE sRNAs in yellow lupine suggests that alterations in its functioning have a great impact on *L. luteus* flower development. The additional element in the form of siRNA that processes *TAS3* mRNA seems to be a new species-specific adjuster of this regulation module.

Function of the Potential miRNA Targets

Our functional analysis of the putative targets identified for miRNAs in lupine indicated their engagement in regulating a number of metabolic – especially 'carbohydrate metabolism' and 'nucleotide metabolism' – pathways (Additional File 5: Figure S4). 'Carbohydrate metabolism' was also one of the most enriched KEGG pathways in our previous *Lupinus luteus* transcriptome analysis [10], and its activation may be an indication of the rebuilding of cell walls or changes in nutrient supply. The next most numerous group of miRNA targets was categorized into the 'Genetic information processing' KEGG pathways, namely, 'spliceosome', 'RNA transport' and 'ubiquitin proteolysis'. This suggests that in yellow lupine flowers most miRNAs regulate processes related to post-transcriptional events and protein degradation. Three KEGG categories within the 'Environmental information processing' category are extremely important in terms of plant development, and they are 'Signal transduction pathways' comprising the MAPK cascade, 'phosphatidylinositol' and 'plant hormone' signaling pathways (Fig. 9, Additional File 6: S5, Additional File

7: S6, Additional File 8: S7). The MAPK pathway is involved in regulating several processes, such as biotic and abiotic stress response (reviewed in [172, 173]), and associated with the functioning of hormones such as ethylene [174] and abscisic acid, engaged in organ abscission and other processes (reviewed in [175, 176]). The MAPK cascade is also an element of the positive feedback loop amplifying the abscission signal [177]. Auxin is not the only hormone whose signal transduction pathway is regulated by sRNAs in yellow lupine. Our KEGG enrichment analyses of the identified target genes for lupine miRNAs indicated that the signal transduction pathways of gibberellin, cytokinin, the already mentioned ethylene and ABA were potentially modulated by miRNAs in yellow lupine, as well (Fig. 9). These data show how important sRNAs are for growth and development regulation.

We also conducted a GO enrichment analysis (Fig. 8, Additional File 2: Table S13). Within the 'Cellular component', 83.3 % of the target genes were categorized as 'cell', with only 4.7 % categorized as 'extracellular region' and 3.9 % as 'cell junction'. This means that miRNAs impacted processes mainly occurring within the cell. As for the 'Molecular function', most of the targets fell into the 'binding' (67.5 %) and 'catalytic activity' (52.2 %) categories. Thus, in yellow lupine flowers, miRNAs were found to most frequently influence molecular interactions and biochemical reaction rates. Within the 'Biological Process' group, most of the targets were categorized as 'cellular' (72.1 %) and 'metabolic process' (63.6 %). What is most interesting is that quite a considerable number of the target genes fell within the 'response to stimulus' and 'signaling' categories, which means that miRNAs modulated the way the plant adapted to environmental stimuli. Surprisingly few genes were categorized into the 'growth' and 'cell proliferation' categories, which indicated that these processes were probably regulated by other factors.

An in-depth analysis of KEGG and GO terms concerning plant hormones (Fig. 8b) showed that most of the miRNAs identified in yellow lupine modulated more than one hormone signaling pathway. For example, in a GO analysis performed exclusively for the targets exhibiting the 'Flower development' term (Fig. 8c), Ll-miR181 belonging to the MIR166 family modulated processes associated with four hormones, namely auxin, gibberellin, jasmonic acid and salicylic acid, by targeting not only transcription factor *AS1*, a central cell division regulator [178], but also Cullin-3A, an element of the ubiquitination complex [179]. Another two members of this family, Ll-miR173 and Ll-miR177, targeted the same gene, 26S proteasome non-ATPase regulatory subunit 8 homolog A (*RPN12A*), involved in the ATP-dependent degradation of ubiquitinated proteins during auxin and cytokinin response [180]. Similarly, a KEGG analysis for the MIR166 family showed that it was involved in the auxin, cytokinin, and brassinosteroid signal transduction pathways (Fig. 9).

Our GO analysis additionally showed for yellow lupine flowers that miRNAs were responsible for guiding the processing of target genes simultaneously involved in multiple processes associated with flower development (Fig. 8c). For example, *AP2* is involved in the specification of floral organ identit [181], and ovule [182] and seed development [183, 184], and in our study it was targeted by ten lupine miRNAs: 8 belonging to the MIR172 family (Ll-miR25, Ll-miR26, Ll-miR27, Ll-miR28, Ll-miR29, Ll-miR30, Ll-miR140, Ll-miR171), one to the MIR166 family (Ll-miR249), and Ll-miR24. On the other hand, seven of these miRNAs additionally targeted a negative flower development regulator, chromodomain-containing protein (*LHP1*), which is a structural component of heterochromatin involved in repressing floral homeotic genes and *FLT*

that regulates flowering time [185, 186]. This highly degenerated and ambiguous model of gene regulation by lupine miRNAs shows that in this plant the adjustment of key biological processes related to fertility is dependent on a complex network of interconnected factors.

Conclusions

In this paper we show our results of next generation sequencing of sRNA, transcriptome and degradome libraries, which allowed us to identify miRNAs, siRNAs and their target genes probably involved in regulating yellow lupine flower development and abscission. These miRNAs and siRNAs, by controlling the expression of their target genes, affect signal transduction pathways of hormones, mainly auxins, and may thus have an impact on the development and fate of flowers growing in particular parts of the inflorescence (Fig. 10). In addition to the purely cognitive aspects of describing the evolutionary conservation and the species specificity of important mechanisms regulating plant development, this work may contribute to the optimization of field crops and to monitoring the impact of various factors on flowering in yellow lupine.

The use of the NGS technique allows for a detailed analysis of the regulatory networks which include sRNAs and their target genes. However, the results of sRNA-seq also contain is a large amount of uncharacterized sRNAs, the function of which may also be significant for the studied processes. More experimental and bioinformatic research is needed to fully describe the complex mechanisms of plant development regulation by low-molecular-weight regulatory RNAs.

Abbreviations

ACA4: Calcium-transporting ATPase 4

AGO: ARGONAUTE

AP: APETALA

APS1: Acid phosphatase 1

ARF: AUXIN RESPONSE FACTOR

ARPN: Basic blue protein

ATHB: Homeobox-leucine zipper protein

ATPS1: ATP sulfurylase 1, chloroplastic

AUX: Auxin

AZ: abscission zone

CER: ECERIFERUM

CIPK6: CBL-interacting serine/threonine-protein kinase 6

DCL: Dicer-like

DE: Differentially expressed

EPSIN2: Clathrin interactor EPSIN 2

ET: Ethylene

FBX6: F-box only protein 6

FPAB: flower pedicel abscissed

FPKM: Fragments per kilobase of transcript per million mapped reads

FPNAB: flower pedicel non abscissed

FUL: FRUITFULL

GA: Gibberellin acid

GGP5: Gamma-glutamyl peptidase 5

GO: Gene ontology

GRF: GROWTH-REGULATING FACTOR

JA: Jasmonic acid

JMJ25: Lysine-specific demethylase JMJ25

KEGG: Kyoto encyclopedia of genes and genomes

LF: lower flower

LFY: LEAFY

MAPK: MITOGEN-ACTIVATED PROTEIN KINASE

MDN-like: Midasin-like

miRNAs: microRNAs

MPE: MPE-cyclase

MYB: MYB DOMAIN PROTEIN

ncRNA: non conding RNA

NFYA9: Nuclear transcription factor Y subunit A-9

NGS: Next generation sequencing

NRX1: Probable nucleoredoxin 1

OFP14: Transcription repressor OFP14

PC: Plastocyanin

RISC: RNA-induced silencing complex

RPM: Reads per million

RPP13-like 1: Putative disease resistance RPP13-like protein 1

RPT1: 26S proteasome regulatory subunit 7

SCR: SCARECROW

SGS: SUPPRESSOR OF GENE SILENCING

siRNA: Small interfering RNA

SOD: Superoxide dismutase [Cu-Zn]

SPL: SQUAMOSA PROMOTER-BINDING-LIKE PROTEIN

SRC2: SOYBEAN GENE REGULATED BY COLD 2

sRNA: Small RNA

TAAR: TIR1/AFB AUXIN RECEPTOR

TCP: TEOSINTE BRANCHED 1, CYCLOIDEA, PROLIFERATING CELL NUCLEAR ANTIGEN FACTOR

TIR1: TRANSPORT INHIBITOR RESPONSE 1

TOE: TARGET OF EAT

UF: upper flower

VPS62: VACUOLAR PROTEIN SORTING-ASSOCIATED PROTEIN 62

Declarations

Ethics approval and consent to participate

Not applicable. This is to confirm that no specific permits were needed for the described experiments, and this study did not involve any endangered or protected species.

Consent for publication

Not applicable.

Availability of data and material

The data supporting the conclusions of this article are within the paper and its additional files. All sequencing reads are deposited in the National Center for Biotechnology Information under the BioProject number PRJNA419564 with the Sequence Read Archive (SRA) study accession SUB3230840.

Competing interests

The authors declare that they have no competing interests.

Funding

This research was funded by The National Science Centre SONATA grant No. 2015/19/D/NZ9/03601 and by the Program Supported by Resolution of the Council of Ministers (RM-111-222-15) in association with the Institute of Plant Genetics, Polish Academy of Sciences.

Authors' contributions

PG conception and design of the experiment, plant and RNA sample preparation, data analysis, interpretation of data and wrote the manuscript; WW, MK, WG plant and RNA sample preparation; WG and MK data analysis and manuscript preparation, JK NGS data analysis.

ACKNOWLEDGEMENTS

We would like to thank Michal Szczesniak and coworkers from Ideas4biology Sp. z o. o. for performing the RNA sequencing data analysis and consulting.

References

1. Prusiński J. Degree of success of legume cultivars registered by the center for cultivar testing over the period of market economy. Acta Sci Pol. 2007;6:3–16.
2. Lucas MM, Stoddard FL, Annicchiarico P, Frías J, Martínez-Villaluenga C, Sussmann D, et al. The future of lupin as a protein crop in Europe. Front Plant Sci. 2015;6:705. doi:10.3389/fpls.2015.00705.
3. Ogura T, Ogihara J, Sunairi M, Takeishi H, Aizawa T, Olivos-Trujillo MR, et al. Proteomic characterization of seeds from yellow lupin (*Lupinus luteus* L.). Proteomics. 2014;14:1543–6. doi:10.1002/pmic.201300511.
4. Van Steveninck RF. Abscission-accelerators in lupins (*Lupinus luteus* L.). Nature. 1959;183:1246–8.

5. Ascough GD, Nogemane N, Mtshali NP, van Staden J, Bornman CH. Flower abscission: environmental control, internal regulation and physiological responses of plants. South African J Bot. 2005;71:287–301. doi:10.1016/S0254-6299(15)30101-0
6. Estornell LH, Agustí J, Merelo P, Talón M, Tadeo FR. Elucidating mechanisms underlying organ abscission. Plant Sci. 2013;199–200:48–60. doi:10.1016/j.plantsci.2012.10.008.
7. Basu MM, González-Carranza ZH, Azam-Ali S, Tang S, Shahid AA, Roberts JA. The manipulation of auxin in the abscission zone cells of *Arabidopsis* flowers reveals that indoleacetic acid signaling is a prerequisite for organ shedding. Plant Physiol. 2013;162:96–106. doi:10.1104/pp.113.216234.
8. Patterson SE, Bleecker AB. Ethylene-dependent and -independent processes associated with floral organ abscission in *Arabidopsis*. Plant Physiol. 2004;134:194–203. doi:10.1104/pp.103.028027.
9. Ma C, Meir S, Xiao L, Tong J, Liu Q, Reid MS, et al. A KNOTTED1-LIKE HOMEOBOX protein regulates abscission in tomato by modulating the auxin pathway. Plant Physiol. 2015;167:844–53. doi:10.1104/pp.114.253815.
10. Glazinska P, Wojciechowski W, Kulasek M, Glinkowski W, Marciniak K, Klajn N, et al. *De novo* transcriptome profiling of flowers, flower pedicels and pods of *Lupinus luteus* (yellow lupine) reveals complex expression changes during organ abscission. Front Plant Sci. 2017;8:641. doi:10.3389/fpls.2017.00641.
11. Marin E, Jouannet V, Herz A, Lokerse AS, Weijers D, Vaucheret H, et al. miR390, *Arabidopsis TAS3* tasiRNAs, and their AUXIN RESPONSE FACTOR targets define an autoregulatory network quantitatively regulating lateral root growth. Plant Cell. 2010;22:1104–17. doi:10.1105/tpc.109.072553.
12. Williams L, Carles CC, Osmont KS, Fletcher JC. A database analysis method identifies an endogenous trans-acting short-interfering RNA that targets the *Arabidopsis ARF2*, *ARF3*, and *ARF4* genes. Proc Natl Acad Sci. 2005;102:9703–8. doi:10.1073/pnas.0504029102.
13. Si-Ammour A, Windels D, Arn-Bouldoires E, Kutter C, Ailhas J, Meins F, et al. miR393 and secondary siRNAs regulate expression of the TIR1/AFB2 auxin receptor clade and auxin-related development of *Arabidopsis* leaves. Plant Physiol. 2011;157:683–91. doi:10.1104/pp.111.180083.
14. D'Ario M, Griffiths-Jones S, Kim M. Small RNAs: Big Impact on Plant Development. Trends Plant Sci. 2017;22:1056–68. doi:10.1016/J.TPLANTS.2017.09.009.
15. Liu H, Yu H, Tang G, Huang T. Small but powerful: function of microRNAs in plant development. Plant Cell Rep. 2018;37:515–28. doi:10.1007/s00299-017-2246-5.
16. Bhogale S, Mahajan AS, Natarajan B, Rajabhoj M, Thulasiram H V, Banerjee AK. MicroRNA156: a potential graft-transmissible microRNA that modulates plant architecture and tuberization in *Solanum tuberosum* ssp. andigena. Plant Physiol. 2014;164:1011–27. doi:10.1104/pp.113.230714.
17. Sun X, Fan G, Su L, Wang W, Liang Z, Li S, et al. Identification of cold-inducible microRNAs in grapevine. Front Plant Sci. 2015;6:595. doi:10.3389/fpls.2015.00595.
18. Koroban NV, Kudryavtseva AV, Krasnov GS, Sadritdinova AF, Fedorova MS, Snezhkina AV, et al. The role of microRNA in abiotic stress response in plants. Mol Biol. 2016;50:337–43. doi:10.1134/S0026893316020102.

19. Jin D, Wang Y, Zhao Y, Chen M. MicroRNAs and their cross-talks in plant development. J Genet Genomics. 2013;40:161–70. doi:10.1016/j.jgg.2013.02.003.
20. Kurihara Y, Watanabe Y. *Arabidopsis* micro-RNA biogenesis through Dicer-like 1 protein functions. Proc Natl Acad Sci. 2004;101:12753–8. doi:10.1073/pnas.0403115101.
21. Reinhart BJ, Weinstein EG, Rhoades MW, Bartel B, Bartel DP. MicroRNAs in plants. Genes Dev. 2002;16:1616–26. doi:10.1101/gad.1004402.
22. Voinnet O. Origin, Biogenesis, and activity of plant microRNAs. Cell. 2009;136:669–87. doi:10.1016/j.cell.2009.01.046.
23. Yu Y, Jia T, Chen X. The “how” and “where” of plant microRNAs. New Phytol. 2017;216:1002–17. doi:10.1111/nph.14834.
24. Teotia S, Tang G. To bloom or not to bloom: role of microRNAs in plant flowering. Mol Plant. 2015;8:359–77. doi:10.1016/J.MOLP.2014.12.018.
25. Yang T, Wang Y, Teotia S, Zhang Z, Tang G. The making of leaves: how small RNA networks modulate leaf development. Front Plant Sci. 2018;9:824. doi:10.3389/fpls.2018.00824.
26. Luo Y, Guo Z, Li L. Evolutionary conservation of microRNA regulatory programs in plant flower development. Dev Biol. 2013;380:133–44. doi:10.1016/J.YDBIO.2013.05.009.
27. Vazquez F, Hohn T. Biogenesis and biological activity of secondary siRNAs in plants. Scientifica (Cairo). 2013;2013:783253. doi:10.1155/2013/783253.
28. Singh A, Gautam V, Singh S, Sarkar Das S, Verma S, Mishra V, et al. Plant small RNAs: advancement in the understanding of biogenesis and role in plant development. Planta. 2018;248:545–58. doi:10.1007/s00425-018-2927-5.
29. Deng P, Muhammad S, Cao M, Wu L. Biogenesis and regulatory hierarchy of phased small interfering RNAs in plants. Plant Biotechnol J. 2018;16:965–75. doi:10.1111/pbi.12882.
30. Lee CH, Carroll BJ. Evolution and diversification of small RNA pathways in flowering plants. Plant Cell Physiol. 2018;59:2169–87. doi:10.1093/pcp/pcy167.
31. Sun Y, Mui Z, Liu X, Yim AK-Y, Qin H, Wong F-L, et al. Comparison of small RNA profiles of *Glycine max* and *Glycine soja* at early developmental stages. Int J Mol Sci. 2016;17. doi:10.3390/ijms17122043.
32. Zhou ZS, Huang SQ, Yang ZM. Bioinformatic identification and expression analysis of new microRNAs from *Medicago truncatula*. Biochem Biophys Res Commun. 2008;374:538–42. doi:10.1016/J.BBRC.2008.07.083.
33. Pokoo R, Ren S, Wang Q, Motes CM, Hernandez TD, Ahmadi S, et al. Genotype- and tissue-specific miRNA profiles and their targets in three alfalfa (*Medicago sativa* L) genotypes. BMC Genomics. 2018;19:913. doi:10.1186/s12864-018-5280-y.
34. Fletcher SJ, Shrestha A, Peters JR, Carroll BJ, Srinivasan R, Pappu HR, et al. The tomato spotted wilt virus genome is processed differentially in its plant host *Arachis hypogaea* and its thrips vector *Frankliniella fusca*. Front Plant Sci. 2016;7:1349. doi:10.3389/fpls.2016.01349.
35. Tsikou D, Yan Z, Holt DB, Abel NB, Reid DE, Madsen LH, et al. Systemic control of legume susceptibility to rhizobial infection by a mobile microRNA. Science. 2018;362:233–6. doi:10.1126/science.aat6907.

36. Wu J, Wang L, Wang S. MicroRNAs associated with drought response in the pulse crop common bean (*Phaseolus vulgaris* L.). Gene. 2017;628:78–86. doi:10.1016/j.gene.2017.07.038.
37. Mantri N, Basker N, Ford R, Pang E, Pardeshi V. The Role of micro-ribonucleic acids in legumes with a focus on abiotic stress response. Plant Genome. 2013;6:0. doi:10.3835/plantgenome2013.05.0013.
38. Ghani A, Din M, Baloch IA, Barozai MYK. Identification of microRNAs in 12 plant species of *Fabaceae*. Pure Appl Biol. 2013;2:104–15. doi:10.19045/bspab.2013.23005.
39. Rodriguez-Medina C, Atkins CA, Mann AJ, Jordan ME, Smith PM. Macromolecular composition of phloem exudate from white lupin (*Lupinus albus* L.). BMC Plant Biol. 2011;11:36. doi:10.1186/1471-2229-11-36.
40. Tang C-Y, Yang M-K, Wu F-Y, Zhao H, Pang Y-J, Yang R-W, et al. Identification of miRNAs and their targets in transgenic *Brassica napus* and its acceptor (Westar) by high-throughput sequencing and degradome analysis. RSC Adv. 2015;5:85383–94. doi:10.1039/C5RA14672K.
41. Zhou R, Wang Q, Jiang F, Cao X, Sun M, Liu M, et al. Identification of miRNAs and their targets in wild tomato at moderately and acutely elevated temperatures by high-throughput sequencing and degradome analysis. Sci Rep. 2016;6:33777. doi:10.1038/srep33777.
42. Fang Y-N, Zheng B-B, Wang L, Yang W, Wu X-M, Xu Q, et al. High-throughput sequencing and degradome analysis reveal altered expression of miRNAs and their targets in a male-sterile cybrid pummelo (*Citrus grandis*). BMC Genomics. 2016;17:591. doi:10.1186/S12864-016-2882-0.
43. Kalvari I, Nawrocki EP, Argasinska J, Quinones-Olvera N, Finn RD, Bateman A, et al. Non-coding RNA analysis using the Rfam database. Curr Protoc Bioinforma. 2018;62:e51. doi:10.1002/cpbi.51.
44. Kalvari I, Argasinska J, Quinones-Olvera N, Nawrocki EP, Rivas E, Eddy SR, et al. Rfam 13.0: shifting to a genome-centric resource for non-coding RNA families. Nucleic Acids Res. 2018;46:D335–42. doi:10.1093/nar/gkx1038.
45. Kozomara A, Griffiths-Jones S. miRBase: annotating high confidence microRNAs using deep sequencing data. Nucleic Acids Res. 2014;42:D68–73. doi:10.1093/nar/gkt1181.
46. Kozomara A, Griffiths-Jones S. miRBase: integrating microRNA annotation and deep-sequencing data. Nucleic Acids Res. 2011;39:D152-7. doi:10.1093/nar/gkq1027.
47. Kozomara A, Birgaoanu M, Griffiths-Jones S. miRBase: from microRNA sequences to function. Nucleic Acids Res. 2019;47:D155–62. doi:10.1093/nar/gky1141.
48. Griffiths-Jones S. The microRNA Registry. Nucleic Acids Res. 2004;32:D109-11. doi:10.1093/nar/gkh023.
49. Griffiths-Jones S, Grocock RJ, van Dongen S, Bateman A, Enright AJ. miRBase: microRNA sequences, targets and gene nomenclature. Nucleic Acids Res. 2006;34:D140-4. doi:10.1093/nar/gkj112.
50. Griffiths-Jones S, Saini HK, van Dongen S, Enright AJ. miRBase: tools for microRNA genomics. Nucleic Acids Res. 2008;36:D154-8. doi:10.1093/nar/gkm952.
51. Altschul SF, Gish W, Miller W, Myers EW, Lipman DJ. Basic local alignment search tool. J Mol Biol. 1990;215:403–10. doi:10.1016/S0022-2836(05)80360-2.

52. Axtell MJ. ShortStack: Comprehensive annotation and quantification of small RNA genes. RNA. 2013;19:740–51. doi:10.1261/rna.035279.112.
53. Chen C, Zeng Z, Liu Z, Xia R. Small RNAs, emerging regulators critical for the development of horticultural traits. Hortic Res. 2018;5:63. doi:10.1038/s41438-018-0072-8.
54. Oliveros J. VENNY. An interactive tool for comparing lists with Venn diagrams. BioinfoGP, CNB-CSIC. http://bioinfogp.cnb.csic.es/tools/venny/index.html. Accessed 6 Mar 2019.
55. Lex A, Gehlenborg N, Strobelt H, Vuillemot R, Pfister H. UpSet: Visualization of Intersecting Sets. IEEE Trans Vis Comput Graph. 2014;20:1983–92. doi:10.1109/TVCG.2014.2346248.
56. Addo-Quaye C, Miller W, Axtell MJ. CleaveLand: a pipeline for using degradome data to find cleaved small RNA targets. Bioinformatics. 2009;25:130–1. doi:10.1093/bioinformatics/btn604.
57. Dai X, Zhuang Z, Zhao PX. psRNATarget: a plant small RNA target analysis server (2017 release). Nucleic Acids Res. 2018;46:W49–54. doi:10.1093/nar/gky316.
58. Zuo J, Wang Q, Han C, Ju Z, Cao D, Zhu B, et al. SRNAome and degradome sequencing analysis reveals specific regulation of sRNA in response to chilling injury in tomato fruit. Physiol Plant. 2017;160:142–54. doi:10.1111/ppl.12509.
59. Chen H, Arsovski AA, Yu K, Wang A. Genome-wide investigation using sRNA-Seq, degradome-Seq and transcriptome-Seq reveals regulatory networks of microRNAs and their target genes in soybean during soybean mosaic virus infection. PLoS One. 2016;11:e0150582. doi:10.1371/journal.pone.0150582.
60. Lin M-C, Tsai H-L, Lim S-L, Jeng S-T, Wu S-H. Unraveling multifaceted contributions of small regulatory RNAs to photomorphogenic development in *Arabidopsis*. BMC Genomics. 2017;18:559. doi:10.1186/s12864-017-3937-6.
61. Wu C, Li X, Guo S, Wong S-M. Analyses of RNA-Seq and sRNA-Seq data reveal a complex network of anti-viral defense in TCV-infected *Arabidopsis thaliana*. Sci Rep. 2016;6:36007. doi: 10.1038/srep36007.
62. Jian H, Ma J, Wei L, Liu P, Zhang A, Yang B, et al. Integrated mRNA, sRNA, and degradome sequencing reveal oilseed rape complex responses to *Sclerotinia sclerotiorum* (Lib.) infection. Sci Rep. 2018;8:10987. doi:10.1038/s41598-018-29365-y.
63. Yang J, Liu X, Xu B, Zhao N, Yang X, Zhang M. Identification of miRNAs and their targets using high-throughput sequencing and degradome analysis in cytoplasmic male-sterile and its maintainer fertile lines of *Brassica juncea*. BMC Genomics. 2013;14:9. doi:10.1186/1471-2164-14-9.
64. He X, Shenkute AG, Wang W, Xu S. Characterization of conserved and novel microRNAs in *Lilium lancifolium* Thunb. by high-throughput sequencing. Sci Rep. 2018;8:2880. doi:10.1038/s41598-018-21193-4.
65. Gao X, Cui Q, Cao Q-Z, Liu Q, He H-B, Zhang D-M, et al. Transcriptome-wide analysis of *Botrytis elliptica* responsive microRNAs and their targets in *Lilium regale* Wilson by high-throughput sequencing and degradome analysis. Front Plant Sci. 2017;8:753. doi:10.3389/fpls.2017.00753.
66. Gao C, Wang P, Zhao S, Zhao C, Xia H, Hou L, et al. Small RNA profiling and degradome analysis reveal regulation of microRNA in peanut embryogenesis and early pod development. BMC Genomics.

2017;18:220. doi:10.1186/s12864-017-3587-8.

67. Ji Y, Chen P, Chen J, Pennerman KK, Liang X, Yan H, et al. Combinations of small RNA, RNA, and degradome sequencing uncovers the expression pattern of microRNA¯mRNA pairs adapting to drought stress in leaf and root of *Dactylis glomerata* L. Int J Mol Sci. 2018;19. doi:10.3390/ijms19103114.
68. Han H, Wang Q, Wei L, Liang Y, Dai J, Xia G, et al. Small RNA and degradome sequencing used to elucidate the basis of tolerance to salinity and alkalinity in wheat. BMC Plant Biol. 2018;18:195. doi:10.1186/s12870-018-1415-1.
69. Li T, Ma L, Geng Y, Hao C, Chen X, Zhang X. Small RNA and degradome sequencing reveal complex roles of miRNAs and their targets in developing wheat grains. PLoS One. 2015;10:e0139658. doi:10.1371/journal.pone.0139658.
70. Chen Z, Li F, Yang S, Dong Y, Yuan Q, Wang F, et al. Identification and functional analysis of flowering related microRNAs in common wild rice (*Oryza rufipogon* Griff.). PLoS One. 2013;8:e82844. doi:10.1371/journal.pone.0082844.
71. Wang ZJ, Huang JQ, Huang YJ, Li Z, Zheng BS. Discovery and profiling of novel and conserved microRNAs during flower development in *Carya cathayensis* via deep sequencing. Planta. 2012;236:613–21. doi:10.1007/s00425-012-1634-x.
72. Ao Y, Wang Y, Chen L, Wang T, Yu H, Zhang Z. Identification and comparative profiling of microRNAs in wild-type *Xanthoceras sorbifolia* and its double flower mutant. Genes Genomics. 2012;34:561–8. doi:10.1007/s13258-012-0065-1.
73. Li X, Jin F, Jin L, Jackson A, Ma X, Shu X, et al. Characterization and comparative profiling of the small RNA transcriptomes in two phases of flowering in *Cymbidium ensifolium*. BMC Genomics. 2015;16:622. doi:10.1186/s12864-015-1764-1.
74. Kim J, Park J, Lim C, Lim J, Ryu J-Y, Lee B-W, et al. Small RNA and transcriptome deep sequencing proffers insight into floral gene regulation in *Rosa* cultivars. BMC Genomics. 2012;13:657. doi:10.1186/1471-2164-13-657.
75. Nag A, Jack T. Sculpting the flower; the role of microRNAs in flower development. In: Timmermans MCP, editor. Plant development. New York:Cold Spring Harbor; 2010. p. 349–78. doi:10.1016/S0070-2153(10)91012-0.
76. Xing S, Salinas M, Höhmann S, Berndtgen R, Huijser P. miR156-targeted and nontargeted SBP-box transcription factors act in concert to secure male fertility in *Arabidopsis*. Plant Cell. 2010;22:3935–50. doi:10.1105/tpc.110.079343.
77. Wang Z, Wang Y, Kohalmi SE, Amyot L, Hannoufa A. SQUAMOSA PROMOTER BINDING PROTEIN-LIKE 2 controls floral organ development and plant fertility by activating ASYMMETRIC LEAVES 2 in *Arabidopsis thaliana*. Plant Mol Biol. 2016;92:661–74. doi:10.1007/s11103-016-0536-x.
78. Yamaguchi A, Wu M-F, Yang L, Wu G, Poethig RS, Wagner D. The microRNA-regulated SBP-Box transcription factor SPL3 is a direct upstream activator of *LEAFY*, *FRUITFULL*, and *APETALA1*. Dev Cell. 2009;17:268–78. doi:10.1016/j.devcel.2009.06.007.

79. Xing S, Salinas M, Garcia-Molina A, Höhmann S, Berndtgen R, Huijser P. *SPL8* and miR156-targeted *SPL* genes redundantly regulate *Arabidopsis* gynoecium differential patterning. Plant J. 2013;75:566–77. doi:10.1111/tpj.12221.
80. Sessions A, Nemhauser JL, McColl A, Roe JL, Feldmann KA, Zambryski PC. ETTIN patterns the *Arabidopsis* floral meristem and reproductive organs. Development. 1997;124:4481–91. http://www.ncbi.nlm.nih.gov/pubmed/9409666. Accessed 7 Mar 2019.
81. Simonini S, Bencivenga S, Trick M, Østergaard L. Auxin-induced modulation of ETTIN activity orchestrates gene expression in *Arabidopsis*. Plant Cell. 2017;29:1864–82. doi:10.1105/tpc.17.00389.
82. Murray F, Kalla R, Jacobsen J, Gubler F. A role for HvGAMYB in anther development. Plant J. 2003;33:481–91. doi:10.1046/j.1365-313X.2003.01641.x.
83. Gubler F, Chandler PM, White RG, Llewellyn DJ, Jacobsen J V. Gibberellin signaling in barley aleurone cells. Control of *SLN1* and *GAMYB* expression. Plant Physiol. 2002;129:191–200. doi:10.1104/pp.010918.
84. Millar AA, Gubler F. The *Arabidopsis GAMYB-like* genes, *MYB33* and *MYB65*, are microRNA-regulated genes that redundantly facilitate anther development. Plant Cell. 2005;17:705–21. doi:10.1105/tpc.104.027920.
85. Achard P, Herr A, Baulcombe DC, Harberd NP. Modulation of floral development by a gibberellin-regulated microRNA. Development. 2004;131:3357–65. doi:10.1242/dev.01206.
86. Tsuji H, Aya K, Ueguchi-Tanaka M, Shimada Y, Nakazono M, Watanabe R, et al. GAMYB controls different sets of genes and is differentially regulated by microRNA in aleurone cells and anthers. Plant J. 2006;47:427–44. doi:10.1111/j.1365-313X.2006.02795.x.
87. Ru P, Xu L, Ma H, Huang H. Plant fertility defects induced by the enhanced expression of microRNA167. Cell Res. 2006;16:457–65. doi:10.1038/sj.cr.7310057.
88. Wu M-F, Tian Q, Reed JW. *Arabidopsis* microRNA167 controls patterns of *ARF6* and *ARF8* expression, and regulates both female and male reproduction. Development. 2006;133:4211–8. doi:10.1242/dev.02602.
89. Barik S, Kumar A, Sarkar Das S, Yadav S, Gautam V, Singh A, et al. Coevolution pattern and functional conservation or divergence of miR167s and their targets across diverse plant species. Sci Rep. 2015;5:14611. doi:10.1038/srep14611.
90. Cecchetti V, Altamura MM, Falasca G, Costantino P, Cardarelli M. Auxin regulates *Arabidopsis* anther dehiscence, pollen maturation, and filament elongation. Plant Cell. 2008;20:1760–74. doi:10.1105/tpc.107.057570.
91. Nagpal P, Ellis CM, Weber H, Ploense SE, Barkawi LS, Guilfoyle TJ, et al. Auxin response factors ARF6 and ARF8 promote jasmonic acid production and flower maturation. Development. 2005;132:4107–18. doi:10.1242/dev.01955.
92. Reeves PH, Ellis CM, Ploense SE, Wu M-F, Yadav V, Tholl D, et al. A regulatory network for coordinated flower maturation. PLoS Genet. 2012;8:e1002506. doi:10.1371/journal.pgen.1002506.

93. Brioudes F, Joly C, Szécsi J, Varaud E, Leroux J, Bellvert F, et al. Jasmonate controls late development stages of petal growth in *Arabidopsis thaliana*. Plant J. 2009;60:1070–80. doi:10.1111/j.1365-313X.2009.04023.x.
94. Tian C, Muto H, Higuchi K, Matamura T, Tatematsu K, Koshiba T, et al. Disruption and overexpression of *Auxin Response Factor 8* gene of *Arabidopsis* affect hypocotyl elongation and root growth habit, indicating its possible involvement in auxin homeostasis in light condition. Plant J. 2004;40:333–43. doi:10.1111/j.1365-313X.2004.02220.x.
95. Yang JH, Han SJ, Yoon EK, Lee WS. Evidence of an auxin signal pathway, microRNA167-ARF8-GH3, and its response to exogenous auxin in cultured rice cells. Nucleic Acids Res. 2006;34:1892–9. doi:10.1093/nar/gkl118.
96. Liu N, Wu S, Van Houten J, Wang Y, Ding B, Fei Z, et al. Down-regulation of *AUXIN RESPONSE FACTORS 6* and *8* by microRNA 167 leads to floral development defects and female sterility in tomato. J Exp Bot. 2014;65:2507–20. doi:10.1093/jxb/eru141.
97. Chen X. A MicroRNA as a translational repressor of *APETALA2* in *Arabidopsis* flower development. Science. 2004;303:2022–5. doi:10.1126/science.1088060.
98. Almeida J, Rocheta M, Galego L. Genetic control of flower shape in *Antirrhinum majus*. Development. 1997;124:1387–92.
99. Galego L, Almeida J. Role of *DIVARICATA* in the control of dorsoventral asymmetry in *Antirrhinum* flowers. Genes Dev. 2002;16:880–91. doi:10.1101/gad.221002.
100. Floyd SK, Bowman JL. Ancient microRNA target sequences in plants. Nature. 2004;428:485–6. doi:10.1038/428485a.
101. Du Q, Wang H. The role of HD-ZIP III transcription factors and miR165/166 in vascular development and secondary cell wall formation. Plant Signal Behav. 2015;10:e1078955. doi:10.1080/15592324.2015.1078955.
102. Zhou G-K, Kubo M, Zhong R, Demura T, Ye Z-H. Overexpression of miR165 affects apical meristem formation, organ polarity establishment and vascular development in *Arabidopsis*. Plant Cell Physiol. 2007;48:391–404. doi:10.1093/pcp/pcm008.
103. Lian H, Li X, Liu Z, He Y. HYL1 is required for establishment of stamen architecture with four microsporangia in *Arabidopsis*. J Exp Bot. 2013;64:3397–410. doi:10.1093/jxb/ert178.
104. Kim J, Jung J-H, Reyes JL, Kim Y-S, Kim S-Y, Chung K-S, et al. microRNA-directed cleavage of *ATHB15* mRNA regulates vascular development in *Arabidopsis* inflorescence stems. Plant J. 2005;42:84–94. doi:10.1111/j.1365-313X.2005.02354.x.
105. Nagasaki H, Itoh J, Hayashi K, Hibara K, Satoh-Nagasawa N, Nosaka M, et al. The small interfering RNA production pathway is required for shoot meristem initiation in rice. Proc Natl Acad Sci U S A. 2007;104:14867–71. doi:10.1073/pnas.0704339104.
106. Nogueira FTS, Madi S, Chitwood DH, Juarez MT, Timmermans MCP. Two small regulatory RNAs establish opposing fates of a developmental axis. Genes Dev. 2007;21:750–5. doi:10.1101/gad.1528607.

107. Tang Z, Zhang L, Xu C, Yuan S, Zhang F, Zheng Y, et al. Uncovering small RNA-mediated responses to cold stress in a wheat thermosensitive genic male-sterile line by deep sequencing. Plant Physiol. 2012;159:721–38. doi:10.1104/pp.112.196048.
108. Palatnik JF, Wollmann H, Schommer C, Schwab R, Boisbouvier J, Rodriguez R, et al. Sequence and expression differences underlie functional specialization of *Arabidopsis* microRNAs miR159 and miR319. Dev Cell. 2007;13:115–25. doi:10.1016/j.devcel.2007.04.012.
109. Rubio-Somoza I, Weigel D. Coordination of flower maturation by a regulatory circuit of three microRNAs. PLoS Genet. 2013;9:e1003374. doi:10.1371/journal.pgen.1003374.
110. Axtell MJ, Snyder JA, Bartel DP. Common functions for diverse small RNAs of land plants. Plant Cell. 2007;19:1750–69. doi:10.1105/tpc.107.051706.
111. Xia R, Xu J, Meyers BC. The emergence, evolution, and diversification of the miR390-TAS3-ARF pathway in land plants. Plant Cell. 2017;7:tpc.00185.2017. doi:10.1105/tpc.17.00185.
112. Hunter C, Willmann MR, Wu G, Yoshikawa M, de la Luz Gutiérrez-Nava M, Poethig SR. Trans-acting siRNA-mediated repression of *ETTIN* and *ARF4* regulates heteroblasty in *Arabidopsis*. Development. 2006;133:2973–81. doi:10.1242/dev.02491.
113. Chitwood DH, Guo M, Nogueira FTS, Timmermans MCP. Establishing leaf polarity: the role of small RNAs and positional signals in the shoot apex. Development. 2007;134:813–23. doi:10.1242/dev.000497.
114. Yoon EK, Yang JH, Lim J, Kim SH, Kim S-K, Lee WS. Auxin regulation of the microRNA390-dependent transacting small interfering RNA pathway in *Arabidopsis* lateral root development. Nucleic Acids Res. 2010;38:1382–91. doi:10.1093/nar/gkp1128.
115. Matsui A, Mizunashi K, Tanaka M, Kaminuma E, Nguyen AH, Nakajima M, et al. tasiRNA-ARF pathway moderates floral architecture in *Arabidopsis* plants subjected to drought stress. Biomed Res Int. 2014;2014:303451. doi:10.1155/2014/303451.
116. Ellis CM, Nagpal P, Young JC, Hagen G, Guilfoyle TJ, Reed JW. *AUXIN RESPONSE FACTOR1* and *AUXIN RESPONSE FACTOR2* regulate senescence and floral organ abscission in *Arabidopsis thaliana*. Development. 2005;132:4563–74. doi:10.1242/dev.02012.
117. Liang G, Yu D. Reciprocal regulation among miR395, *APS* and *SULTR2;1* in *Arabidopsis thaliana*. Plant Signal Behav. 2010;5:1257–9. doi:10.4161/PSB.5.10.12608.
118. Nazar R, Umar S, Khan NA. Exogenous salicylic acid improves photosynthesis and growth through increase in ascorbate-glutathione metabolism and S assimilation in mustard under salt stress. Plant Signal Behav. 2015;10:e1003751. doi:10.1080/15592324.2014.1003751.
119. Herrmann J, Ravilious GE, McKinney SE, Westfall CS, Lee SG, Baraniecka P, et al. Structure and mechanism of soybean ATP sulfurylase and the committed step in plant sulfur assimilation. J Biol Chem. 2014;289:10919–29. doi:10.1074/jbc.M113.540401.
120. Wang M, Wang Q, Zhang B. Response of miRNAs and their targets to salt and drought stresses in cotton (*Gossypium hirsutum* L.). Gene. 2013;530:26–32. doi:10.1016/j.gene.2013.08.009.

121. Kawashima CG, Yoshimoto N, Maruyama-Nakashita A, Tsuchiya YN, Saito K, Takahashi H, et al. Sulphur starvation induces the expression of microRNA-395 and one of its target genes but in different cell types. Plant J. 2009;57:313–21. doi:10.1111/j.1365-313X.2008.03690.x.
122. Li SF, Milliken ON, Pham H, Seyit R, Napoli R, Preston J, et al. The *Arabidopsis* MYB5 transcription factor regulates mucilage synthesis, seed coat development, and trichome morphogenesis. Plant Cell. 2009;21:72–89. doi:10.1105/tpc.108.063503.
123. Camargo-Ramírez R, Val-Torregrosa B, San Segundo B. MiR858-mediated regulation of flavonoid-specific MYB transcription factor genes controls resistance to pathogen infection in *Arabidopsis*. Plant Cell Physiol. 2018;59:190–204. doi:10.1093/pcp/pcx175.
124. Inagaki S, Miura-Kamio A, Nakamura Y, Lu F, Cui X, Cao X, et al. Autocatalytic differentiation of epigenetic modifications within the *Arabidopsis* genome. EMBO J. 2010;29:3496–506. doi:10.1038/emboj.2010.227.
125. Bourdenx B, Bernard A, Domergue F, Pascal S, Léger A, Roby D, et al. Overexpression of *Arabidopsis ECERIFERUM1* promotes wax very-long-chain alkane biosynthesis and influences plant response to biotic and abiotic stresses. Plant Physiol. 2011;156:29–45. doi:10.1104/pp.111.172320.
126. Vaucheret H, Mallory AC, Bartel DP. AGO1 homeostasis entails coexpression of *MIR168* and *AGO1* and preferential stabilization of miR168 by AGO1. Mol Cell. 2006;22:129–36. doi:10.1016/j.molcel.2006.03.011.
127. Dong J, Kim ST, Lord EM. Plantacyanin plays a role in reproduction in *Arabidopsis*. Plant Physiol. 2005;138:778–89. doi:10.1104/pp.105.063388.
128. Song Z, Zhang L, Wang Y, Li H, Li S, Zhao H, et al. Constitutive expression of miR408 improves biomass and seed yield in *Arabidopsis*. Front Plant Sci. 2017;8:2114. doi:10.3389/fpls.2017.02114.
129. Sieber P, Gheyselinck J, Gross-Hardt R, Laux T, Grossniklaus U, Schneitz K. Pattern formation during early ovule development in *Arabidopsis thaliana*. Dev Biol. 2004;273:321–34. doi:10.1016/J.YDBIO.2004.05.037.
130. Liu D, Song Y, Chen Z, Yu D. Ectopic expression of miR396 suppresses *GRF* target gene expression and alters leaf growth in *Arabidopsis*. Physiol Plant. 2009;136:223–36. doi:10.1111/j.1399-3054.2009.01229.x.
131. Lee S-J, Lee BH, Jung J-H, Park SK, Song JT, Kim JH. GROWTH-REGULATING FACTOR and GRF-INTERACTING FACTOR specify meristematic cells of gynoecia and anthers. Plant Physiol. 2018;176:717–29. doi:10.1104/PP.17.00960.
132. Liang G, He H, Li Y, Wang F, Yu D. Molecular mechanism of microRNA396 mediating pistil development in *Arabidopsis*. Plant Physiol. 2014;164:249–58. doi:10.1104/pp.113.225144.
133. Liu H, Guo S, Xu Y, Li C, Zhang Z, Zhang D, et al. OsmiR396d-regulated *OsGRFs* function in floral organogenesis in rice through binding to their targets *OsJMJ706* and *OsCR4*. Plant Physiol. 2014;165:160–74. doi:10.1104/pp.114.235564.
134. Kawarazaki T, Kimura S, Iizuka A, Hanamata S, Nibori H, Michikawa M, et al. A low temperature-inducible protein AtSRC2 enhances the ROS-producing activity of NADPH oxidase AtRbohF. Biochim

Biophys Acta. 2013;1833:2775–80. doi:10.1016/j.bbamcr.2013.06.024.

135. Kamiya N, Itoh J-I, Morikami A, Nagato Y, Matsuoka M. The *SCARECROW* gene's role in asymmetric cell divisions in rice plants. Plant J. 2003;36:45–54. doi:10.1046/j.1365-313X.2003.01856.x.
136. Wang H, Niu Q-W, Wu H-W, Liu J, Ye J, Yu N, et al. Analysis of non-coding transcriptome in rice and maize uncovers roles of conserved lncRNAs associated with agriculture traits. Plant J. 2015;84:404–16. doi:10.1111/tpj.13018.
137. Held K, Pascaud F, Eckert C, Gajdanowicz P, Hashimoto K, Corratgé-Faillie C, et al. Calcium-dependent modulation and plasma membrane targeting of the AKT2 potassium channel by the CBL4/CIPK6 calcium sensor/protein kinase complex. Cell Res. 2011;21:1116–30. doi:10.1038/cr.2011.50.
138. Jagadeeswaran G, Zheng Y, Li Y-F, Shukla LI, Matts J, Hoyt P, et al. Cloning and characterization of small RNAs from *Medicago truncatula* reveals four novel legume-specific microRNA families. New Phytol. 2009;184:85–98. doi:10.1111/j.1469-8137.2009.02915.x.
139. Mourrain P, Béclin C, Elmayan T, Feuerbach F, Godon C, Morel JB, et al. *Arabidopsis SGS2* and *SGS3* genes are required for posttranscriptional gene silencing and natural virus resistance. Cell. 2000;101:533–42. doi:10.1016/S0092-8674(00)80863-6.
140. Xie Z, Johansen LK, Gustafson AM, Kasschau KD, Lellis AD, Zilberman D, et al. Genetic and functional diversification of small RNA pathways in plants. PLoS Biol. 2004;2:E104. doi:10.1371/journal.pbio.0020104.
141. Song Q-X, Liu Y-F, Hu X-Y, Zhang W-K, Ma B, Chen S-Y, et al. Identification of miRNAs and their target genes in developing soybean seeds by deep sequencing. BMC Plant Biol. 2011;11:5. doi:10.1186/1471-2229-11-5.
142. Windels D, Vazquez F. miR393: Integrator of environmental cues in auxin signaling? Plant Signal Behav. 2011;6:1672–5. doi:10.4161/psb.6.11.17900.
143. Vidal EA, Araus V, Lu C, Parry G, Green PJ, Coruzzi GM, et al. Nitrate-responsive miR393/AFB3 regulatory module controls root system architecture in *Arabidopsis thaliana*. Proc Natl Acad Sci U S A. 2010;107:4477–82. doi:10.1073/pnas.0909571107.
144. Navarro L, Dunoyer P, Jay F, Arnold B, Dharmasiri N, Estelle M, et al. A plant miRNA contributes to antibacterial resistance by repressing auxin signaling. Science. 2006;312:436–9. doi:10.1126/science.1126088.
145. Zhang W, Gao S, Zhou X, Chellappan P, Chen Z, Zhou X, et al. Bacteria-responsive microRNAs regulate plant innate immunity by modulating plant hormone networks. Plant Mol Biol. 2011;75:93–105. doi:10.1007/s11103-010-9710-8.
146. Zhao C-Z, Xia H, Frazier TP, Yao Y-Y, Bi Y-P, Li A-Q, et al. Deep sequencing identifies novel and conserved microRNAs in peanuts (*Arachis hypogaea* L.). BMC Plant Biol. 2010;10:3. doi:10.1186/1471-2229-10-3.
147. Iglesias MJ, Terrile MC, Windels D, Lombardo MC, Bartoli CG, Vazquez F, et al. MiR393 regulation of auxin signaling and redox-related components during acclimation to salinity in *Arabidopsis*. PLoS One. 2014;9:e107678. doi:10.1371/journal.pone.0107678.

148. Li H, Dong Y, Yin H, Wang N, Yang J, Liu X, et al. Characterization of the stress associated microRNAs in *Glycine max* by deep sequencing. BMC Plant Biol. 2011;11:170. doi:10.1186/1471-2229-11-170.
149. Chen Z-H, Bao M-L, Sun Y-Z, Yang Y-J, Xu X-H, Wang J-H, et al. Regulation of auxin response by miR393-targeted Transport Inhibitor Response protein 1 is involved in normal development in *Arabidopsis*. Plant Mol Biol. 2011;77:619–29. doi:10.1007/s11103-011-9838-1.
150. Bonnet E, Van de Peer Y, Rouzé P. The small RNA world of plants. New Phytol. 2006;171:451–68. doi:10.1111/j.1469-8137.2006.01806.x.
151. Quint M, Gray WM. Auxin signaling. Curr Opin Plant Biol. 2006;9:448–53. doi:10.1016/j.pbi.2006.07.006.
152. Damodharan S, Zhao D, Arazi T. A common miRNA160-based mechanism regulates ovary patterning, floral organ abscission and lamina outgrowth in tomato. Plant J. 2016;86:458–71. doi:10.1111/tpj.13127.
153. Hendelman A, Buxdorf K, Stav R, Kravchik M, Arazi T. Inhibition of lamina outgrowth following *Solanum lycopersicum AUXIN RESPONSE FACTOR 10* (*SlARF10*) derepression. Plant Mol Biol. 2012;78:561–76. doi:10.1007/s11103-012-9883-4.
154. Peng T, Sun H, Qiao M, Zhao Y, Du Y, Zhang J, et al. Differentially expressed microRNA cohorts in seed development may contribute to poor grain filling of inferior spikelets in rice. BMC Plant Biol. 2014;14:196. doi:10.1186/s12870-014-0196-4.
155. Zhu Q-H, Spriggs A, Matthew L, Fan L, Kennedy G, Gubler F, et al. A diverse set of microRNAs and microRNA-like small RNAs in developing rice grains. Genome Res. 2008;18:1456–65. doi:10.1101/gr.075572.107.
156. Rodriguez RE, Mecchia MA, Debernardi JM, Schommer C, Weigel D, Palatnik JF. Control of cell proliferation in *Arabidopsis thaliana* by microRNA miR396. Development. 2010;137:103–12. doi:10.1242/dev.043067.
157. Yi R, Zhu Z, Hu J, Qian Q, Dai J, Ding Y. Identification and expression analysis of microRNAs at the grain filling stage in rice (*Oryza sativa* L.) via deep sequencing. PLoS One. 2013;8:e57863. doi:10.1371/journal.pone.0057863.
158. Guo N, Zhang Y, Sun X, Fan H, Gao J, Chao Y, et al. Genome-wide identification of differentially expressed miRNAs induced by ethephon treatment in abscission layer cells of cotton (*Gossypium hirsutum*). Gene. 2018;676:263–8. doi:10.1016/j.gene.2018.08.057.
159. Hu G, Fan J, Xian Z, Huang W, Lin D, Li Z. Overexpression of *SlREV* alters the development of the flower pedicel abscission zone and fruit formation in tomato. Plant Sci. 2014;229:86–95. doi:10.1016/j.plantsci.2014.08.010.
160. Li M, Liang Z, He S, Zeng Y, Jing Y, Fang W, et al. Genome-wide identification of leaf abscission associated microRNAs in sugarcane (*Saccharum officinarum* L.). BMC Genomics. 2017;18:754. doi:10.1186/s12864-017-4053-3.
161. Xu T, Wang Y, Liu X, Lv S, Feng C, Qi M, et al. Small RNA and degradome sequencing reveals microRNAs and their targets involved in tomato pedicel abscission. Planta. 2015;242:963–84.

doi:10.1007/s00425-015-2318-0.

162. Smith LM, Burbano HA, Wang X, Fitz J, Wang G, Ural-Blimke Y, et al. Rapid divergence and high diversity of miRNAs and miRNA targets in the Camelineae. Plant J. 2015;81:597–610. doi:10.1111/tpj.12754.
163. Curaba J, Singh MB, Bhalla PL. miRNAs in the crosstalk between phytohormone signalling pathways. J Exp Bot. 2014;65:1425–38. doi:10.1093/jxb/eru002.
164. Guilfoyle TJ, Hagen G. Auxin Response Factors. Curr Opin Plant Biol. 2007;10:453–60. doi:10.1016/j.pbi.2007.08.014.
165. Lau S, Jurgens G, De Smet I. The evolving complexity of the auxin pathway. Plant Cell. 2008;20:1738–46. doi:10.1105/tpc.108.060418.
166. Rhoades MW, Reinhart BJ, Lim LP, Burge CB, Bartel B, Bartel DP. Prediction of plant microRNA targets. Cell. 2002;110:513–20. doi:10.1093/bioinformatics/btq233.
167. Ulmasov T, Hagen G, Guilfoyle TJ. Activation and repression of transcription by auxin-response factors. Proc Natl Acad Sci U S A. 1999;96:5844–9. doi:10.1073/pnas.96.10.5844.
168. Allen E, Xie Z, Gustafson AM, Carrington JC, Achard P, Herr A, et al. microRNA-directed phasing during trans-acting siRNA biogenesis in plants. Cell. 2005;121:207–21. doi:10.1016/j.cell.2005.04.004.
169. Axtell MJ, Jan C, Rajagopalan R, Bartel DP. A two-hit trigger for siRNA biogenesis in plants. Cell. 2006;127:565–77. doi:10.1016/j.cell.2006.09.032.
170. Xie F, Zhang B. microRNA evolution and expression analysis in polyploidized cotton genome. Plant Biotechnol J. 2015;13:421–34. doi:10.1111/pbi.12295.
171. Zhang C, Li G, Zhu S, Zhang S, Fang J. tasiRNAdb: a database of ta-siRNA regulatory pathways. Bioinformatics. 2014;30:1045–6. doi:10.1093/bioinformatics/btt746.
172. Sinha AK, Jaggi M, Raghuram B, Tuteja N. Mitogen-activated protein kinase signaling in plants under abiotic stress. Plant Signal Behav. 2011;6:196–203. doi:10.4161/PSB.6.2.14701.
173. Jalmi SK, Sinha AK. ROS mediated MAPK signaling in abiotic and biotic stress- striking similarities and differences. Front Plant Sci. 2015;6:769. doi:10.3389/fpls.2015.00769.
174. Ouaked F, Rozhon W, Lecourieux D, Hirt H. A MAPK pathway mediates ethylene signaling in plants. EMBO J. 2003;22:1282–8. doi:10.1093/emboj/cdg131.
175. Finkelstein R. Abscisic Acid synthesis and response. Arab B. 2013;11:e0166. doi:10.1199/tab.0166.
176. Sawicki M, Ait Barka E, Clement C, Vaillant-Gaveau N, Jacquard C. Cross-talk between environmental stresses and plant metabolism during reproductive organ abscission. J Exp Bot. 2015;66:1707–19. doi:10.1093/jxb/eru533.
177. Patharkar OR, Walker JC. Floral organ abscission is regulated by a positive feedback loop. Proc Natl Acad Sci U S A. 2015;112:2906–11. doi:10.1073/pnas.1423595112.
178. Sun Y, Zhou Q, Zhang W, Fu Y, Huang H. *ASYMMETRIC LEAVES1* , an *Arabidopsis* gene that is involved in the control of cell differentiation in leaves. Planta. 2002;214:694–702. doi:10.1007/s004250100673.

179. Dieterle M, Thomann A, Renou J-P, Parmentier Y, Cognat V, Lemonnier G, et al. Molecular and functional characterization of *Arabidopsis* Cullin 3A. Plant J. 2004;41:386–99. doi:10.1111/j.1365-313X.2004.02302.x.
180. Smalle J, Kurepa J, Yang P, Babiychuk E, Kushnir S, Durski A, et al. Cytokinin growth responses in *Arabidopsis* involve the 26S proteasome subunit RPN12. Plant Cell. 2002;14:17–32. doi:10.1105/TPC.010381.
181. Krogan NT, Hogan K, Long JA. APETALA2 negatively regulates multiple floral organ identity genes in *Arabidopsis* by recruiting the co-repressor TOPLESS and the histone deacetylase HDA19. Development. 2012;139:4180–90. doi:10.1242/dev.085407.
182. Elliott RC, Betzner AS, Huttner E, Oakes MP, Tucker WQ, Gerentes D, et al. *AINTEGUMENTA*, an *APETALA2-like* gene of *Arabidopsis* with pleiotropic roles in ovule development and floral organ growth. Plant Cell. 1996;8:155–68. 10.1105/tpc.8.2.155.
183. Ohto M, Floyd SK, Fischer RL, Goldberg RB, Harada JJ. Effects of APETALA2 on embryo, endosperm, and seed coat development determine seed size in *Arabidopsis*. Sex Plant Reprod. 2009;22:277–89. doi:10.1007/s00497-009-0116-1.
184. Ohto MA, Fischer RL, Goldberg RB, Nakamura K, Harada JJ. Control of seed mass by APETALA2. Proc Natl Acad Sci U S A. 2005;102:3123–8. doi:10.1073/pnas.0409858102.
185. Exner V, Aichinger E, Shu H, Wildhaber T, Alfarano P, Caflisch A, et al. The chromodomain of LIKE HETEROCHROMATIN PROTEIN 1 is essential for H3K27me3 binding and function during *Arabidopsis* development. PLoS One. 2009;4:e5335. doi:10.1371/journal.pone.0005335.
186. Takada S, Goto K. Terminal flower 2, an *Arabidopsis* homolog of heterochromatin protein 1, counteracts the activation of flowering locus T by constans in the vascular tissues of leaves to regulate flowering time. Plant Cell. 2003;15:2856–65. doi:10.1105/tpc.016345.
187. Poznań Plant Breeders LTD.: information on yellow lupine cv. Taper. http://phr.pl/sklep/lubin-zolty-taper/(2019). Accessed 05 Apr 2019.
188. Langmead B. Aligning Short Sequencing Reads with Bowtie. In: Pyne S, Prakasa Rao BLS, Rao SB, editors. Current Protocols in Bioinformatics. Hoboken, NJ, USA: John Wiley & Sons, Inc.; 2010. p. Unit 11.7.32. doi:10.1002/0471250953.bi1107s32.
189. Wickham H. Ggplot2 : elegant graphics for data analysis. Springer Verlag New York; 2016.
190. Auguie B. gridExtra: Miscellaneous Functions for “Grid” Graphics. R package version 2.3. 2017. https://cran.r-project.org/web/packages/gridExtra/gridExtra.pdf Accessed 11 Mar 2019.
191. Love MI, Huber W, Anders S. Moderated estimation of fold change and dispersion for RNA-seq data with DESeq2. Genome Biol. 2014;15:550. doi:10.1186/s13059-014-0550-8.
192. Gu Z, Eils R, Schlesner M. Complex heatmaps reveal patterns and correlations in multidimensional genomic data. Bioinformatics. 2016;32:2847–9. doi:10.1093/bioinformatics/btw313.
193. Gu Z, Gu L, Eils R, Schlesner M, Brors B. circlize implements and enhances circular visualization in R. Bioinformatics. 2014;30:2811–2. doi:10.1093/bioinformatics/btu393.

194. Galili T. dendextend: an R package for visualizing, adjusting and comparing trees of hierarchical clustering. Bioinformatics. 2015;31:3718–20. doi:10.1093/bioinformatics/btv428.

195. Kramer MF. Stem-loop RT-qPCR for miRNAs. Curr Protoc Mol Biol. 2011;95:15.10.1-15.10.15. doi:10.1002/0471142727.mb1510s95.

196. Varkonyi-Gasic E, Hellens RP. Quantitative stem-loop RT-PCR for detection of microRNAs. In: Kodama H, Komamine A, editors. RNAi and Plant Gene Function Analysis. Methods in Molecular Biology (Methods and Protocols). Clifton, N.J.:Humana Press; 2011. p. 145–57. doi:10.1007/978-1-61779-123-9_10.

197. Haas BJ, Papanicolaou A, Yassour M, Grabherr M, Blood PD, Bowden J, et al. *De novo* transcript sequence reconstruction from RNA-seq using the Trinity platform for reference generation and analysis. Nat Protoc. 2013;8:1494–512. doi:10.1038/nprot.2013.084.

198. Young MD, Wakefield MJ, Smyth GK, Oshlack A. Gene ontology analysis for RNA-seq: accounting for selection bias. Genome Biol. 2010;11:R14. doi:10.1186/gb-2010-11-2-r14.

199. Huo Z, Tang S, Park Y, Tseng G. P-value evaluation, variability index and biomarker categorization for adaptively weighted Fisher's meta-analysis method in omics applications. http://arxiv.org/abs/1708.05084 (2017). Accessed 9 Mar 2019.

Tables

Table 1. Summary of read and general annotation of small RNA-seq data.

	FPAB	FPNAB	LF1	LF2	LF3	LF4	UF1	UF2	UF3	UF4
All reads										
unique	5915879,5	6387744,5	6755903	6725750	6401622,5	6434224,5	6633250	6525844,5	6061243,5	6188739,5
redundant	15042451	14794948	15357830	15397345	15132153	15067593	15368697	15249713	14996762	15226142
Annotation										
Unique										
miRBase	424	388	449	399	346	412	467	336	360	410
hairpin	2001	1832	1713	1610	1738	1801	1815	1699	1750	1995
Rfam	45858	31044	25877	29300	34998	33577	31265	33221	36206	43875
unknown	5867598	6354480,5	6727865	6694441,5	6364541,5	6398435	6599704	6490589,5	6022928	6142461
All										
miRBase	580674	562932	364583	351641	394114	410044	368739	448377	571963	471398
hairpin	298173	319855	208266	234335	286889	274200	192098	236605	298894	301915
Rfam	731119	493959	299502	386808	581709	528515	522096	499417	555178	727483
unknown	13432486	13418203	14485480	14424562	13869443	13854835	14285765	14065314	13570728	13725347

Table 2. Rfam annotation summary.

	FPAB	FPNAB	LF1	LF2	LF3	LF4	UF1	UF2	UF3	UF4
tRNA	4742	3467	2537	3245	3771	4209	2914	3617	4115	4645
rRNA	33810	23320	19921	22331	27302	25453	24092	25477	27557	34641
snoRNA	2164	893	496	561	540	591	1125	683	827	748
Intro	1480	1238	1094	1201	1403	1340	1166	1339	1407	1546
Retro	829	800	681	707	792	742	803	766	751	852
U1	415	100	64	103	83	66	62	84	124	124
U2	620	323	263	261	286	294	275	308	312	346
U3	433	244	150	172	169	163	189	184	245	215
U4	248	61	51	63	54	54	58	67	91	82
U5	69	10	12	15	16	16	13	9	13	21
U6	349	81	52	81	64	58	102	76	90	108
Total	45858	31044	25877	29300	34998	33577	31265	33221	36206	43875

Table 3. Novel miRNAs identified in *Lupinus luteus*.

miRNA ID	Sequence (5'-3')	Size (nt)	Precursor (RNA-seq ID)	LP (nt)	MFE (kcal/mol)	Target description (degradome/psRNAtarget)
Ll-miRn1	TTGCCAATTCCACCCATGCCTA	22	TRINITY_DN58100_c0_g3_i1	125	-59,90	SUPPRESSOR OF GENE SILENCING 3
Ll-miRn2	TCACTCCAACTTTGACCTTCT	21	TRINITY_DN50576_c0_g2_i1	215	-84,70	65-kDa microtubule-associated protein 7
Ll-miRn3	TGAAGAGGGAGGGAGACTGATG	22	TRINITY_DN77107_c0_g1	185	-86,50	SRC2 homolog
Ll-miRn4	GTAGCACCATCAAGATTCACA	21	TRINITY_DN43941_c0_g1_i1	151	-60,30	RCC1 and BTB domain-containing protein 2
Ll-miRn5	TGGAATAGTGAATGAGACATC	21	TRINITY_DN52736_c3_g2_i2	102	-38,70	Probable cinnamyl alcohol dehydrogenase 9
Ll-miRn6	TGCTATCCATCCTGAGTTTCA	21	TRINITY_DN54182_c6_g1_i1	133	-47,90	Probable amino acid permease 7
Ll-miRn7	AGAGGTGTATGGCACAAGAGA	21	TRINITY_DN53175_c1_g6_i1	85	-36,60	Probable protein phosphatase 2C
Ll-miRn8	TGAAGTGTTTGGGGGAACTCC	21	TRINITY_DN44441_c0_g1_i1	102	-37,40	ATP sulfurylase 1
Ll-miRn9	TCGGACCAGGCTTTATTCCTT	21	TRINITY_DN50586_c0_g1_i3	167	-65,60	Homeobox-leucine zipper protein REVOLUTA
Ll-miRn10	ATGTTGTGATGGGAATCAATG	21	TRINITY_DN67022_c0_g1_i1	84	-43,50	CBL-interacting serine/threonine-protein kinase 6
Ll-miRn11	TAAAGACCTCATTCTCTCATG	21	TRINITY_DN31556_c0_g1_i1	130	-62,80	Vacuolar protein sorting-associated protein 62
Ll-miRn12	AGGTCATCTTGCAGCTTCAAT	21	TRINITY_DN52990_c2_g1_i5	71	-36,84	DNA-directed RNA polymerase I subunit 1
Ll-miRn15	TTCGGCTTTCTACTTCTCATG	21	TRINITY_DN54101_c8_g2_i10	156	-66,20	Transcription termination factor MTERF8
Ll-miRn16	AGTTCTTTAGATGGGCTGGACGCC	24	TRINITY_DN52523_c6_g2_i1	83	-36,50	Amino acid transporter AVT6A
Ll-miRn17	TGTCTCATTCTCTATCTCAAG	21	TRINITY_DN51068_c0_g1_i2	142	-64,30	IST1-like protein
Ll-miRn18	AATAGGGCACATCTCTCATGG	22	TRINITY_DN46596_c0_g1_i1	112	-49,00	E3 ubiquitin-protein ligase HOS1
Ll-miRn19	TCCAAAGGGATCGCATTGATTT	22	TRINITY_DN53637_c4_g2_i4	110	-48.10	AUXIN SIGNALING F-BOX 3
Ll-miRn21	TGAGCATGAGGATAAGGACGG	21	TRINITY_DN50271_c0_g3_i1	246	-144,90	Tetratricopeptide repeat protein 1
Ll-miRn22	TATCATTCCATACATCGTCTCG	21	TRINITY_DN50592_c0_g4_i2	80	-33,60	Putative disease resistance RPP13-like protein 1
Ll-miRn24	ATTGTCACTGTATCATTCACCATT	24	TRINITY_DN52987_c0_g1_i1	104	-32,30	Zinc finger CCCH domain-containing protein 55
Ll-miRn25	TGGTACAAAAAGTGGGGCAAC	21	TRINITY_DN48871_c3_g1_i9	151	-43,90	Nuclear transcription factor Y subunit A-9
Ll-miRn26	TGTTGTTTTCTGGTAAAAATA	21	TRINITY_DN58488_c1_g2_i4	99	-33,80	Auxin-responsive protein IAA27
Ll-	ATTAGATCATGTGGCAGTTTCACC	24	TRINITY_DN51506_c3_g2_i5	77	-36,60	U-box domain-containing

miRn27						protein 33
ll-miRn28	TACGGGTGTCCTCACCTCTGAT	22	TRINITY_DN70730_c0_g1_i1	98	-36,90	**ISWI chromatin-remodeling complex ATPase**
ll-miRn29	TGGGATAGAGAGTGAGATACC	21	TRINITY_DN51068_c0_g1_i2	125	-67,80	Ethylene-responsive transcription factor ERF017
ll-miRn30	TTCGTTTGTGTGCAGACTCTGT	22	TRINITY_DN57730_c1_g9_i2	105	-42,70	**Endoribonuclease Dicer homolog 2**
ll-miRn31	GCGTACCAGGAGCCATGCATG	21	TRINITY_DN58934_c0_g4_i1	149	-60,20	Calcium-transporting ATPase 4
ll-miRn32	AAGGGTTGTTTACAGAGTTTA	21	TRINITY_DN51330_c0_g1_i1	128	-55,40	26S proteasome regulatory subunit 7

Table 4. Differentially expressed miRNAs identified in comparisons of flower development stages between lower and upper parts of the raceme with
Padj < 0.05.

Flower development						
ID	miRNA sequence	miRBase annotation	log_2FC	p-value	padj	Target description (psRNAtarget/degradome)
Lower flowers development						
LF2 vs LF1						
Ll-miRn22	TATCATTCCATACATCGTCTCG	new	0,71	0,0000	0,0004	Putative disease resistance RPP13-like protein 1
Ll-miR401	TTGACAGAAGAGAGTGAGCAC	gma-miR156k	0,61	0,0003	0,0032	**Squamosa promoter-binding-like protein 2**
Ll-miR265	TCGGACCAGGCTTCATTCCTT	ata-miR166c-3p	0,61	0,0001	0,0007	**Homeobox-leucine zipper protein ATHB-15**
Ll-miRn27	ATTAGATCATGTGGCAGTTTCACC	new	0,51	0,0028	0,0241	U-box domain-containing protein 33
Ll-miR454	TTTGGATTGAAGGGAGCTCTT	aly-miR159b-3p	0,47	0,0000	0,0000	Transcription factor GAMYB
Ll-miR124	TGACAGAAGAGAGTGAGCAC	ama-miR156	0,43	0,0021	0,0193	**Squamosa promoter-binding-like protein 13B**
Ll-miR247	TCGCTTGGTGCAGGTCGGGAA	aly-miR168a-5p	-0,68	0,0000	0,0000	AGO1
Ll-miR102	CGCTGTCCATCCTGAGTTTCA	bra-miR390-3p	-0,69	0,0000	0,0003	TAS3
Ll-miR115	CTCGTTGTCTGTTCGACCTTG	ppe-miR858	-0,76	0,0000	0,0001	**Transcription repressor MYB5**
Ll-miR53	ATCATGCTATCCCTTTGGATT	gma-miR393c-3p	-1,02	0,0034	0,0278	**Midasin-like**
Ll-miR82	CCCGCCTTGCATCAACTGAAT	aly-miR168a-3p	-1,31	0,0000	0,0000	FAD-linked sulfhydryl oxidase ERV1
Ll-miRn10	ATGTTGTGATGGGAATCAATG	new	-1,37	0,0000	0,0000	**CBL-interacting Ser/Thr -protein kinase 6**
Ll-miRn3	TGAAGAGGGAGGGAGACTGATG	new	-1,43	0,0006	0,0060	**SRC2 homolog**
Ll-miR198	GTTCAATAAAGCTGTGGGAA	osa-miR396a-3p	-1,75	0,0000	0,0000	ECERIFERUM 1
Ll-miRn31	GCGTACCAGGAGCCATGCATG	new	-1,99	0,0001	0,0007	Calcium-transporting ATPase 4
Ll-miR200	GTTCAATAAAGCTGTGGGAAG	aly-miR396a-3p	-2,00	0,0000	0,0000	ECERIFERUM 1
Ll-miR155	GCTCAAGAAAGCTGTGGGAGA	gma-miR396b-3p	-2,04	0,0000	0,0000	**Lysine-specific demethylase JMJ25**
Ll-miR199	GTTCAATAAAGCTGTGGGAAA	ata-miR396e-3p	-2,31	0,0000	0,0000	ECERIFERUM 1
LF3 vs LF2						
Ll-miR258	TCGGACCAGGCTTCATTCCCG	cpa-miR166d	0,91	0,0000	0,0001	Homeobox-leucine zipper protein ATHB-15
Ll-miRn1	TTGCCAATTCCACCCATGCCTA	new	0,87	0,0000	0,0008	**SUPPRESSOR OF GENE SILENCING 3**
Ll-miR9	AAGCTCAGGAGGGATAGCGCC	aly-miR390a-5p	0,78	0,0005	0,0100	**TAS3**
Ll-miR118	CTGAAGTGTTTGGGGGAACTC	aly-miR395d-3p	0,70	0,0000	0,0007	**ATP sulfurylase 1, chloroplastic**
Ll-miR264	TCGGACCAGGCTTCATTCCTC	aqc-miR166a	0,66	0,0037	0,0401	**Homeobox-leucine zipper protein ATHB-15**
Ll-miRn22	TATCATTCCATACATCGTCTCG	new	0,46	0,0032	0,0401	Putative disease resistance RPP13-like protein 1

Ll-miR384	TTCCACAGCTTTCTTGAACTT	aly-miR396b-5p	-0,35	0,0033	0,0401	MPE-cyclase
Ll-miR115	CTCGTTGTCTGTTCGACCTTG	ppe-miR858	-0,59	0,0048	0,0426	**Transcription repressor MYB5**
Ll-miR200	GTTCAATAAAGCTGTGGGAAG	aly-miR396a-3p	-0,62	0,0000	0,0000	ECERIFERUM 1
Ll-miR108	CGTGTTCTCAGGTCGCCCCTG	ppe-miR398b	-1,08	0,0044	0,0426	Plastocyanin
Ll-miR60	ATGCACTGCCTCTTCCCTGGC	ahy-miR408-3p	-1,09	0,0024	0,0385	**Basic blue protein**
			LF4 vs LF3			
ND						
			Upper flowers development			
			UF2 vs UF1			
Ll-miR119	TGAAGTGTTTGGGGGAACTCC	sly-miR395a	1,22	0,0000	0,0019	**ATP sulfurylase 1, chloroplastic**
Ll-miR452	TTTGGATTGAAGGGAGCTCTC	lus-miR159b	0,74	0,0001	0,0019	**Gamma-glutamyl peptidase 5**
Ll-miR118	CTGAAGTGTTTGGGGGAACTC	aly-miR395d-3p	0,64	0,0001	0,0019	**ATP sulfurylase 1, chloroplastic**
Ll-miR177	GGAATGTTGTCTGGCTCGAGG	aly-miR166a-5p	0,50	0,0002	0,0033	Transcription factor RADIALIS
Ll-miR174	GGAATGTTGGCTGGCTCGAGG	mtr-miR166e-5p	-0,45	0,0002	0,0033	**Nucleolar GTP-binding protein 1**
Ll-miR285	TGAAGCTGCCAGCATGATCTTA	mdm-miR167h	-0,56	0,0023	0,0286	**Auxin response factor 6**
Ll-miRn10	ATGTTGTGATGGGAATCAATG	new	-0,96	0,0008	0,0117	**CBL-interacting Ser/Thr-protein kinase 6**
Ll-miR155	GCTCAAGAAAGCTGTGGGAGA	gma-miR396b-3p	-1,17	0,0000	0,0000	**Lysine-specific demethylase JMJ25**
			UF3 vs UF2			
Ll-miR258	TCGGACCAGGCTTCATTCCCG	cpa-miR166d	0,70	0,0022	0,0323	Homeobox-leucine zipper protein ATHB-15
Ll-miR247	TCGCTTGGTGCAGGTCGGGAA	aly-miR168a-5p	-0,40	0,0005	0,0113	AGO1
Ll-miR102	CGCTGTCCATCCTGAGTTTCA	bra-miR390-3p	-0,96	0,0000	0,0004	TAS3
Ll-miR199	GTTCAATAAAGCTGTGGGAAA	ata-miR396e-3p	-0,97	0,0000	0,0001	ECERIFERUM 1
Ll-miR60	ATGCACTGCCTCTTCCCTGGC	ahy-miR408-3p	-1,01	0,0008	0,0145	**Basic blue protein**
Ll-miR200	GTTCAATAAAGCTGTGGGAAG	aly-miR396a-3p	-1,02	0,0000	0,0000	ECERIFERUM 1
Ll-miR100	CGCTATCCATCCTGAGTTTCA	aly-miR390a-3p	-1,10	0,0001	0,0021	TAS3
Ll-miR99	CGCTATCCATCCTGAGTTTC	gma-miR390a-3p	-1,16	0,0014	0,0228	TAS3
Ll-miR53	ATCATGCTATCCCTTTGGATT	gma-miR393c-3p	-1,19	0,0001	0,0017	**Midasin-like**
Ll-miR155	GCTCAAGAAAGCTGTGGGAGA	gma-miR396b-3p	-1,45	0,0000	0,0000	**Lysine-specific demethylase JMJ25**
			UF4 vs UF3			
Ll-	TTGTGTTCTCAGGTCACCCCT	stu-miR398b-3p	1,09	0,0003	0,0098	**Probable nucleoredoxin 1**

miR438						
Ll-miR281	TGAAGCTGCCAGCATGATCTGA	ata-miR167b-5p	0,92	0,0001	0,0048	Auxin response factor 6 and ARF8
Ll-miR445	TTTGGACTGAAGGGAGCTCCT	atr-miR319b	0,84	0,0000	0,0009	Transcription factor TCP4
Ll-miR9	AAGCTCAGGAGGGATAGCGCC	aly-miR390a-5p	0,78	0,0004	0,0098	**TAS3**
Ll-miR346	TGGAGAAGCAGGGCACGTGCA	aly-miR164a-5p	0,73	0,0029	0,0359	CUP-SHAPED COTYLEDON 2
Ll-miR280	TGAAGCTGCCAGCATGATCTG	atr-miR167	0,66	0,0010	0,0207	Auxin response factor 6 and ARF8
Ll-miR130	CTTGGACTGAAGGGAGCTCCC	ppt-miR319c	0,65	0,0001	0,0034	**Transcription factor MYB33**
Ll-miR115	CTCGTTGTCTGTTCGACCTTG	ppe-miR858	-0,67	0,0019	0,0333	**Transcription repressor MYB5**
Ll-miR100	CGCTATCCATCCTGAGTTTCA	aly-miR390a-3p	-0,70	0,0025	0,0337	TAS3
Ll-miRn11	TAAAGACCTCATTCTCTCATG	new	-0,83	0,0037	0,0386	**Vacuolar protein sorting-associated protein 62**
Ll-miR99	CGCTATCCATCCTGAGTTTC	gma-miR390a-3p	-0,86	0,0038	0,0386	TAS3
Ll-miR102	CGCTGTCCATCCTGAGTTTCA	bra-miR390-3p	-0,91	0,0025	0,0337	TAS3

Table 5. Differentially expressed miRNAs identified in comparisons between flowers from lower and upper parts of the raceme with Padj < 0.05.

Flowers from upper and lower parts of receme						
ID	miRNA sequence	miRBase annotation	log_2FC	p-value	padj	Target description (psRNAtarget/degradome)
UF1 vs LF1						
LI-miR281	TGAAGCTGCCAGCATGATCTGA	ata-miR167b-5p	-0,47	0,0002	0,0054	Auxin response factor 6 and ARF8
LI-miRn30	TTCGTTTGTGTGCAGACTCTGT	new	-0,49	0,0009	0,0221	**Endoribonuclease Dicer homolog 2**
LI-miR118	CTGAAGTGTTTGGGGGAACTC	aly-miR395d-3p	-0,58	0,0000	0,0000	**ATP sulfurylase 1, chloroplastic**
LI-miR102	CGCTGTCCATCCTGAGTTTCA	bra-miR390-3p	-0,71	0,0000	0,0000	TAS3
LI-miRn29	TGGGATAGAGAGTGAGATACC	new	-1,00	0,0000	0,0000	Ethylene-responsive transcription factor ERF017
LI-miR94	CGATGTTGGTGAGGTTCAATC	gma-miR171k-5p	-1,09	0,0012	0,0253	Transcription factor MYB4
LI-miR198	GTTCAATAAAGCTGTGGGAA	osa-miR396a-3p	-1,10	0,0000	0,0001	ECERIFERUM 1
LI-miR82	CCCGCCTTGCATCAACTGAAT	aly-miR168a-3p	-1,25	0,0000	0,0000	FAD-linked sulfhydryl oxidase ERV1
LI-miR200	GTTCAATAAAGCTGTGGGAAG	aly-miR396a-3p	-1,44	0,0000	0,0000	ECERIFERUM 1
LI-miR199	GTTCAATAAAGCTGTGGGAAA	ata-miR396e-3p	-1,47	0,0000	0,0000	ECERIFERUM 1
LI-miRn25	TGGTACAAAAAGTGGGGCAAC	new	-1,82	0,0001	0,0030	Nuclear transcription factor Y subunit A-9
LI-miRn3	TGAAGAGGGAGGGAGACTGATG	new	-2,11	0,0000	0,0000	**SRC2 homolog**
UF2 vs LF2						
LI-miR433	TTGGCATTCTGTCCACCTCC	ahy-miR394	3,11	0,0000	0,0000	**F-box only protein 6**
LI-miR341	TGGACTGAAGGGAGCTCCTTC	gma-miR319q	3,07	0,0000	0,0000	**Transcription factor TCP2**
LI-miR424	TTGGACTGAAGGGAGCTCCCT	aau-miR319	1,98	0,0000	0,0000	Transcription factor TCP4
LI-miR423	TTGGACTGAAGGGAGCTCCCA	mtr-miR319c-3p	1,91	0,0000	0,0000	Transcription factor TCP4
LI-miR224	TCCAAAGGGATCGCATTGATCC	aly-miR393a-5p	1,88	0,0002	0,0052	**TRANSPORT INHIBITOR RESPONSE 1**
LI-miR131	TTGGACTGAAGGGAGCTCCT	mes-miR319h	1,78	0,0000	0,0000	Transcription factor TCP2
LI-miR332	TGCCTGGCTCCCTGTATGCC	bdi-miR160f	1,63	0,0015	0,0262	**Auxin response factor 18**
LI-miR130	TTGGACTGAAGGGAGCTCCC	ppt-miR319c	1,60	0,0000	0,0000	**Transcription factor MYB33**
LI-miR329	TGCCTGGCTCCCTGAATGCCA	ahy-miR160-5p	1,56	0,0024	0,0381	**Auxin response factor 16**
LI-miR199	GTTCAATAAAGCTGTGGGAAA	ata-miR396e-3p	0,66	0,0005	0,0095	ECERIFERUM 1
LI-miR200	GTTCAATAAAGCTGTGGGAAG	aly-miR396a-3p	0,31	0,0001	0,0030	ECERIFERUM 1
UF3 vs LF3						
LI-miR433	TTGGCATTCTGTCCACCTCC	ahy-miR394	2,59	0,0000	0,0009	**F-box only protein 6**
LI-miR333	TGCCTGGCTCCCTGTATGCCA	aly-miR160a-5p	2,18	0,0002	0,0072	**Auxin response factor 18**
LI-miR332	TGCCTGGCTCCCTGTATGCC	bdi-miR160f	1,88	0,0006	0,0210	**Auxin response factor 18**

LI-miR224	TCCAAAGGGATCGCATTGATCC	aly-miR393a-5p	1,87	0,0018	0,0498	**TRANSPORT INHIBITOR RESPONSE 1**
LI-miR115	CTCGTTGTCTGTTCGACCTTG	ppe-miR858	0,78	0,0001	0,0072	**Transcription repressor MYB5**
LI-miR453	TTTGGATTGAAGGGAGCTCTG	bdi-miR159b-3p	-0,57	0,0002	0,0072	**RING-type zinc-finger**
LI-miR229	TCCACAGGCTTTCTTGAACTG	ata-miR396a-5p	-1,94	0,0013	0,0404	**Growth-regulating factor 5**
LI-miR432	TTGGATTTTTATTTAGGACGG	osa-miR5490	-2,29	0,0001	0,0072	**Acid phosphatase 1**
LI-miR311	TGAGGAATCACTAGTAGTCGT	osa-miR5794	-2,32	0,0001	0,0072	**Uncharacterized WD repeat-containing protein**
LI-miR92	CGATCTTGAGGCAGGAACTGAG	osa-miR1861b	-4,11	0,0000	0,0000	Clathrin interactor EPSIN 2
LI-miR251	TCGGACCAGGCTTCAATCCCT	ata-miR5168-3p	-5,13	0,0000	0,0000	Homeobox-leucine zipper protein ATHB-15
			UF4 vs LF4			
LI-miR445	TTTGGACTGAAGGGAGCTCCT	atr-miR319b	0,75	0,0001	0,0078	Transcription factor TCP4
LI-miR100	CGCTATCCATCCTGAGTTTCA	aly-miR390a-3p	-0,97	0,0006	0,0452	TAS3

Table 6. Differentially expressed miRNAs identified in comparisons between pedicels collected from abscised or non-abscised flowers (FPAB vs FPNAB) with Padj < 0.05.

Flower pedicels						
ID	miRNA sequence	miRBase annotation	log_2FC	p-value	padj	Target description (psRNAtarget/degradome)
FPAB vs FPNAB						
Ll-miR281	TGAAGCTGCCAGCATGATCTGA	ata-miR167b-5p	4,77	0,0000	0,0000	Auxin response factor 6 and ARF8
Ll-miR39	AGATCATGTGGCAGTTTCACC	ahy-miR167-3p	4,65	0,0000	0,0000	Transcription repressor OFP14
Ll-miR280	TGAAGCTGCCAGCATGATCTG	atr-miR167	3,73	0,0000	0,0000	Auxin response factor 6 and ARF8
Ll-miR283	TGAAGCTGCCAGCATGATCTGG	aly-miR167d-5p	3,19	0,0000	0,0000	Auxin response factor 6 and ARF8
Ll-miR276	TGAAGCTGCCAGCATGATCT	bna-miR167d	2,74	0,0000	0,0005	Auxin response factor 6 and ARF8
Ll-miRn18	AATAGGGCACATCTCTCATGG	new	2,26	0,0001	0,0006	E3 ubiquitin-protein ligase HOS1
Ll-miR193	GTCGTTGTAGTATAGTGG	gma-miR6300	2,18	0,0001	0,0006	-
Ll-miR438	TTGTGTTCTCAGGTCACCCCT	stu-miR398b-3p	2,09	0,0000	0,0000	**Probable nucleoredoxin 1**
Ll-miR325	TGCCAAAGGAGAGTTGCCCTG	aly-miR399b-3p	1,95	0,0000	0,0000	Inorganic phosphate transporter 1-4
Ll-miR364	TGTGTTCTCAGGTCACCCCTT	aly-miR398a-3p	1,94	0,0010	0,0071	**Superoxide dismutase [Cu-Zn]**
Ll-miR415	TTGAGCCGTGCCAATATCACG	aly-miR171b-3p	1,80	0,0017	0,0117	**Scarecrow-like protein 6**
Ll-miR366	TGTGTTCTCAGGTCGCCCCTG	aqc-miR398b	1,66	0,0005	0,0042	Superoxide dismutase [Cu-Zn]
Ll-miR260	TCGGACCAGGCTTCATTCCCT	csi-miR166d	1,07	0,0078	0,0450	**Homeobox-leucine zipper protein ATHB-14**
Ll-miR273	TCTCGTTGTCTGTTCGACCTT	cme-miR858	1,02	0,0037	0,0223	**Transcription factor MYB78**
Ll-miR402	TTGACAGAAGATAGAGAGC	hbr-miR156	-0,89	0,0008	0,0060	Squamosa promoter-binding protein 1
Ll-miRn21	TGAGCATGAGGATAAGGACGG	new	-1,18	0,0000	0,0000	**Tetratricopeptide repeat protein 1**
Ll-miR198	GTTCAATAAAGCTGTGGGAA	osa-miR396a-3p	-1,24	0,0024	0,0159	ECERIFERUM 1
Ll-miRn5	TGGAATAGTGAATGAGACATC	new	-1,25	0,0003	0,0024	Probable cinnamyl alcohol dehydrogenase 9
Ll-miR102	CGCTGTCCATCCTGAGTTTCA	bra-miR390-3p	-1,27	0,0003	0,0027	TAS3
Ll-miR199	GTTCAATAAAGCTGTGGGAAA	ata-miR396e-3p	-1,49	0,0005	0,0039	ECERIFERUM 1
Ll-miR200	GTTCAATAAAGCTGTGGGAAG	aly-miR396a-3p	-1,61	0,0001	0,0009	ECERIFERUM 1
Ll-miR44	AGCTGCTGACTCGTTGGTTCA	mtr-miR4414a-5p	-1,76	0,0012	0,0084	Non-specific phospholipase C1
Ll-miR151	GCGTATGAGGAGCCAAGCATA	gma-miR160a-3p	-1,90	0,0007	0,0055	E3 ubiquitin-protein ligase RFWD3
Ll-miR57	TGAAGTGTTTGGGGGAACTC	gma-miR395i	-2,01	0,0000	0,0000	**ATP sulfurylase 1, chloroplastic**
Ll-	GGAACGTTGGCTGGCTCGAGG	ata-miR166c-5p	-2,02	0,0072	0,0425	Probable methyltransferase PMT21

miR170						
ll-miR119	TGAAGTGTTTGGGGGAACTCC	sly-miR395a	-2,23	0,0000	0,0000	**ATP sulfurylase 1, chloroplastic**
ll-miRn3	TGAAGAGGGAGGGAGACTGATG	new	-2,26	0,0027	0,0171	**SRC2 homolog**
ll-miR118	CTGAAGTGTTTGGGGGAACTC	aly-miR395d-3p	-2,47	0,0000	0,0000	**ATP sulfurylase 1, chloroplastic**
ll-miR99	CGCTATCCATCCTGAGTTTC	gma-miR390a-3p	-2,65	0,0001	0,0006	TAS3
ll-miR100	CGCTATCCATCCTGAGTTTCA	aly-miR390a-3p	-2,75	0,0000	0,0000	TAS3
ll-miR162	GCTCTCTAAGCTTCTGTCATCA	aly-miR157b-3p	-2,90	0,0000	0,0003	Dr1 homolog
ll-miR94	CGATGTTGGTGAGGTTCAATC	gma-miR171k-5p	-3,01	0,0000	0,0000	Transcription factor MYB4
ll-miRn32	AAGGGTTGTTTACAGAGTTTA	new	-3,18	0,0000	0,0000	26S proteasome regulatory subunit 7
ll-miR174	GGAATGTTGGCTGGCTCGAGG	mtr-miR166e-5p	-3,46	0,0000	0,0000	**Nucleolar GTP-binding protein 1**

Figures

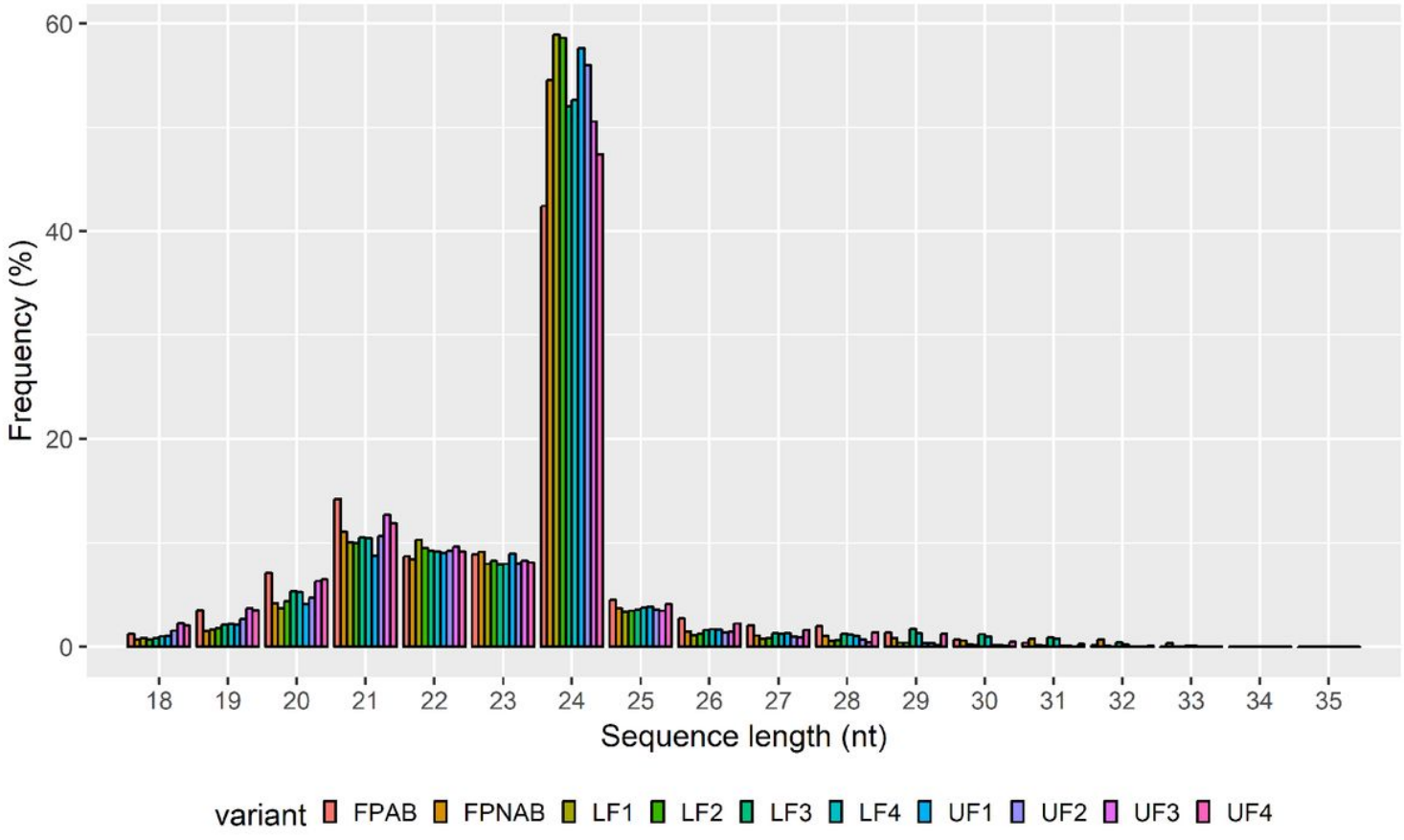

Figure 1

Nucleotide length distribution of small RNAs from all ten libraries. Y-axis represents the percentage frequency of the sRNA sequences identified in this study, X-axis represents sRNA length.

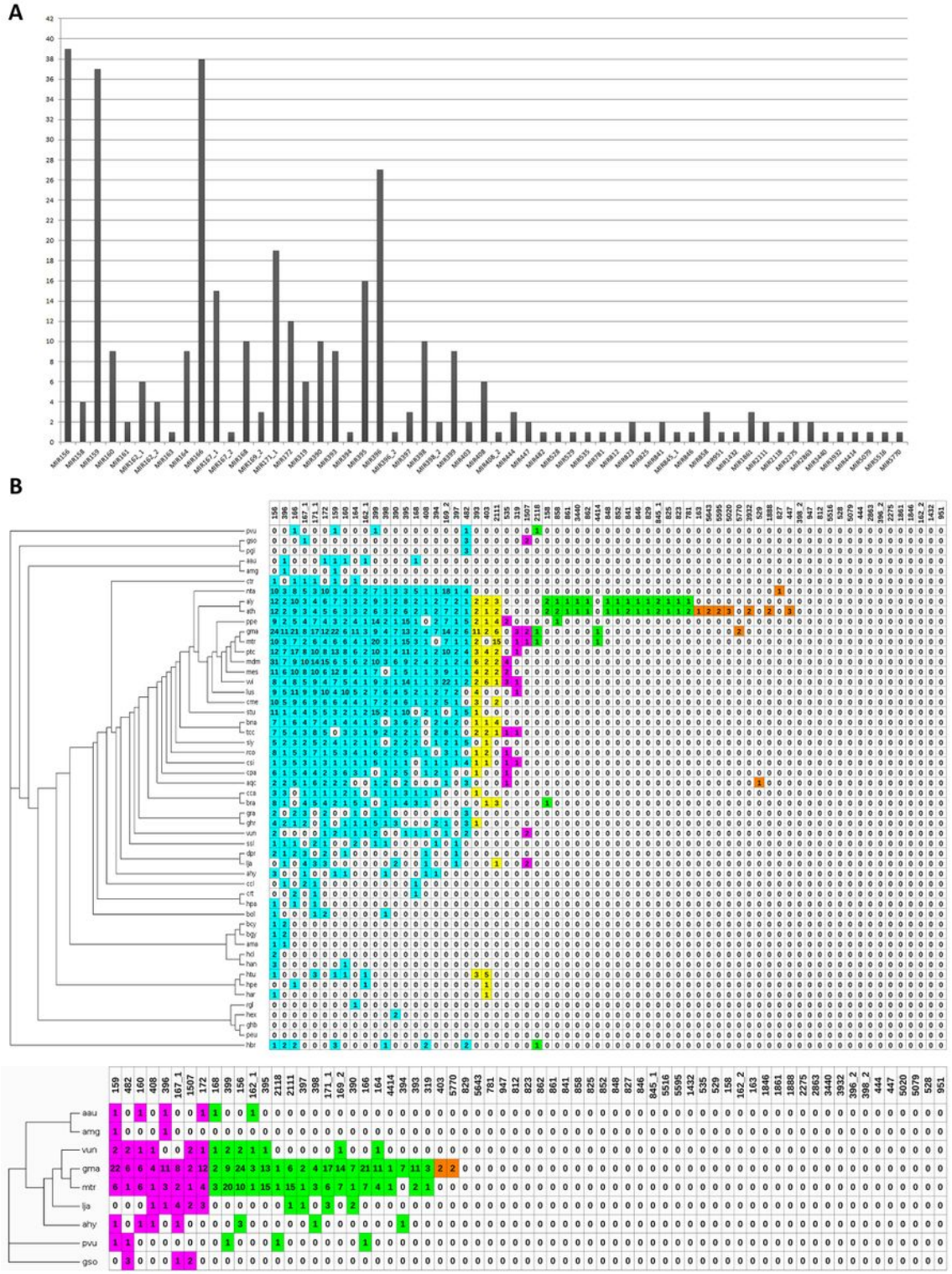

Figure 2

Identification and evolutionary conservation of known miRNA families in Lupinus luteus. (a) The distribution of known miRNA family sizes in L. luteus. (b) Comparison of known miRNA families in L. luteus and their 52 homologs in Eudicotyledons species present in miRBase (upper panel) and 9 Fabaceae species (lower panel). Known miRNA families of L. luteus identified from small RNA-seq are listed in the top row. The colors represent relative miRNA families classified into different groups with similar

conservation. Blue, yellow, magenta, green and orange represent relative miRNA families with homologs across more than 20, 10-19, 5-9, 2-4 species and in 1 species, respectively. Aau, Acacia auriculiformis; amg, Acacia mangium; aqc, Aquilegia caerulea; aly, Arabidopsis lyrata, ath, Arabidopsis thaliana; ahy, Arachis hypogaea; ama, Avicennia marina; bna, Brassica napus, bol, Brassica oleracea; bra, Brassica rapa; bcy, Bruguiera cylindrica; bgy, Bruguiera gymnorhiza; cpa, Carica papaya; ccl, Citrus clementina; crt, Citrus reticulata; csi, Citrus sinensis; ctr, Citrus trifoliata; cme, Cucumis melo; cca, Cynara cardunculus; dpr, Digitalis purpurea; gma, Glycine max; gso, Glycine soja; ghb, Gossypium herbaceum; ghr, Gossypium hirsutum; gra, Gossypium raimondii; han, Helianthus annuus; har, Helianthus argophyllus; hci, Helianthus ciliaris; hex, Helianthus exilis; hpa, Helianthus paradoxus; hpe, Helianthus petiolaris; htu, Helianthus tuberosus; hbr, Hevea brasiliensis; lus, Linum usitatissimum; lja, Lotus japonicus; mdm, Malus domestica; mes, Manihot esculenta; mtr, Medicago truncatula; nta, Nicotiana tabacum; pgi, Panax ginseng; pvu, Phaseolus vulgaris; peu, Populus euphratica; ptc, Populus trichocarpa; ppe, Prunus persica; rgl, Rehmannia glutinosa; rco, Ricinus communis; ssl, Salvia sclarea; sly, Solanum lycopersicum; stu, Solanum tuberosum; tcc, Theobroma cacao; vun, Vigna unguiculata, vvi, Vitis vinifera.

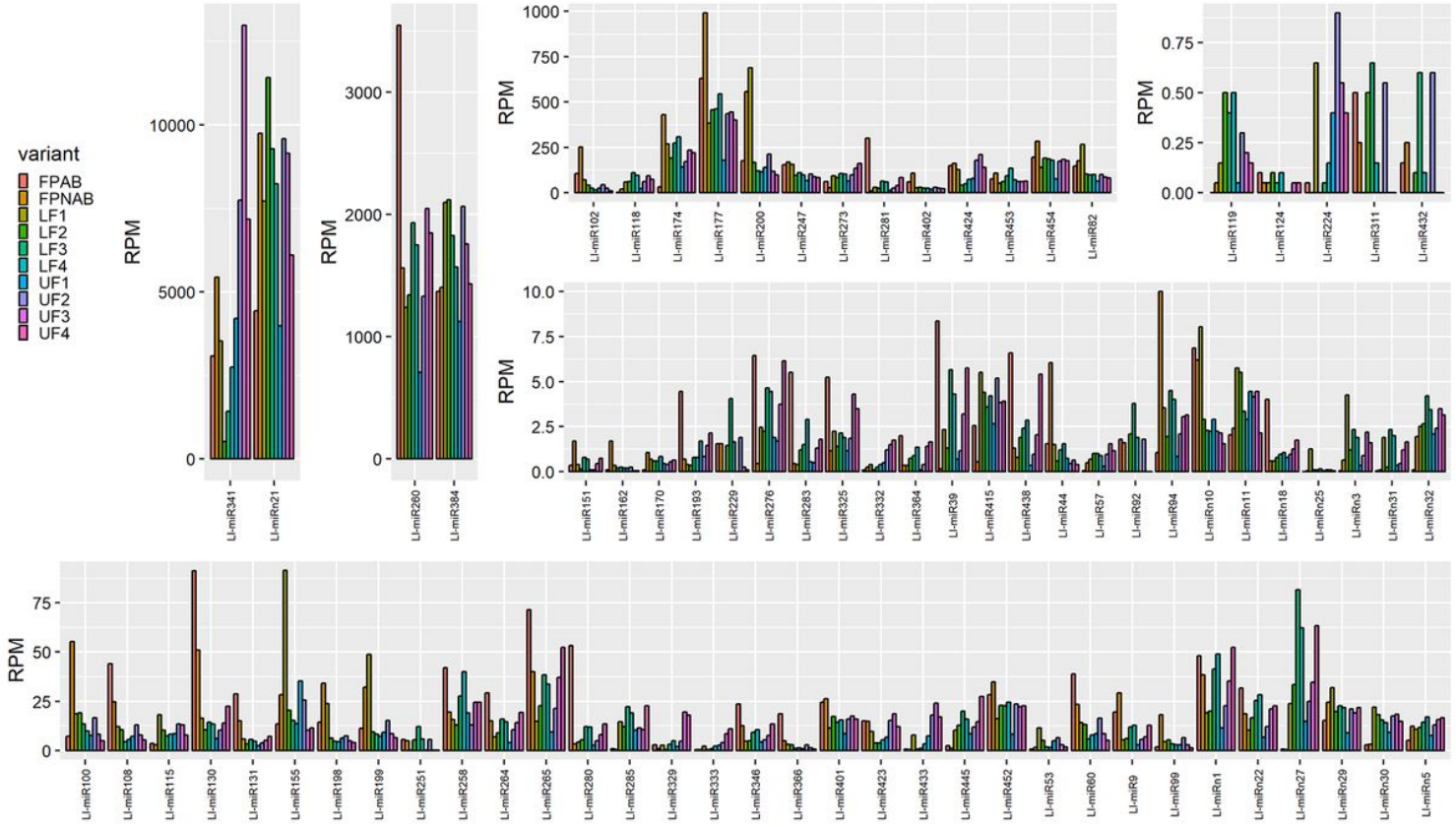

Figure 3

Diversity of miRNA expression (reads per million, RPM) in yellow lupine flowers. All graphs together show complete data concerning differential miRNA expression in the experiment described herein.

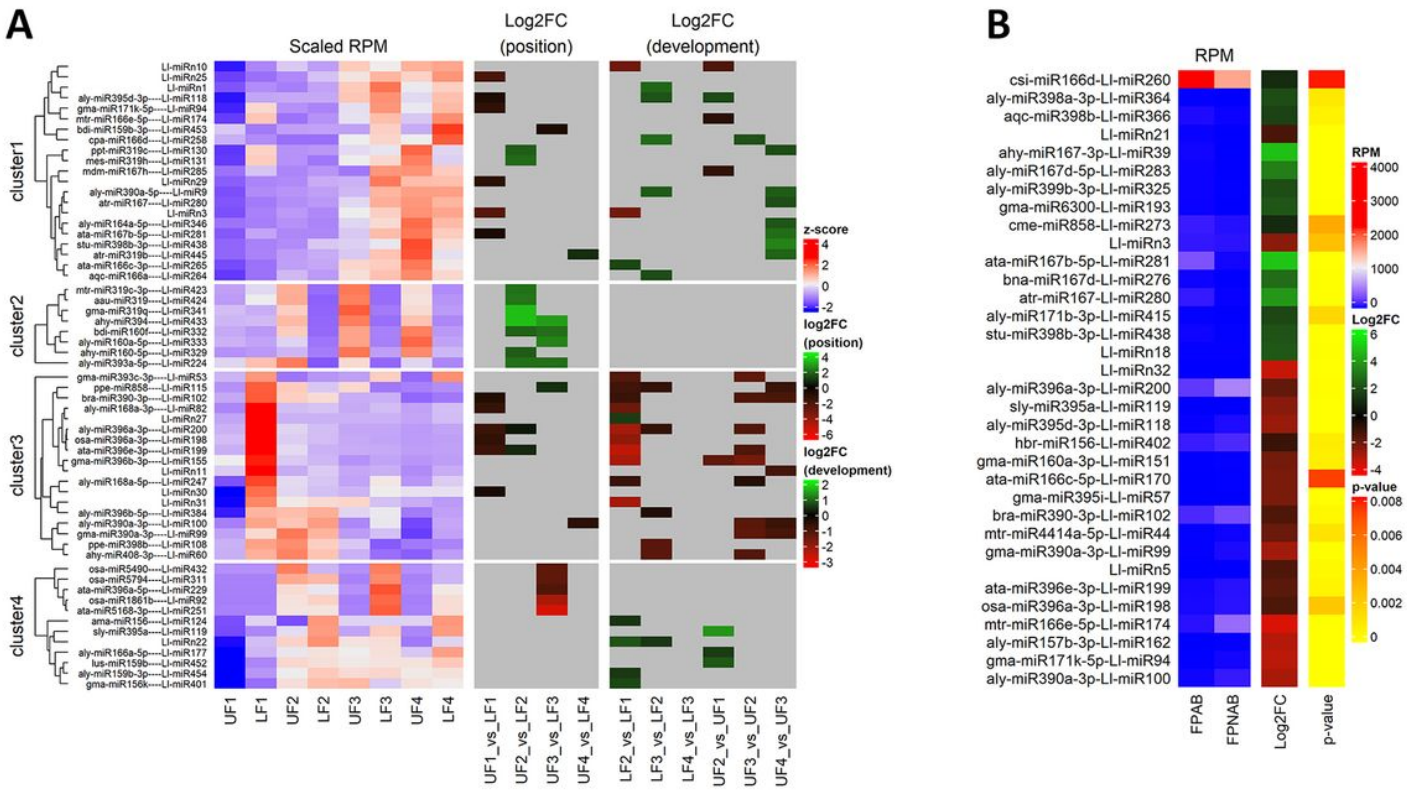

Figure 4

Differential miRNA expression in lupine flowers and flower pedicels. (a) Heatmaps of z-scaled miRNA expression (scaled RPM) and log2 fold changes for either position of the flower on the raceme (Log2FC position), or identified between consecutive stages of flower development (Log2FC development). Grey indicates insignificant changes. (b) Heatmaps of miRNA expression, log2 fold changes (Log2FC) and p-values for flower pedicels with an active or inactive abscission zone. The miRNA names are shown on the right vertical axis. Red and green represent the up-regulated and down-regulated miRNAs, respectively.

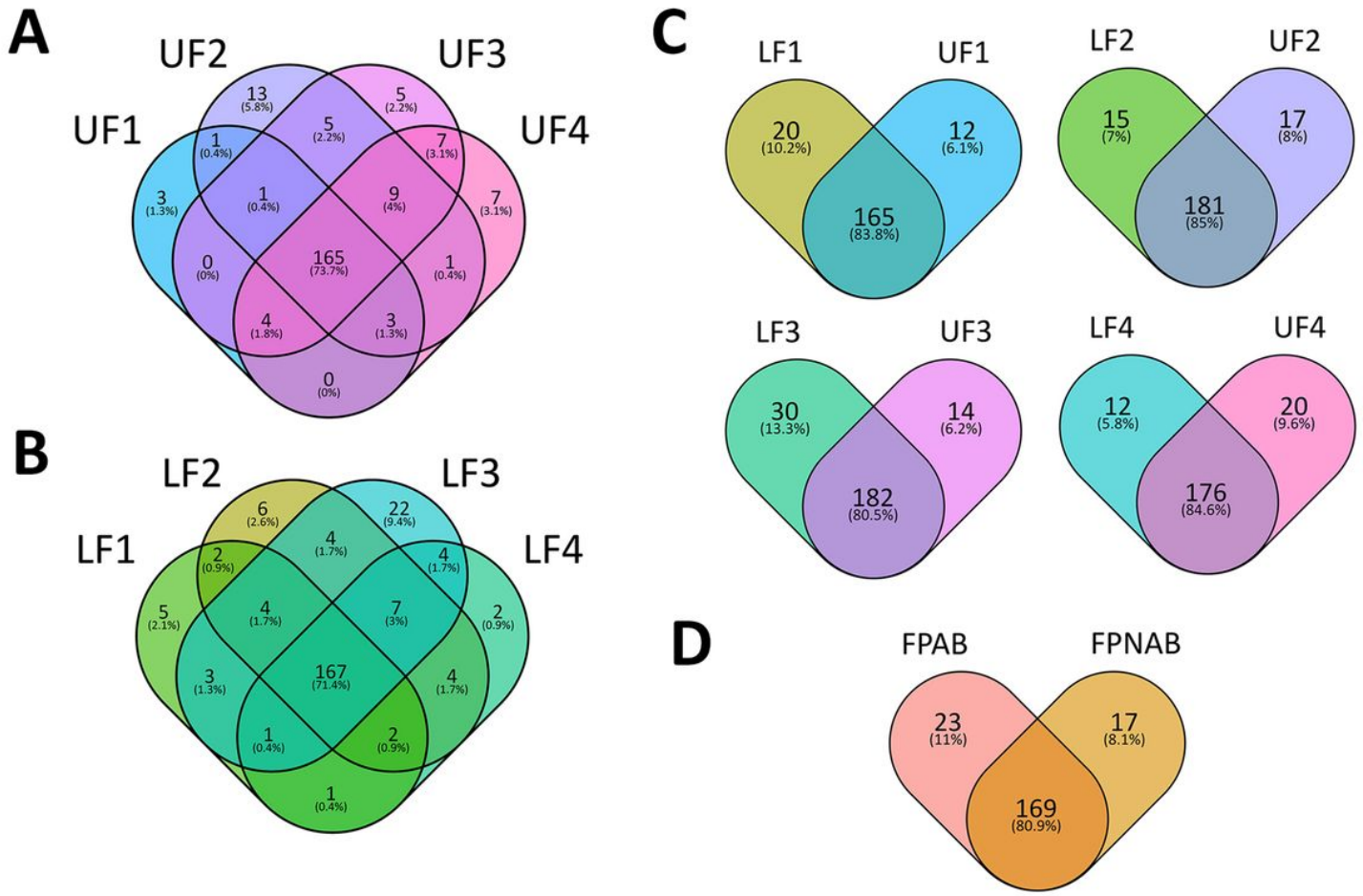

Figure 5

Venn diagrams showing distribution of yellow lupine miRNAs in: (a) upper flowers, (b) lower flowers, (c) both upper and lower flowers in particular stages of their development, (d) pedicels of abscising flowers or flowers maintained on the plant.

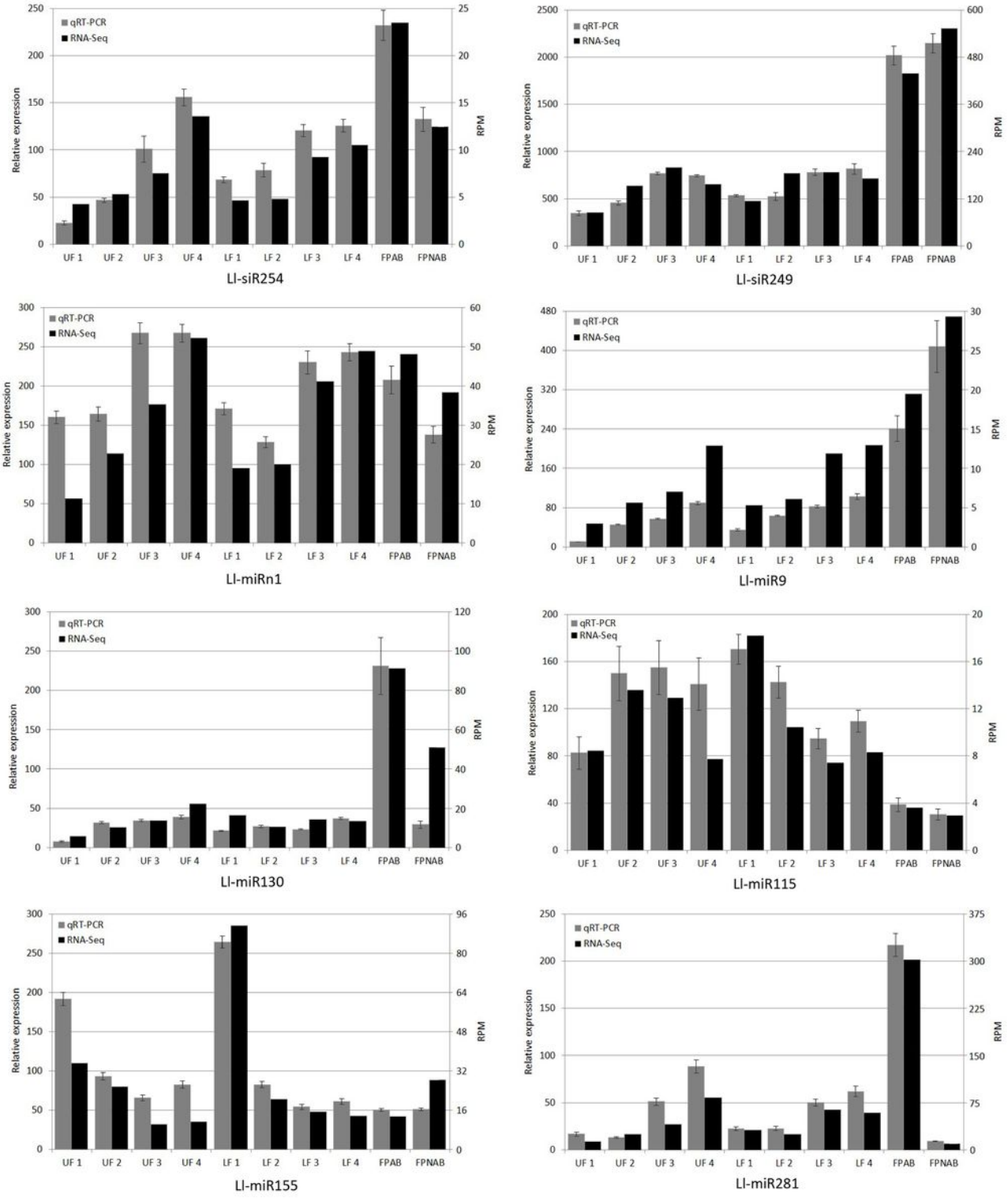

Figure 6

SL RT-qPCR validation of selected sRNAs in L. lupinus. Grey indicates the miRNA expression levels determined by qPCR normalized to the Actin housekeeping gene. Black indicates the miRNA expression levels determined by deep sequencing. Vertical bars indicate the standard errors in three repetitions.

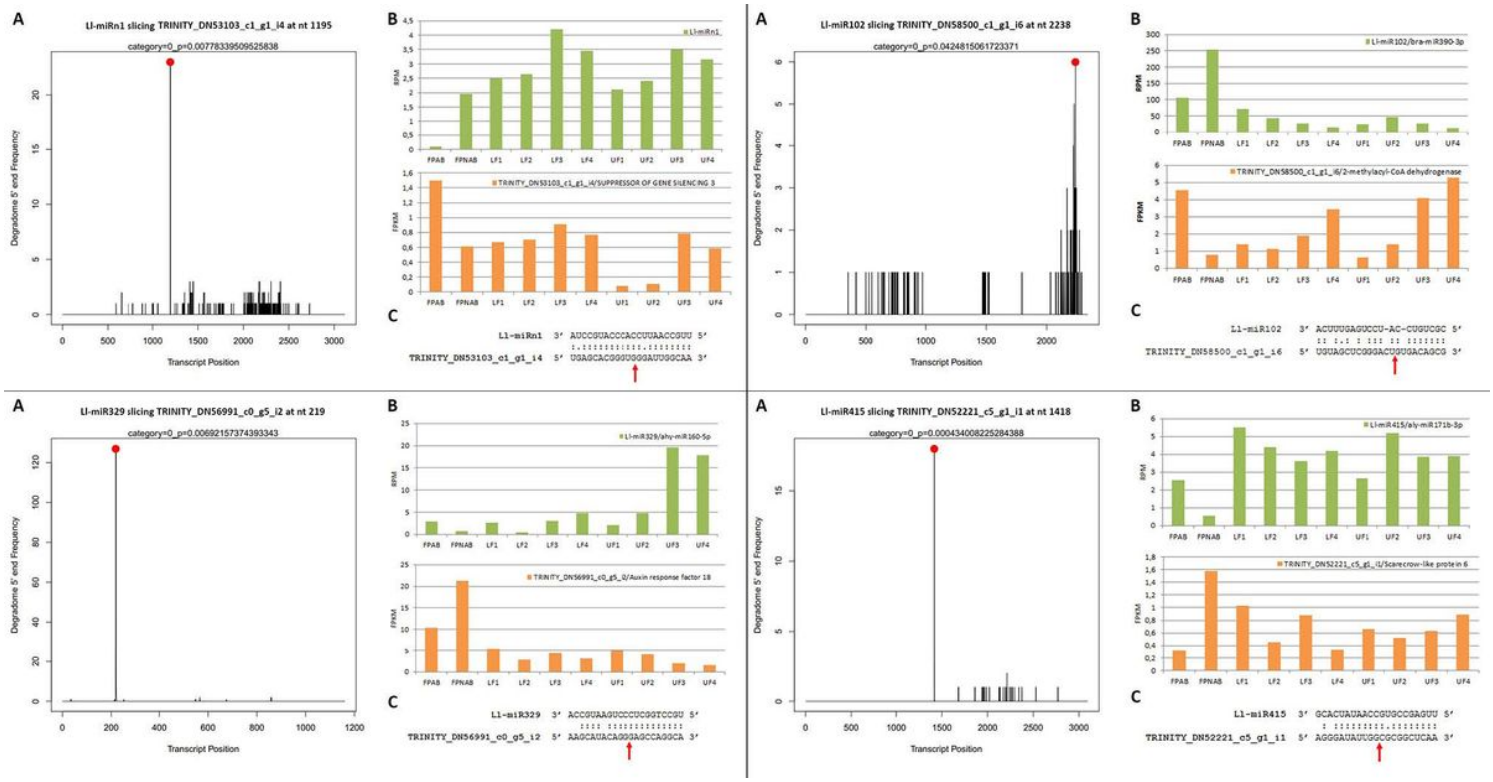

Figure 7

Examples of post-transcriptional regulation of miRNA targets in yellow lupine. (a) T-plots of miRNA targets confirmed by degradome sequencing. The T-plots show the distribution of the degradome tags along the full length of the target gene sequence. The cleavage site of each transcript is indicated by a red dot. (b) Comparison of the expression levels of miRNAs and their targets in flowers from upper and lower whorls of yellow lupine racemes, and flower pedicels, as determined by deep sequencing. (c) miRNA-mRNA alignments. The red arrows represent the cleavage site nucleotides on the target genes.

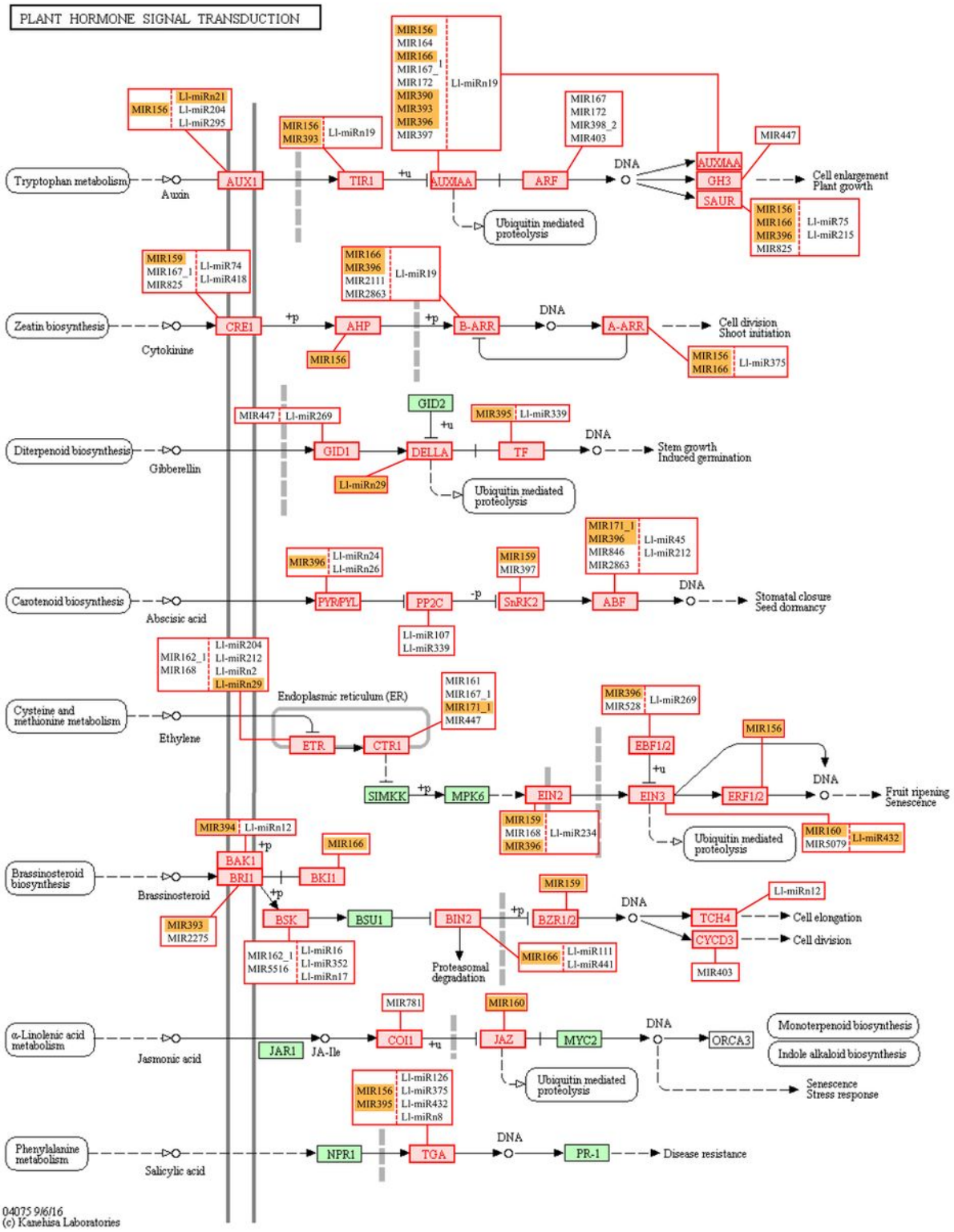

Figure 8

KEGG pathways related to plant hormone signal transduction targeted by known and novel miRNAs./ Plant hormone signal transduction pathways and the related miRNAs. Orange indicates DE miRNAs.

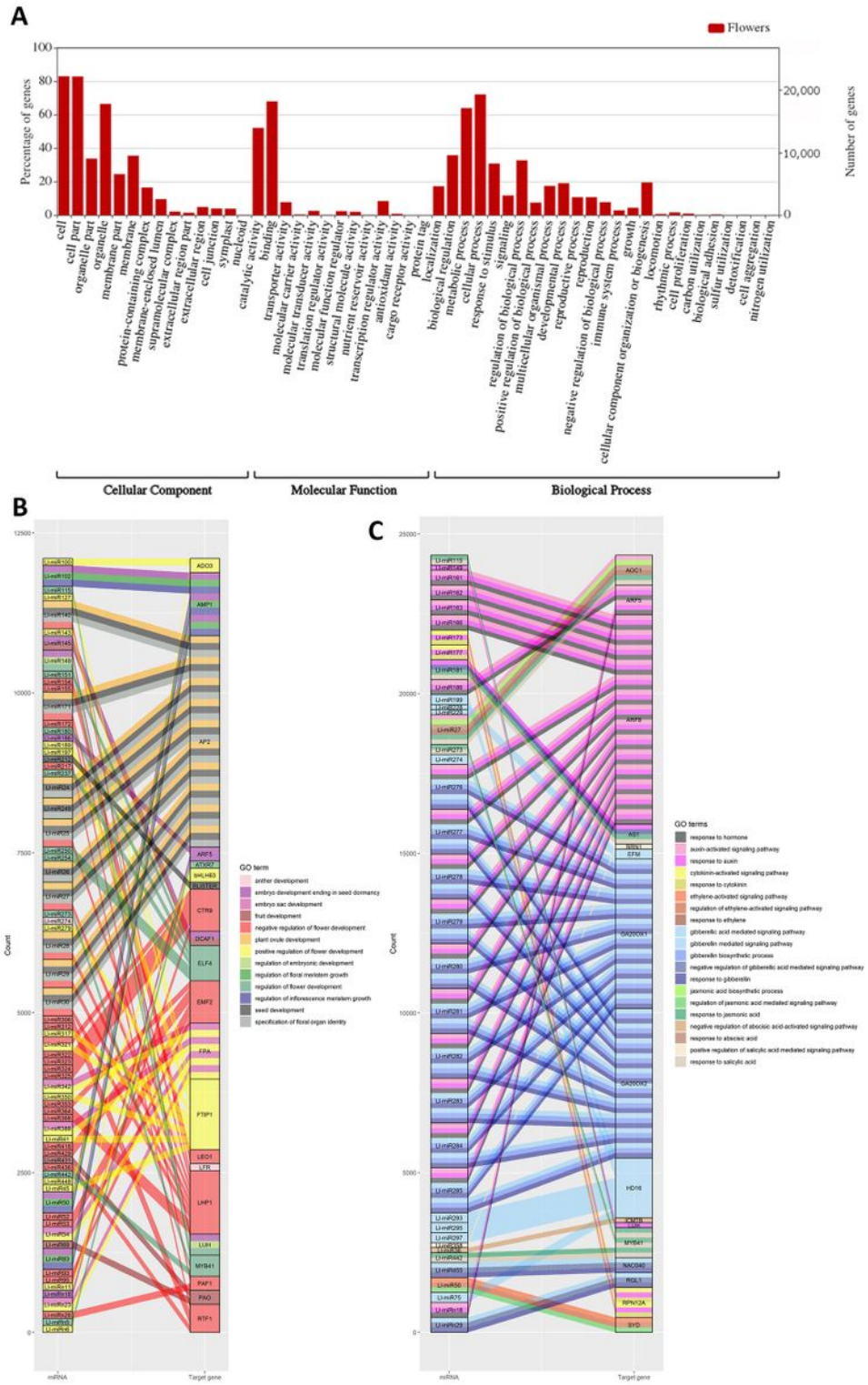

Figure 9

GO analysis of miRNA target genes in yellow lupine. (a) Visualization of GO categories annotated to predicted target genes of known and novel miRNAs in yellow lupine. (b-c) Alluvial diagrams showing participation of Lupinus luteus miRNAs in processes categorized to selected GO terms associated with (b) plant hormones or (c) flower development via regulation of their target genes.

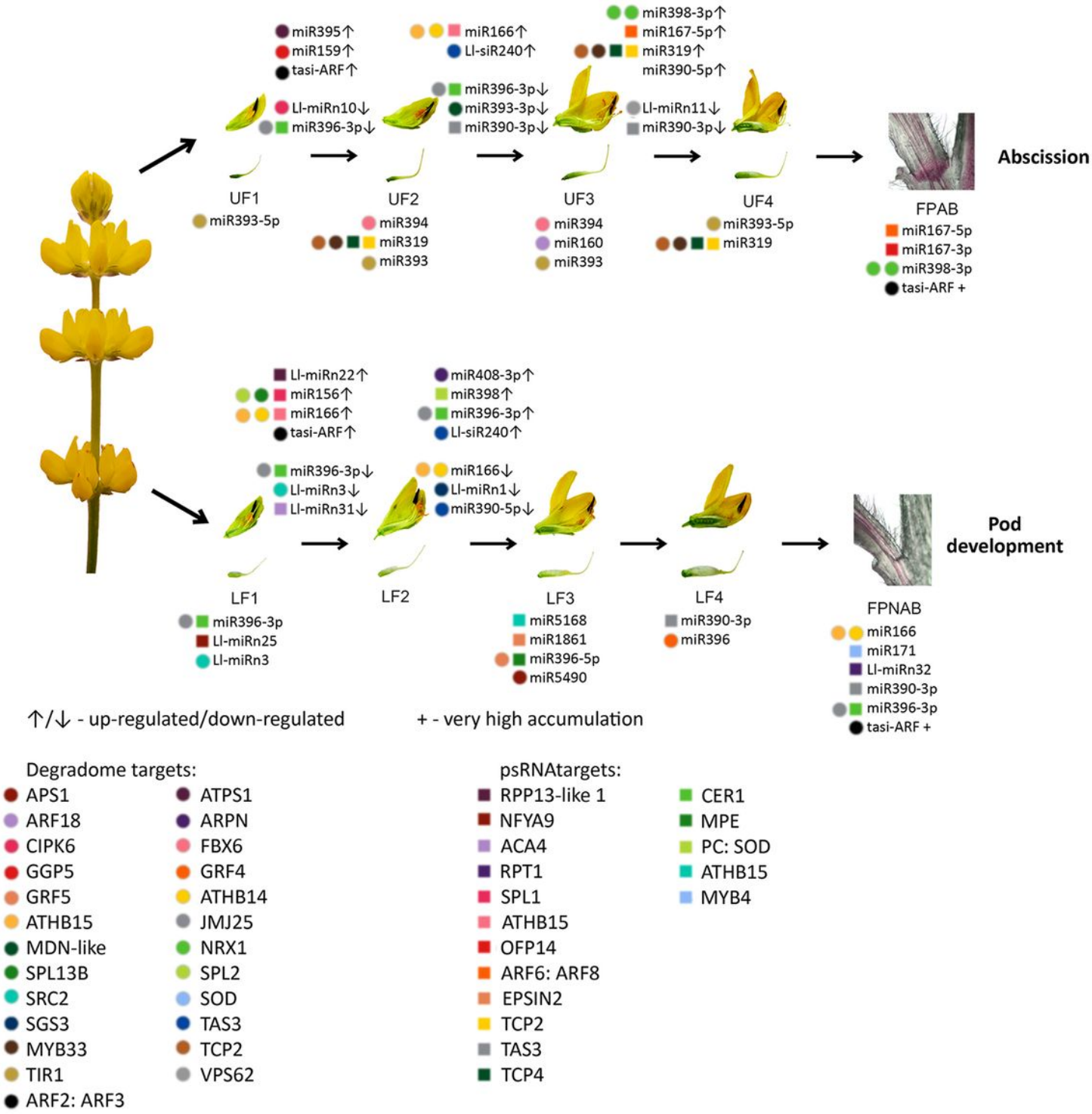

Figure 10

MiRNAs and siRNAs participating in yellow lupine flower development and abscission. Scheme based on the results of current analysis. Arrows pointing upwards and downwards represent sequences that are up or down-regulated in the transition between two developmental stages, respectively. The plus sign marks significantly expressed sequences. Colored circles represent targets found in the degradome, colored squares represent targets found using psRNATarget, as listed below. Multiple markers indicate that

sequence has multiple targets. Full target gene names can be found at abbreviation list. Pictures from left to right are as follows: 4-whorl inflorescence of yellow lupine, flower cross-sections and isolated pistils for each stage of development, cross-sections of abscissing and non-abscissing flower pedicels stained with phloroglucinol-HCL solution.

Supplementary Files

This is a list of supplementary files associated with this preprint. Click to download.

- additionalfile120032019.xlsx
- Additionalfile5FigureS4.pdf
- Additionalfile3FigureS2.pdf
- Additionalfile4FigureS3.pdf
- Additionalfile8FigureS7.pdf
- additionalfile220032019.xlsx
- Additionalfile7FigureS6.pdf
- Additionalfile6FigureS5.pdf